"In presenting the dissertation as a partial fulfillment of the requirements for an advanced degree from the Georgia Institute of Technology, I agree that the Library of the Institution shall make it available for inspection and circulation in accordance with its regulations governing materials of this type. I agree that permission to copy from, or to publish from, this dissertation may be granted by the professor under whose direction it was written, or, in his absence, by the dean of the Graduate Division when such copying or publication is solely for scholarly purposes and does not involve potential financial gain. It is understood that any copying from, or publication of, this dissertation which involves potential financial gain will not be allowed without written permission.

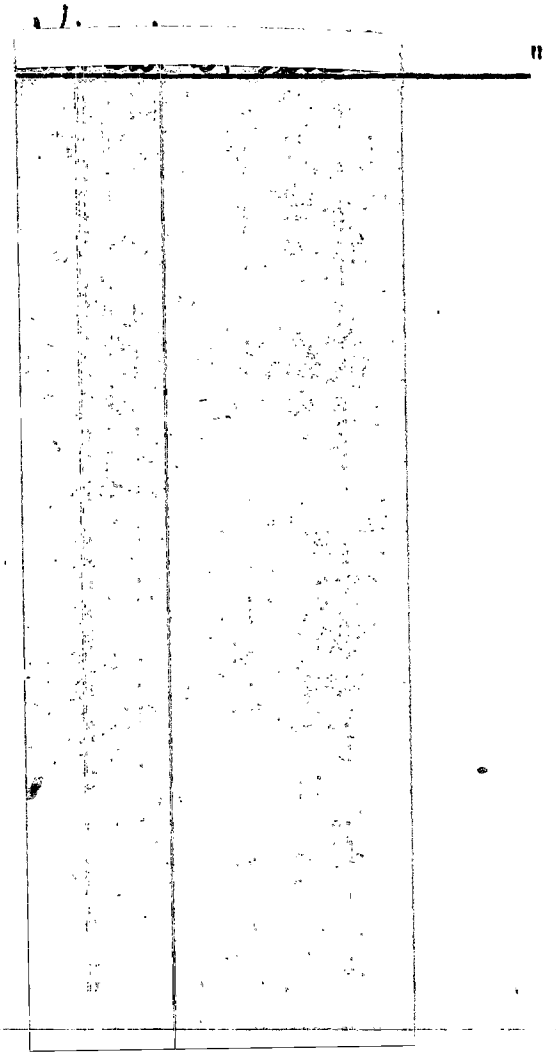

THE DECAY OF Ir^{192}

A THESIS

Presented to

the Faculty of the Graduate Division

Georgia Institute of Technology

In Partial Fulfillment

of the Requirements for the Degree

Doctor of Philosophy in the School

of Physics

By

Vincent Wymore Shiel

May 1957

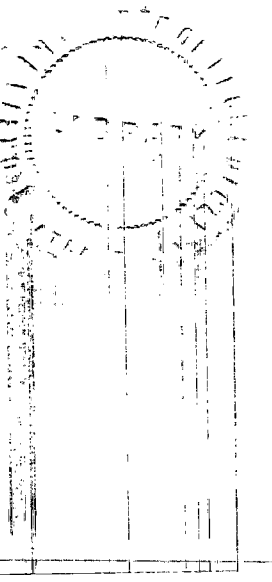

12R
N/C

THE DECAY OF Ir^{192}

Approved

Thesis Advisor

Date Approved by
Chairman

May 24, 1957

ACKNOWLEDGMENTS

The completion of this research was made possible by the Graduate Division Fellowships which the author held during 1955-1957. The research project was supported in part by the National Science Foundation. The author wishes to acknowledge Drs. L. D. Wyly and C. H. Braden both for suggesting the thesis topic and for supplying many hours of constructive consultation. The author also wishes to acknowledge Mr. E. T. Patronis for helpful advice on the electronics, Mr. H. G. Dulaney for assistance in making the calculations for Figs. 11 and 12, and Mr. R. E. Anderson for the construction of the mechanical apparatus.

TABLE OF CONTENTS

Page

APPENDICES

LIST OF TABLES

LIST OF FIGURES

Figure Page

THESIS ABSTRACT

THE DECAY OF Ir^{192}

(124 pages)

by Vincent Wymore Shiel
Advisor Dr. D. David Wyly

Even though the radioactive decay of Ir^{192} had been studied by many investigators, several ambiguities existed in the spin assignments to the excited levels of Os^{192}, Pt^{192}, and the ground state of Ir^{192}. Ir^{192} decays by negatron emission, (beta decay), into Pt^{192} and by K-capture into Os^{192}. The positioning of the energy levels in Pt^{192} and Os^{192} and the energies and relative intensities of the accompanying gamma-rays were known. Furthermore, multipolarities of the more intense gamma-rays had been assigned; the spins of many of the energy levels were delimited to only a few possibilities, and the parities of many of the levels were established. The existence of at least three beta groups connecting Ir^{192} and Pt^{192} was postulated, but direct measurements had been performed only on the beta group with the highest energy.

Gamma-gamma angular correlation techniques have proved valuable for determining the spins of nuclear energy levels when the multipolarities of the gamma-rays have been assigned by other measurements and when the spins of the levels are limited to only a relatively few possibilities. Therefore, it was decided to study the decay of Ir^{192} by the use of gamma-gamma angular correlation, scintillation counter techniques and attempt to remove the uncertainties of the spins of some of the energy levels. Furthermore, it was decided to investigate the beta decay of Ir^{192} using beta-gamma coinci-

dence techniques and beta-gamma angular correlation techniques in order to provide direct experimental evidence supporting the decay scheme.

The apparatus used in this research may be described as follows: the detectors are standard scintillation detectors. For gamma-ray detection a sodium iodide (thallium activated) crystal is coupled to a photomultiplier; for electron detection an anthracene crystal is used and the source and detector are contained in a vacuum chamber. The amplifiers and pulse height analyzers are commercial instruments. The coincidence circuit is of the fast-slow type using pulse-height analysis to choose the desired gamma or beta energy. The resolving time is about 10^{-7} second. The fast pulses to the coincidence circuit are taken from the amplifier discriminator output and the accidental coincidences are determined by insertion of a delay in one of these outputs. In beta-gamma work, the gamma-gamma background is determined by insertion of a lucite electron absorber in front of the electron detector.

The experimental procedure may be described as follows: the Ir^{192} was produced at the Oak Ridge National Laboratory by irradiation of iridium with thermal neutrons. Sources were prepared by evaporation of Na_2IrCl_2 in HCl solution on 0.25 mil rubber hydrochloride backing. The gamma-rays studied in this research showed no change in relative intensities over a period of more than one year; therefore, radioactive impurities are probably not present in appreciable quantities.

Gamma-gamma coincidence studies were performed in order to determine which gamma-gamma angular correlation experiments were feasible. From these studies it was decided that the following gamma-gamma angular correlation experiments could be performed: 468-300 kev, 600-300 kev, 600-600 kev, 485-205 kev, and 416-468 kev. Measurements were made at

angles of 90°, 270°, and 180° for the 600-600 and 485-205 kev cascades and at angles of 90°, 270°, 135°, 225°, and 180° for the other cascades.

The beta-ray singles spectrum was examined; however, little information can be gained from such a study since the observed spectrum is a composite of several beta groups. Therefore, beta-gamma coincidence studies were made with the 468 and 600 kev gamma-rays. The resulting Fermi plots indicate the existence of two beta groups with endpoint energies near 670 and 540 kev respectively. The fact that the Fermi plots are approximately straight lines indicates that energy degradation of the electrons due to scattering is not appreciable, and that beta-gamma angular correlation experiments with the 468 and 600 kev gamma-rays are meaningful. These beta-gamma angular correlation experiments were performed and the angular distribution obtained is very nearly isotropic.

The experimental gamma-gamma angular correlation data after suitable corrections are compared to the various theoretical possibilities corresponding to the different spin possibilities for the pertinent nuclear state. From such comparisons it is possible to assign a spin of three to the 690 kev level in Os^{192} and to the 921 and 1201 kev levels in Pt^{192}. The assignment of spin three to the 1201 kev level in Pt^{192} requires an admixture of about 8.5 per cent M1 radiation in the 588 kev transition. The interference in the 485-205 kev angular correlation experiment prevents an accurate assignment of the admixture of M1 radiation in the 485 kev transition, but it is probably less than six per cent. The interference in the 600-300 kev cascade also prevents an accurate assignment of the admixture of M1 radiation in the 604 kev transition, but it is probably less than five per cent. Interference in the 416-468 kev experiment from

other gamma-ray cascades makes the data for this experiment lack significance. The assignment of spin three to the level at 921 kev in Pt^{192} indicates that the spin of Ir^{192} is five. Odd parity and a high spin for Ir^{192} may be reconciled with the shell model by assignment of the odd proton to an $h_{11/2}$ orbital and the odd neutron to an $i_{13/2}$ orbital.

The beta-gamma coincidence data lend support to the generally accepted decay scheme. The beta-gamma angular correlation experiment between the 670 kev beta group and the 468 kev gamma-ray gives an isotropic angular distribution which is expected if the spin of Ir^{192} is five. The angular correlation experiment with the 540 kev beta group also gives an isotropic distribution. However, this angular distribution consists of a superposition of three cascades which preclude a significant interpretation.

CHAPTER I

INTRODUCTION

One of the most urgent needs in physics today is the need to develop a comprehensive theory of the nucleus. Such a theory should predict accurately the energy levels of the nuclei, the spins, moments, and parities of these levels, and the properties of the transitions connecting these levels. At the present time no complete theory exists although partially successful theories such as the shell model (1) and the collective model (2) are known. The nuclear experimentalist therefore not only tries to check the predictions of the limited theories in existence but, more important, also seeks to provide a source of accurate information about nuclei in order to guide the theorists and to serve as checks for future more comprehensive theories.

One method of compiling such information is by the study of the radiations accompanying radioactive decay. This thesis is such a study of the radiations associated with the decay of Ir^{192} by the use of scintillation counter spectroscopy and angular correlation techniques. The results of this work have been published in the Physical Review (3).

History of Angular Correlation Techniques

Appendix A discusses the fundamental properties of nuclear spin states and radiations and may be consulted as needed by the reader.

The basic situation in an angular correlation experiment is as follows: A nucleus emits in rapid succession two radiations R_1 and R_2.

The correlation function $W(\Theta)$ is defined as follows: $W(\Theta)\, d\Omega$ is the relative probability that R_2 is emitted into the solid angle element $d\Omega$ at an angle Θ with respect to R_1 (4). The fundamental problem is the determination of this correlation function.

The original work on angular correlation was done in 1940 by Hamilton (5). Hamilton, following a suggestion of Dunworth (6), made a theoretical investigation of the correlation between the directions of propagation of quanta (gamma rays) emitted in two successive transitions of a nucleus. He pointed out that the correlation was a function of the angular momenta (spins) of the states of the nucleus and of the multipolarities of the transitions involved, and he indicated that these correlation measurements would hold particular interest as a means of investigating the spins of the nuclear energy levels.

Following Hamilton's theoretical work, several attempts were made to observe such a correlation. At that time the experiments were performed using Geiger-Mueller detectors which have a very low efficiency for detecting gamma radiations and lack the ability to distinguish between radiations of different energies. With one exception (7), until 1947 all results seemed to indicate that the correlation function was isotropic.

In 1946, Goertzel (8) reexamined the theory and extended it to take into account the effect of the magnetic field at the nucleus due to extranuclear electrons. He suggested that this effect might be in part responsible for the small angular correlations observed experimentally. However, in 1947, Brady and Deutsch (9) studied coincidences between successive gamma rays in the decay of Co^{60}, Sc^{46}, Y^{86}, and

Cs^{134} and found a pronounced anisotropy in the first two cases but none in Y^{86} and Cs^{134}. Furthermore, they studied Co^{60} in a solid chloride, an acqueous solution, and gaseous cobalt nitrosyl carbonyl with essentially the same degree of anisotropy observed in each case. This seemed to indicate that the effect of extranuclear electrons was small, at least in this particular case.

The present angular correlation technique using scintillation counters as detectors was first used in 1948 by Brady and Deutsch (10). They studied the decay of six nuclides and found an anisotropy in every case. The use of scintillation counters increased the rate at which data could be accumulated by a factor of one hundred over that obtained using Geiger counters. Brady and Deutsch showed that their results agreed with Hamilton's theory in four of the cases if the transitions were electric quadrupole and if a 4-2-0 spin sequence was assumed. The remaining two cases seemed to require mixing of different multipolarities in the gamma radiations in order to obtain agreement with the theory. In the complete report of this work Brady and Deutsch (11) showed that the effects of external magnetic fields and chemical binding upon the correlation were small. The earlier failures to obtain anisotropic results appear to be due to the use of inadequate experimental techniques.

At this time Brady and Deutsch suggested that data were urgently needed which determined precisely the internal conversion coefficients of the various gamma radiations in radioactive decay. These internal conversion coefficients enable one to determine the multipolarities of the transitions independently of angular correlation measurements.[1]

---

[1] For further discussion of this point see Appendix A.

Since 1948 gamma-gamma angular correlation measurements have taken their place as an established tool in nuclear spectroscopy. In the last few years the general theory of angular correlations has been highly developed. The correlation function $W(\Theta)$ is usually expanded in a series of even order Legendre polynomials:

$$W(\Theta) = 1 + A_2 P_2(\cos\Theta) + A_4 P_4(\cos\Theta) + \ldots\ldots$$

Biedenharn and Rose (12) have tabulated the correlation coefficients A_2, A_4, etc. as functions of the multipolarities of the gamma transitions R_1 and R_2 and the spins of the nuclear levels connected by R_1 and R_2. Experimentally, one measures the rate at which coincidences between R_1 and R_2 occur as a function of the angle between the directions of emission of R_1 and R_2. After proper correction for the finite solid angles subtended by the counters, one compares the experimental correlation function with the various theoretical possibilities. In a number of cases the multipolarities of R_1 and R_2 have been previously determined, and frequently the spins and parities of two of the levels are known. In such a case the angular correlation experiment yields the spin of the third level.

The status of beta-gamma angular correlations as a tool in spectroscopy is not as well established as that of gamma-gamma techniques. The original theoretical work on beta-gamma correlations was done by Falkoff and Uhlenbeck (13). They discussed the theory under the assumptions that the nuclear charge was zero and that the beta interaction was pure.[2] They found that in certain cases of forbidden beta decay a

---

[2] That is, not a mixture of the five different types of beta interactions (14).

correlation should exist which depends upon the exact nature of the interaction,[3] the degree of forbiddenness, and the energy of the beta particles observed. They showed that no angular correlation is expected whenever (a) the beta transition is allowed; (b) the beta transition is forbidden but has the allowed shape of its energy spectrum; (c) one counts only low energy beta particles. The theory was extended to remove the assumptions of zero nuclear charge and pure beta interaction by Fuchs and Lennox (15), Morita, Yamada, and Fugita (16), (17), (18), (19), (20) and by Biedenharn and Rose (12). However, the results are still not in a form in which they can be applied easily.

Since 1949 numerous attempts have been made to observe an anisotropic beta-gamma angular correlation. However, only a few have been observed (4). Recently, Novey, Freedman, Porter and Wagner (21) carefully studied the beta-gamma directional correlation in Re^{186}. Their results were essentially in agreement with the theory.

Review of Previous Research on Ir^{192}

The decay of Ir^{192} has been studied by numerous investigators. The early workers were hindered by inadequate experimental apparatus, and their results will not be discussed. In 1952 Muller et al (22) applied Dumond's curved crystal spectrometer (23) to a study of the gamma radiations accompanying the decay of Ir^{192}. They measured the energies and intensities of eleven gamma radiations. Cork (24), Pringle (25), (26), and Johns and Nablo (27) further investigated the gamma radiations accompanying the decay and proposed a decay scheme

---

[3] For example, pseudoscaler or tensor etc.

for Ir^{192}. In 1955, Baggerly et al (28) rediscussed the decay very carefully and proposed a decay scheme which was similar to the one previously proposed in the Pt^{192} branch but contained minor changes in the Os^{192} branch. This scheme is shown in Fig. 1.

A summary of the essential arguments for positioning the energy levels as shown in Fig. 1 is as follows: assignment to either the platinum or osmium branch is assured by comparing the energies of the gamma-rays as determined by gamma spectrometer measurements with the respective K-conversion lines as measured in a beta-ray spectrometer[4] (28).

Pt^{192} branch.--Intensity measurements of the 316 kev line indicate that it is by far the most intense line and hence is very likely the ground state transition. Therefore, level B is placed at 316 kev. Numerous observers have noted coincidences between the 316 kev and 468 kev transitions (28), (29), (30), (31), and hence level D is placed at 784 kev. Levels C and E are placed on the basis of the observed triple coincidences among the 296, 308 and 316 kev gamma transitions (29), (30), (31) and because of the fact that the 136 kev and 172 kev lines fit in well with level C at 612 kev. The 612 kev transition is placed as a transition from C to A for energy reasons. The coincidences observed between the 588 kev and 612 kev lines (31), (28), (30) place level G at 1201 kev. The 602 kev transition is placed between levels E and B for energy reasons. Levels F and H are fixed by the energies of the other observed gamma radiations (27). The fact that the energies for all the transitions fit so well is an indication that the decay scheme is correct.

---

[4] With sufficiently high resolution the differences in the binding energy of the K electrons in platinum and osmium may be observed.

Relative Intensities of Gamma-Rays are Given in Parentheses. Energies are in kev. Spin and Parity Assignments are Indicated. The Scheme is Based on Work Done by Baggerly et al (28).

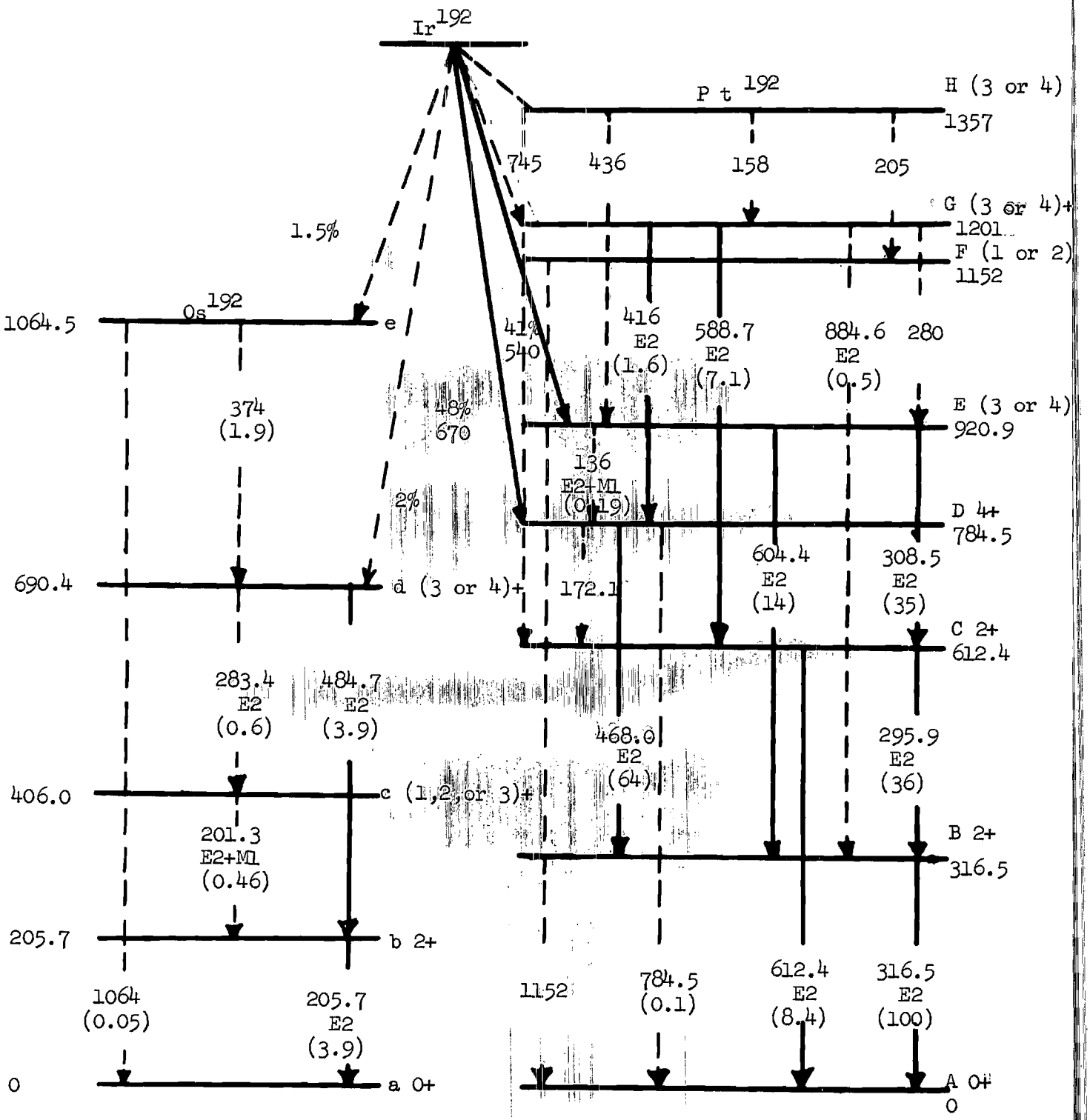

Figure 1. Decay Scheme of Ir^{192}

Os^{192} branch.--Coulomb excitation of natural osmium has revealed two deexcitation peaks - one at 155 kev due to Os^{188} and a broad peak at 200 kev (32). It seems likely that either the 201 kev or 205 kev transition is the ground-state transition. From internal conversion data it appears that the 201 kev line is a mixture of M1 and E2 while the 205 kev line is pure E2. Therefore, the 205 line must be the ground state transition (see Appendix A) (28). The other levels were placed as shown for energy reasons, and the ordering of the 283 kev and 201 kev lines is arbitrary on the basis of existing data (28).

The beta radiations accompanying the decay have not been studied as comprehensively as have the gamma radiations. Several investigators have measured the end point energy of the most energetic beta group (33), (34), (35), and their results are in good agreement. The energies and intensities of the remaining groups as shown in Fig. 1 were determined by Baggerly et al (28) by studying the total intensity of the gamma radiations into and out of the various levels. Using these intensities and energies Baggerly et al have shown that the transitions to levels D, E and G are probably first forbidden.[5]

The spins and parities of the energy levels as shown in Figure 1 were determined as follows: Pt^{192} and Os^{192} are both nuclei which have an even number of protons and neutrons. An empirical rule of nuclear systematics states that all even-even nuclei have ground state spins of zero and even parity. The internal conversion coefficients of

---

[5]Baggerly et al have calculated the log ft values of the beta transitions to levels D, E and G. Their calculations give values of 8.3, 8.1 and 8.1 respectively which indicate first forbidden transitions (See Appendix A).

the more intense gamma rays have been measured by Baggerly et al (28). From these measurements they were able to assign the dominant multipolarities to many of the transitions. These multipolarities then delimit the spins of the levels. Since the 316, 205, and 612 kev transitions are dominantly E2, and since they proceed to a state of spin zero, the spins of states B, C, and b are taken to be 2 and the parities even. Several investigators have studied the angular correlation between the 468 and 316 kev transitions in order to determine the spin of level D (26), (28), (30), (3). Their results are in good agreement and indicate that a spin of 4 is correct for this level. Even parities are assigned to levels D, E, G, e, and d on the basis of the dominantly E2 nature of the transitions (28). Baggerly et al (28) assign a spin of 4 to level G on the basis of angular correlation measurements for the 589-612 kev cascade; however, no data are given. Kelley and Wiedenbeck (30) also examined this correlation but do not interpret the data as fixing the spin at 4. The spin of level G must be considered in doubt. Since level G decays to levels D (spin 4) and C (spin 2) primarily by E2 transitions, its spin must be 2, 3 or 4. Certain beta decay arguments[6] further delimit its spin to either 3 or 4. Also the spins of levels E and d may be delimited to either 3 or 4 by beta decay arguments (28). The fact that the beta transitions are first forbidden fixes the parity of the Ir^{192} nucleus as odd. First forbidden beta transitions proceed to levels of spin 3 or 4 (levels D, E, G) but not to levels of spin 2 (levels B, C); therefore, the spin of Ir^{192} is probably 5 or 6 (28).

---

[6] The beta decay arguments mentioned here and in the following are discussed in Appendix A.

Purpose of This Research

The spins of levels E, G, and d and the ground-state spin of Ir^{192} were in doubt. The purpose of this research was to determine these spins and to add evidence in support of the decay scheme.

The level spins have been determined by gamma-gamma angular correlation techniques, and in each of the above mentioned cases a definite spin has been assigned. Some beta-gamma angular correlation data have been obtained, and in the course of the experiments certain facts supporting the decay scheme have been verified.

CHAPTER II

INSTRUMENTATION AND EQUIPMENT

The equipment used for this research was standard scintillation spectrometers with a coincidence circuit permitting the study of coincidences between radiations of selected energies. The method used is, in principle, similar to that used at Oak Ridge by McGowan (37). A block diagram of the apparatus is shown in Fig. 2. Most of this apparatus had already been constructed when this research began; therefore, the discussion of the construction and operation of the equipment is very brief.

The detectors used are of two types. For gamma-ray detection, the counters consist of cylindrical sodium iodide (thallium activated) crystals coupled to Dumont 6292 or RCA 6655 photomultiplier tubes by the use of Dow Corning high vacuum grease. The crystals are available commercially from Harshaw Chemical Company and are approximately 1 1/2 inches in diameter and 1 inch thick. The photomultiplier tubes are surrounded by magnetic shields to reduce effects due to the magnetic field of the earth and other stray magnetic fields.

For electron detection, the counter consists of a cylindrical anthracene crystal coupled through a lucite light piper to a photomultiplier tube by the use of Dow Corning high vacuum grease. The light piper is 1 inch in diameter and 1 inch high. The anthracene crystal is 1 inch in diameter and 3 mm thick. It was calculated that this thickness was the minimum required for total absorption of electrons in the energy

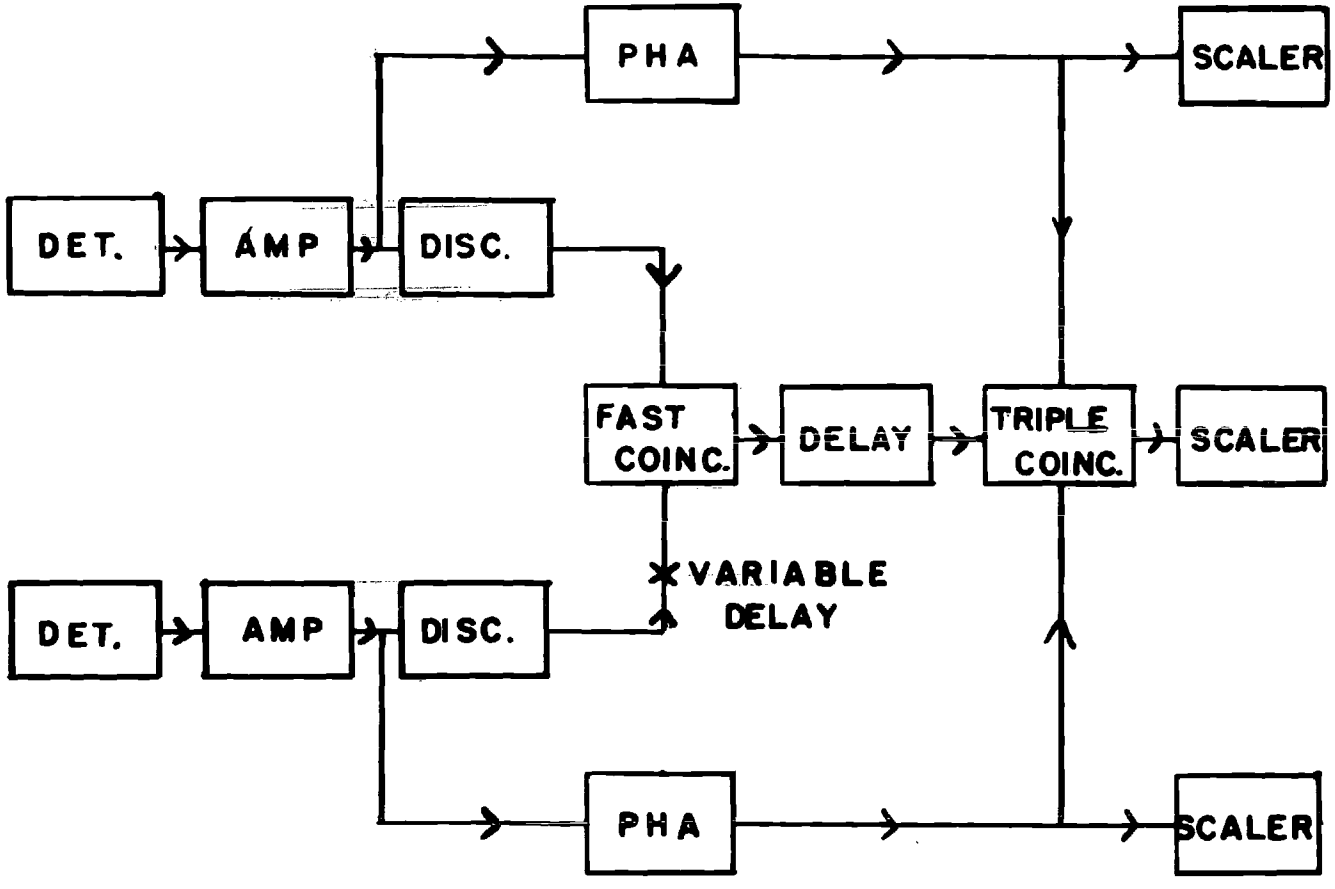

Figure 2. Block Diagram of the Apparatus

range of interest. An increase in the thickness of the anthracene crystal increases the gamma-ray efficiency of the detector which is undesirable. A thin aluminum foil, 0.2 mils thick, is placed over the section of the crystal into which the electrons enter for the purpose of reflecting light pulses back into the crystal. A photograph of this electron counter, disassembled, is shown in Fig. 3. The electron counter and source are both mounted within a vacuum chamber for electron work. A vacuum chamber is used to reduce scattering and energy degradation of the electrons. O-rings (supplied by Goshen Rubber and Mfg. Co., Goshen, Indiana) and Apiezon Q sealing compound (supplied by James G. Biddle Co., Philadelphia, Pennsylvania) are used as vacuum seals, and the chamber is evacuated by a Welch Duo-Seal vacuum pump.

A photograph of the detectors as set up for gamma-gamma angular correlation work is shown in Fig. 4. One gamma counter is fixed, and the other gamma counter may be rotated in a circle about the source in order to obtain data at different angles. For electron-gamma angular correlation experiments, the fixed gamma counter is replaced by an electron detector, and a vacuum chamber is necessary.

During the first part of this work regulated rectifier high voltage power supplies were used; these were replaced by battery supplies containing eleven 90 volt and two 67 1/2 volt batteries. The following potential differences were applied between the various electrodes of the photomultiplier tube: cathode and first dynode - 180 volts, first dynode and second dynode - 135 volts, other successive dynodes - 90 volts. A cathode follower arrangement is used to feed the signals from the photomultiplier to the amplifier.

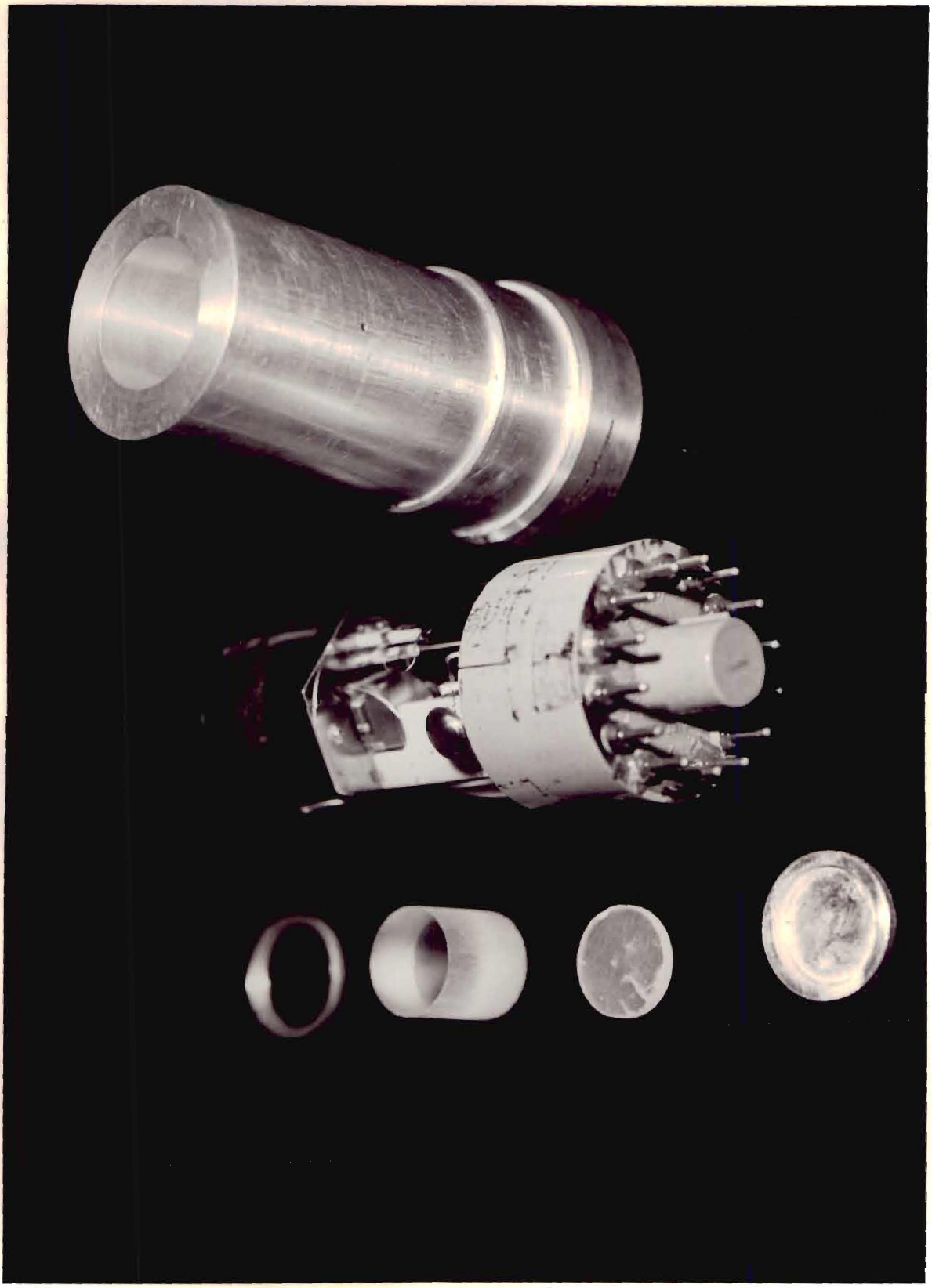

Figure 3. Photograph of the Electron Counter

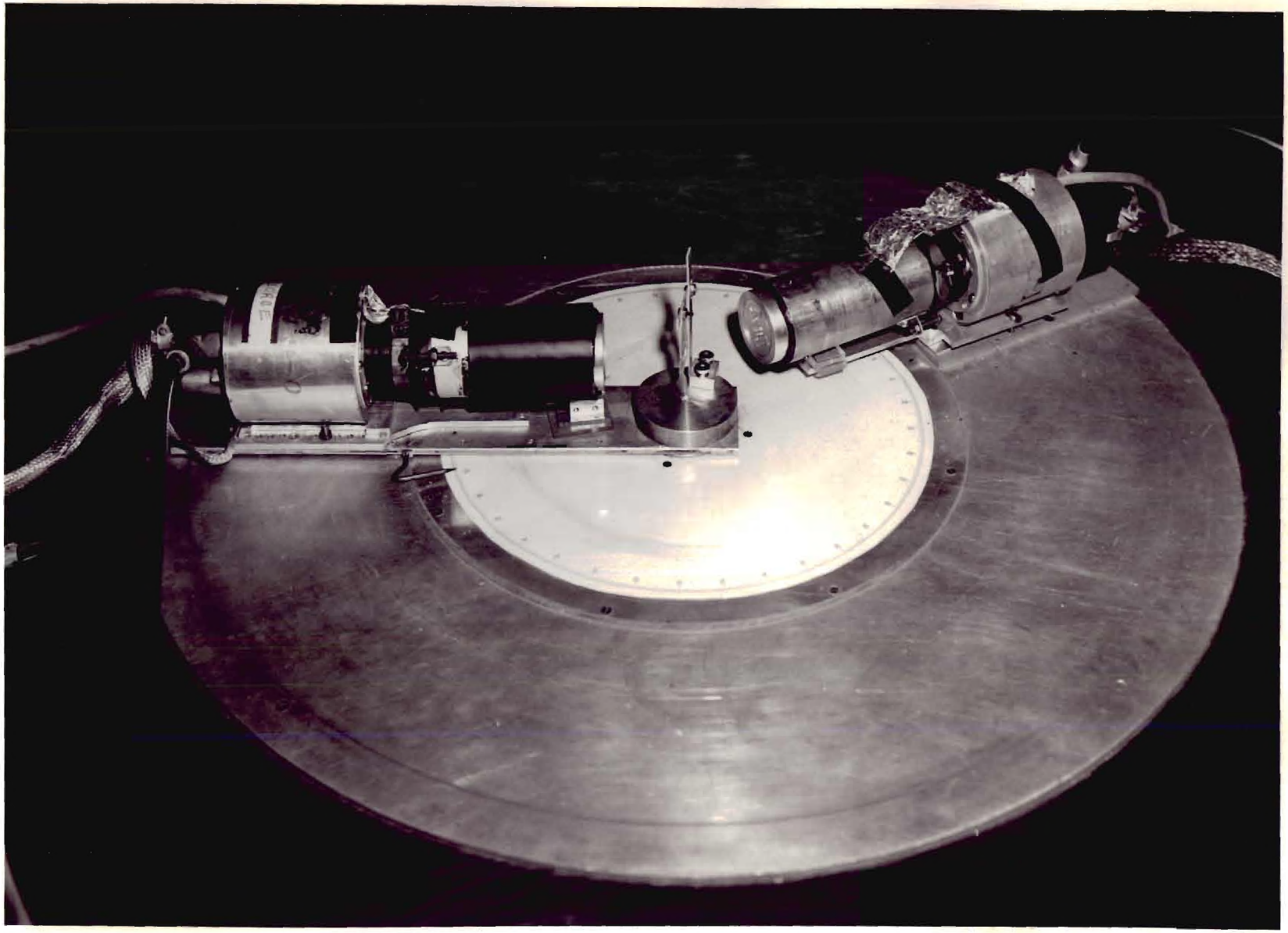

Figure 4. Photograph of the Detectors During a Gamma-Gamma Angular Correlation Experiment

The amplifiers are Atomic Instrument Company amplifiers Model 204B modified slightly to improve overload characteristics by insertion of crystal diodes in some of the grid circuits to remove overshoots. The discriminators shown in Fig. 2 are the integral discriminators in the Model 204B amplifiers.

The pulse height analyzers are Atomic Instrument Company single channel differential analyzers Model 510. The scalers are Atomic Instrument Company Model 1020A scalers. The variable delay shown in Fig. 2 is a lumped-parameter delay line with delays available from 0 to 0.90 microsecond in steps of 0.05 microsecond.[1]

The remainder of the apparatus represented in Fig. 2 is the coincidence circuit. A more detailed block diagram of this circuit is shown in Fig. 5. This coincidence method is essentially of the fast-slow type proposed by McGowan (37), (38). The particular circuits used are those discussed by Elmore and Sands (39), (40), and the circuit described here was designed and built by Dr. C. H. Braden and Dr. L. D. Wyly.

The operation of the coincidence circuit may be described as follows: the pulses from the discriminators[2] in the Model 204B amplifiers are fed into the input pulse shortner. At this state, after some amplification, the pulse is shaped by a shorted delay line (41). The length of this delay line determines the width of the pulse and thereby the resolution of the fast coincidence circuit. The fast coincidence circuit

---

[1]This variable delay was produced by Tel Instrument Company, Paterson Avenue, East Rutherford, New Jersey.

[2]The amplitude of pulses from the discriminators is independent of the amplifier output pulse.

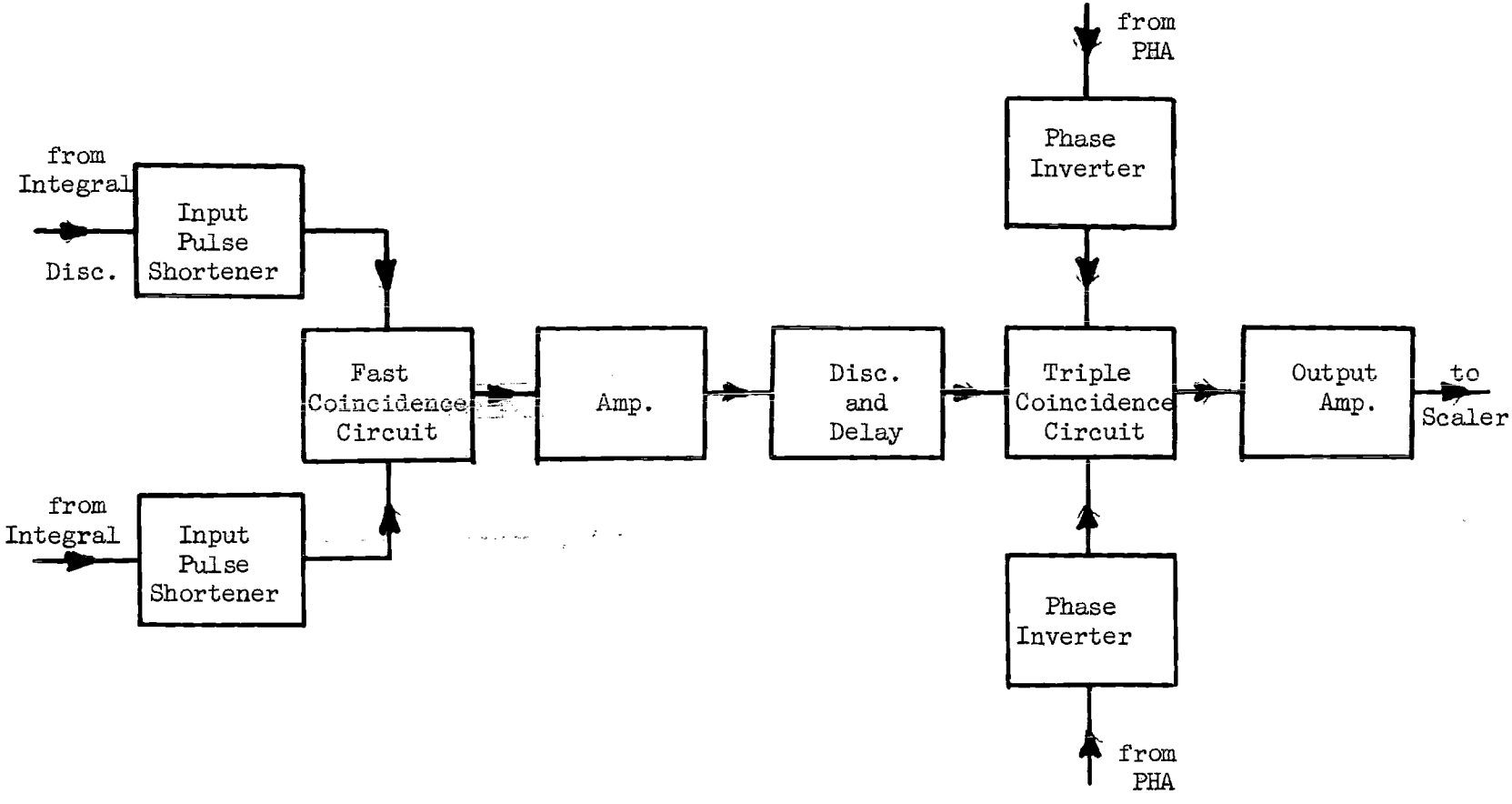

Figure 5, Block Diagram of the Coincidence Circuit

utilizes crystal diodes and was proposed by Elmore (40). The discriminator and delay is essentially a univibrator (39). The resolving time may be varied within limits by setting the bias of the input of the univibrator. A rheostat permits an accurate setting of this bias thereby giving a fine adjustment on the resolving time. It is necessary to delay the fast coincidence pulses to allow for the time required for the energy selected pulses to go through the pulse height analyzers; this delay is achieved by adjusting the time constant of the univibrator. The triple coincidence circuit receives two pulses from identical pulse height analyzers which are aligned in time with the fast coincidence pulse. This triple coincidence circuit is also a crystal diode circuit (39). Experiment shows that this circuit will operate with a resolving time as small as 80 milli-microseconds.

To be assured of the proper operation of the apparatus, it is necessary to consider two requirements which the circuits must satisfy. First, it must be ascertained that insertion of the variable delay into one channel actually does eliminate all real coincidences so that a determination of the resolving time[3] based on data taken with the delay in one channel is correct. In order to check this method of determining the resolving time, two independent radioactive sources, one for each counter, were used to measure the resolving time. If the sources are independent, all coincidence counts are accidentals and the resolving time may be calculated. The results of independent source measurements

---

[3]The resolving time, τ , may be calculated from the expression: accidental coincidence rate = $2\tau N_1 N_2$ where N_1 and N_2 are the counting rates of the two detectors.

and measurements based on the insertion of a delay are in agreement if delays greater than 0.20 microsecond are used.

Second, it is absolutely necessary to be sure that the coincidence circuit is aligned properly so that all of the real coincidences are counted. Due to the finite rise time of the pulse from the amplifiers the time alignment of the output pulse from the discriminator is a function of the amplitude of the amplifier output (or input) for a fixed discriminator trigger level. Therefore, the time alignment of a pulse appearing at the fast coincidence stage may be changed by varying the discriminator trigger level. This provides a fine adjustment for aligning two signals at the fast coincidence stage. A course adjustment for this alignment is provided by the variable delay in one of the channels. If both spectrometers are set on gamma-rays of a fixed energy which are in coincidence, then, by using these adjustments the coincidence rate may be maximized. This maximization process determines where the variable delay and discriminator trigger levels should be set for proper operation. Fortunately, the settings of the trigger levels are not critical. In fact, a change of 0.05 microsecond in the time alignment of the pulses at the fast coincidence stage only affects the coincidence rate by a small amount. However, a change of 0.10 microsecond eliminates almost all of the real coincidences. After the real coincidence rate is maximized, a pulser is connected to the two amplifiers; each gain is set to give the same size output as before, and the time alignment of the signals at the fast coincidence stage is checked with an oscilloscope triggered by the output of one of the amplifiers. This time alignment with the pulser in use is recorded and used to align the

equipment for further experiments rather than going through the process of maximizing the real coincidence rate. If one of the spectrometers is to be used to count radiations of varying energies, the pulser is used to determine the proper setting of the discriminator for alignment of the signals of different amplitudes at the fast coincidence stage.

CHAPTER III

EXPERIMENTAL PROCEDURE AND RESULTS

Gamma-Gamma Work

In essence three types of experiments were performed on the gamma rays following the decay of Ir^{192}. The three types may be called single spectra determination, coincidence spectra determination, and angular correlation experiments. The method of source preparation for these experiments is the same and will be discussed first; then the three types of experiments will be discussed. The major experimental tools used in the research are angular correlation measurements; therefore, the section describing angular correlation measurements is somewhat more detailed than the other two.

Source Preparation

The Ir^{192} was produced at the Oak Ridge National Laboratory by irradiation of iridium with thermal neutrons. Sources were prepared by evaporation of Na_2IrCl_2 in HCl solution on 0.25-mil rubber hydrochloride backing. In gamma ray work the thickness of the source is of little importance, so care was not taken to produce uniformly thin sources. The sources used were of the order of 0.9 cm. in diameter. The gamma-rays studied in this work showed no change in relative intensities over a period of one year, indicating that radioactive impurities are not present in appreciable quantities in the source.

Singles Spectra Determination Experiments

Although the intensities of the gamma radiations accompanying this

decay were fairly well known when this work began, there were no published results indicating how the spectrum would look when examined by a scintillation spectrometer. Therefore, the first data taken were to determine this gamma-ray spectrum. Good resolution requires the use of a very narrow window width (0.05 volts) on the pulse height analyzer. Furthermore, the counting intervals were short (10 sec.) in order to minimize the distortions that various instabilities (in power supply, amplifier, pulse height analyzer base line and window width) would cause. Under these conditions the detector gave a resolution of approximately 9 per cent and a peak to valley ratio of 34 to 1 as measured using the 661 kev gamma rays of Cs^{137}.[1] A number of these singles spectra have been taken at different times with essentially the same results.

Figure 6 shows a typical plot of the gamma spectrum obtained. Data were taken above 700 pulse height divisions, (above 700 kev), and evidence for a peak was found; however, the counting rate was so low that these gamma-rays could not be used in coincidence experiments. Therefore these high energy radiations will not be discussed. In order to interpret this spectrum it is necessary to understand the response of a scintillation spectrometer to a monoenergetic gamma-ray. Bell (42) has discussed very carefully the various factors influencing the response of a scintillation counter. Gamma-rays interact with a phosphor by three major processes - Compton scattering, photoelectric effect, and pair production. Pair production requires at least 1.02 mev of energy, and since none of the radiations observed in Ir^{192} have this much energy,

---

[1] Resolution is defined as the full width (in pulse height analyzer divisions) at half maximum divided by the pulse height analyzer reading at the maximum. The peak to valley ratio is the counting rate at the peak divided by the rate obtained in the valley on the low energy side of the photoelectric peak.

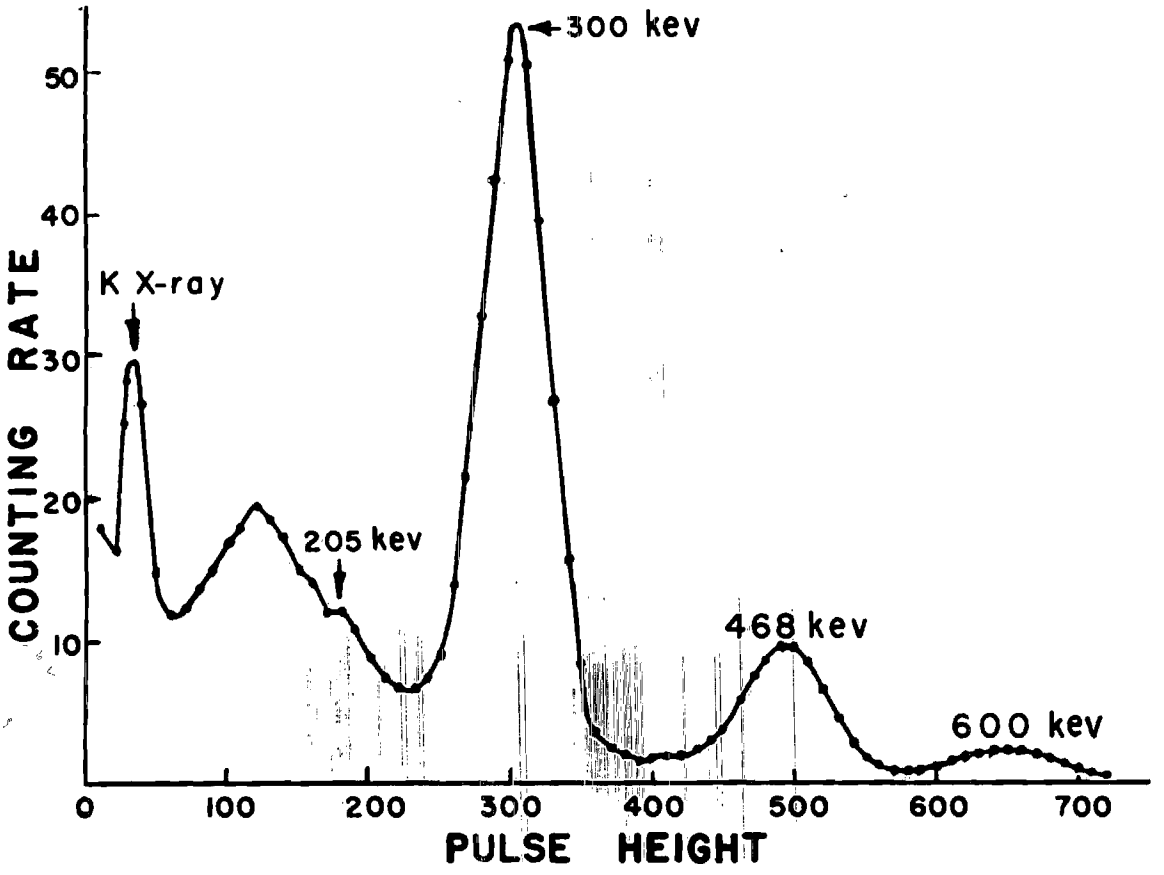

Figure 6. Gamma-Ray Singles Spectrum of Ir^{192}

this process will not be considered. In the photoelectric effect the gamma-ray produces a photoelectron which is absorbed in the crystal. This effect usually gives a pulse corresponding to the total energy of the gamma-radiation. When the photoelectric effect takes place in the crystal an X-ray is produced. This X-ray may or may not be absorbed in the crystal. If it is not absorbed a pulse corresponding to an energy lower than the gamma-ray energy results. Such pulses form what are known as escape peaks. The Compton process transfers some of the gamma-ray energy to an electron which is absorbed and leaves the remainder as a scattered photon which may or may not be totally absorbed. If absorbed the full energy is again realized. If not absorbed this process then yields a pulse which may correspond to something less than the total energy of the gamma radiation. It may easily be shown that if the Compton scattered photon escapes from the crystal a continuous distribution of pulses corresponding to energies between

$$E = \frac{2E_\gamma^2}{M_o c^2 + 2E_\gamma}$$

and E = 0 is obtained, where E_γ is the energy of the incident radiation in kev and $M_o c^2$, the rest mass energy of the electron, is 511 Kev. The most likely occurrence is for

$$E = \frac{2E_\gamma^2}{M_o c^2 + 2E_\gamma} .$$

In general, if a monoenergetic gamma-ray of less than 1 Mev is examined by a scintillation spectrometer the following are observed (42): A large peak corresponding to the incident gamma-ray energy (the photo-

electric peak plus multiple processes leading to total absorption of the radiation), a continuous distribution corresponding to the Compton distribution as described above and perhaps a small peak superimposed on the Compton distribution at $E = \frac{E_\gamma}{1 + 2E_\gamma / M_o c^2}$ due to backscattering of the gamma-ray from some of the nearby apparatus.[2]

Keeping these facts in mind it is possible to interpret Fig. 6. The three highest energy peaks are photoelectric peaks due to the 600 kev group of lines, the 468 kev (and 485 kev) line, and the 300 kev group. The difference in peak heights as shown in Fig. 6 is due to the actual differences in intensities of the radiations and also to the decrease in crystal detection efficiency with increasing energy. The interpretation of the lower energy distributions is somewhat more difficult. The sharp peak observed at a low energy is due to the K X-rays arising from the K capture decay of Ir^{192} into Os^{192} and to K X-rays occurring when internal conversion takes place in either the Os^{192} or Pt^{192} branch. Calculation shows that the Compton edges of the 600 kev, 468 kev, and 300 kev lines are at 421 kev, 303 kev, and 162 kev respectively. The backscatter peaks of the 600 kev, 468 kev and 300 kev lines should lie at 179 kev, 166 kev, and 138 kev respectively. By making a straight line energy calibration using the 600 kev, 468 kev, 300 kev, and K X-ray peaks as calibration points, it appears that the unresolved

---

[2]The expression for the energy of the degraded photon in a Compton process, $E_{\gamma'}$, is given by

$$E_{\gamma'} = \frac{E_\gamma}{(1 + E_\gamma/M_o c^2)(1 - \cos\phi)}$$

where ϕ is the angle between the incident photon direction and the scattered photon direction. For backscattering $\phi = 180°$, and

$$E_{\gamma'} = \frac{E_\gamma}{1 + 2E_\gamma/M_o c^2} .$$

peak appearing in Fig. 6 just below 200 pulse height divisions is at approximately 205 kev, and that the sharp peak at 120 pulse height divisions is at approximately 136 kev. Since none of the Compton edges or backscatter peaks as calculated above occurs at 205 kev it appears fairly certain that the unresolved peak at 205 kev is due primarily to the 205 kev gamma-ray in Os^{192}. The peak at 136 kev is probably due to a composite of the 136 kev gamma line in Pt^{192} and the backscatter peak of the 300 kev group, but it is believed to be mainly due to the backscatter peak.

Since this work on the single spectrum was completed, a report of work done with scintillation counters on Ir^{192} has been published by Kelley and Wiedenbeck (30). The spectrum shown by them is almost identical to the one shown in Fig. 6. Kelley and Wiedenbeck have interpreted all the features of the spectrum except the peaks at 136 kev and 205 kev. Their interpretations of all the other features of the spectrum are in agreement with the ones discussed above.

Coincidence Spectra

In order to determine which gamma-gamma angular correlations were feasible it was necessary to do considerable coincidence work. This type of study enables one to determine what sort of coincidence rate may be expected and also enables one to evaluate the effect other gamma-ray cascades have on the one of interest. Furthermore, sometimes coincidence curves show up gamma transitions which cannot be observed on the singles spectrum.

In general, to take a coincidence spectrum, one of the scintillation spectrometers is set on a certain gamma radiation and then all or part of the gamma spectrum is swept with the other spectrometer.

Data are taken in sufficiently long time intervals to assure satisfactory statistics. In order to obtain coincidence data as rapidly as possible it is necessary to place the scintillation detectors as close as possible to the source and to use a strong source. The strength of the source which can be most efficiently used is determined by the resolving time of the apparatus. With this apparatus resolving times as small as 80 milli-microsecond may be used. If one attempts to operate with shorter resolving times, the real coincidence rate begins to decrease thereby indicating that the apparatus is not counting all the real coincidences. The resolving time determines the number of accidental coincidences which will be counted, and hence, in general one operates with as short a resolving time as possible. For a fixed resolving time one can show that an increase in the source strength beyond a point which gives approximately equal numbers of reals and accidentals is not profitable[3] (43).

Figure 7 shows plots of several of the coincidence spectra. In all cases the fixed energy spectrometer used as wide a window as possible to include most of the line in question but not to include counts from other transitions. The spectrometer which was used to sweep the spectrum had as narrow a window as possible in order to improve the energy resolution. In general, the counting intervals were of the order of 10 or 15 minutes at each point, and the points were taken sufficiently close together to show up all peaks. The method by which the date were analyzed is discussed in Appendix B.

---

[3]As the source strength, S, increases the number of accidentals increases as S^2 while the number of real coincidences increases as S. See Appendix C.

Figure 7a shows the coincidence spectrum with the 468 kev line. Comparison of the spectrum with the decay scheme shows that peaks occur at the proper places in all cases. In fact, the coincidence peak due to the 416 kev gamma line can be seen on the coincidence spectrum but not on the singles spectrum. Figure 7b shows the coincidence spectrum with the 600 kev group of lines. Again the spectrum agrees with the decay scheme in all cases if the line at 136 kev is interpreted as consisting, at least partially, of backscattering from the 300 kev lines. The coincidence spectrum with the 136 kev peak was examined briefly. The spectrum showed peaks at 136, 300, 468, and 600 kev but no indication of a peak at 205 kev. The fact that the 136 kev peak is in coincidence with itself indicated that a considerable portion is due to 300 kev backscattering, and therefore it did not appear worthwhile to examine it further. The absence of coincidences between the 136 kev peak and the 205 kev unresolved peak indicates that the 205 kev line may be in a different branch from the 300 kev lines. Therefore, the coincidence spectrum with the 205 kev line was taken from approximately 280 kev to 500 kev. The results are shown in Fig. 7c. The peak at 300 kev may be interpreted as due to the Compton distribution of the 468 kev and 600 kev lines lying under the 205 kev line;[4] the peak at approximately 470 kev must be due to the 485 kev-205 kev cascade in the Os^{192} branch since there is nothing at 205 kev which could be in coincidence

---

[4]The Compton edges of the 468 kev and 600 kev lines lie at 305 and 420 kev respectively. Therefore the counting rate of a spectrometer set at 205 kev will include counts from the 468 kev and 600 kev lines. These lines are in coincidence with the 300 kev lines; therefore, a coincidence peak is expected at 300 kev.

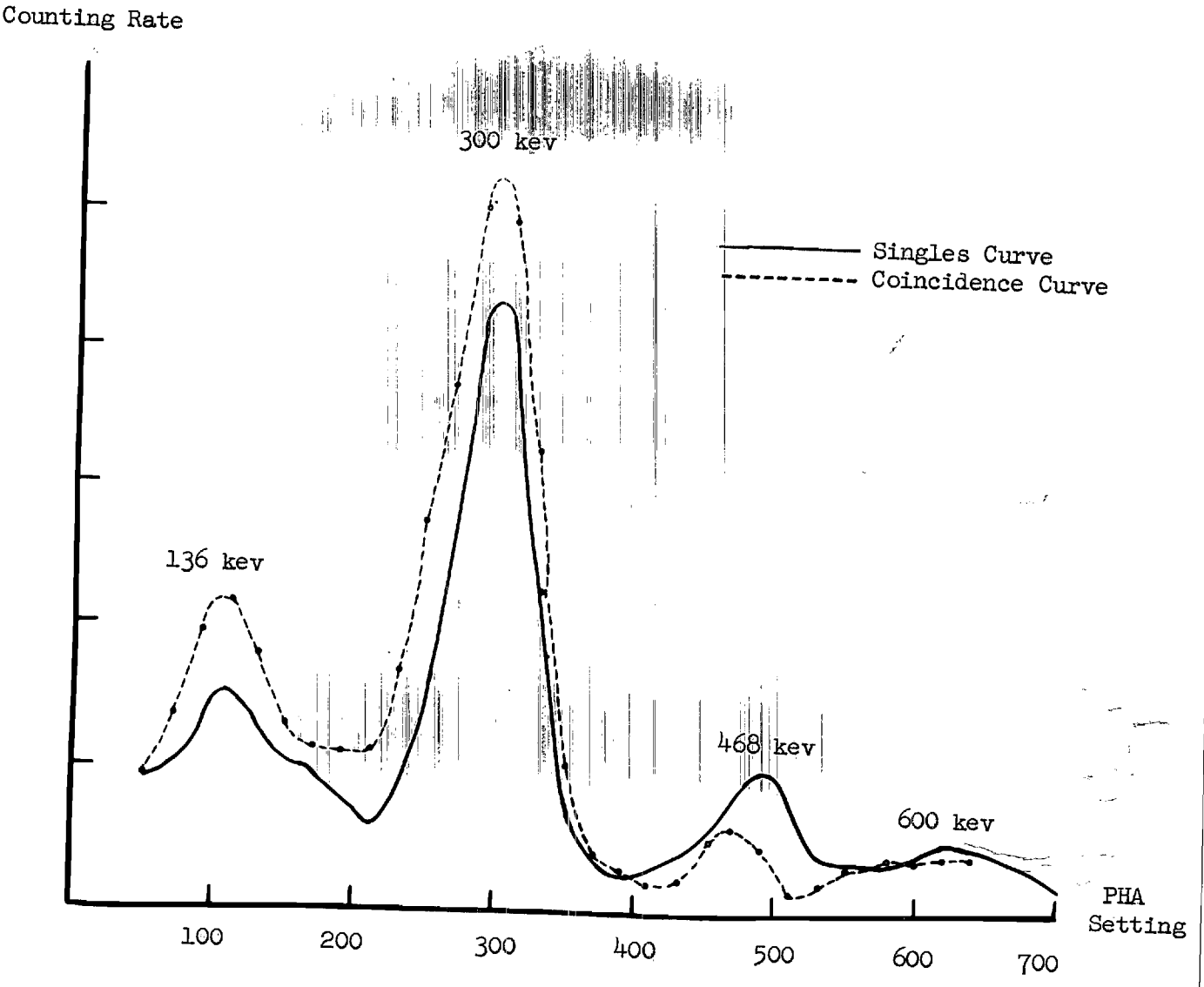

Figure 7a. Coincidence Spectrum with the 468 kev Gamma-Ray

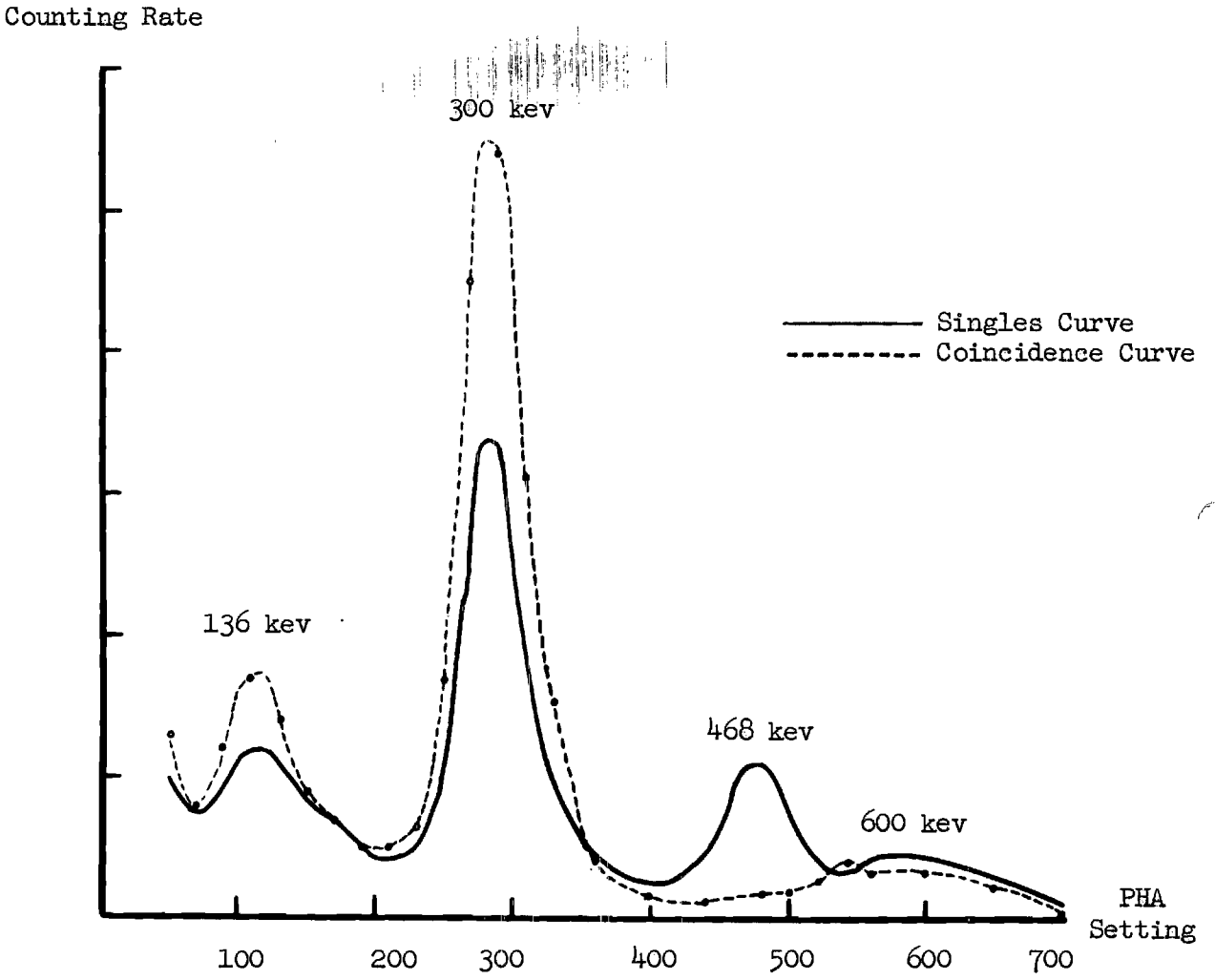

Figure 7b. Coincidence Spectrum with the 600 kev Gamma-Rays

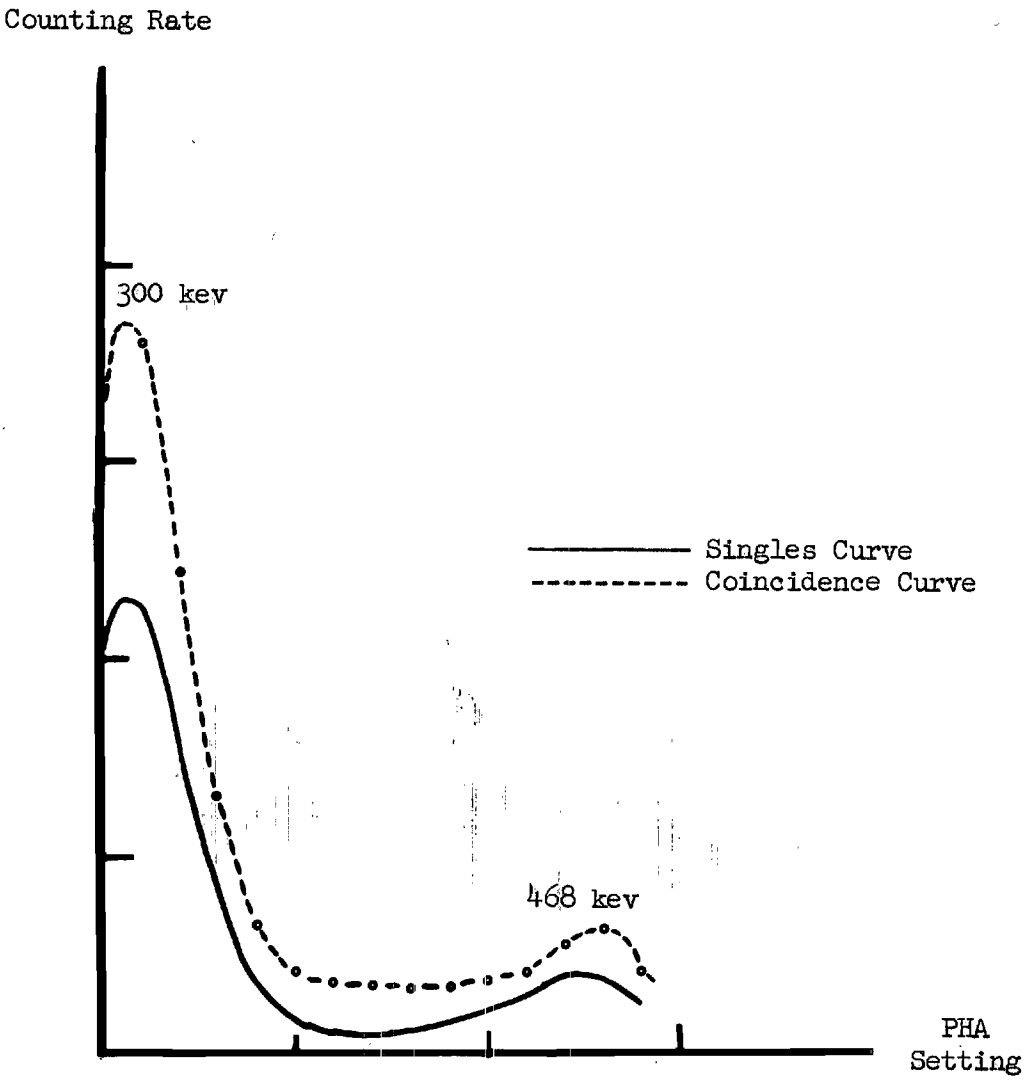

Figure 7c. Coincidence Spectrum with the 205 kev Gamma-Ray

with the 468 kev line in Pt^{192}. The K X-ray coincidence spectrum has been studied at this laboratory by A. L. Stanford and E. T. Patronis (44). Their results indicate coincidences between K X-rays and the 136 kev, 205 kev, 300 kev, and 468-485 kev lines. The coincidence peak at the 205 kev line is almost completely resolved and is a good indication that the 205 kev line is actually in the Os^{192} branch.[5] It should also be noted that a line at 374 kev as reported by Johns and Nablo (27) and Baggerly et al (28) was not detected in any of the above coincidence experiments.

Angular Correlation Measurements

The purpose of an angular correlation experiment is the determination of the correlation coefficients A_2, A_4, etc. Usually one is interested in only A_2 and A_4.[6] In order to determine these two coefficients it is necessary to take data at three angles - 90°, 135°, and 180°. The accuracy with which A_2 and A_4 are determined is dependent upon the number of real coincidences counted at each angle. For example, if 10,000 reals are counted at each angle, the counting statistics limit the accuracy of the coefficients to approximately two per cent. It is desirable to obtain data at all three angles if possible; if data are taken at only two angles, 90° and 180°, then

---

[5] K X-rays occur in the Os^{192} branch since it is formed from Ir^{192} by K capture. K X-rays also occur in the Pt^{192} branch due to internal conversion. Therefore, coincidences between K X-rays and all the gamma radiations are expected. Since the internal conversion coefficients are small most of the X-rays probably occur due to K capture, and therefore any Os^{192} lines should appear stronger on a K X-ray coincidence spectrum than on a singles spectrum.

[6] See Chapter V of this thesis. In almost all of the angular correlation experiments previously performed, it has been found that the data agree with theory if A_2 and A_4 are taken to be not equal to zero and higher order coefficients are assumed to be zero.

A_2 can be calculated only if an assumption is made as to the value of A_4.

The following is a brief discussion of the general problems which occur in all angular correlation experiments.

1. Number of Angles at Which Data Should Be Taken

Three angles are sufficient to determine A_2 and A_4; two are not. Therefore, data should be taken at three or more angles unless the counting rates are so low that the acquisition of these data would require an unreasonable amount of time, or unless the extra information gained is uninterpretable due to interference effects from other cascades. The three angles usually selected are 90°, 135° and 180°. As pointed out in Chapter V $W(\Theta)$ is a function of even order Legendre Polynomials; therefore, if data are taken at 270° and 225° the results must be the same as for 90° and 135° respectively. A further check of consistency is therefore obtained by taking data at the five angles 90°, 135°, 180°, 225° and 270°.

2. Source Strength

The source should be made of such strength that the ratio of real coincidences to accidental coincidences is approximately one or more.

3. Distance From Source to Detectors

The distance from source to detector determines the solid angle subtended by the detector. This solid angle determines the coincidence rate and the angular resolution of the apparatus. To increase counting rates the distance must be decreased; to improve angular resolution the distance must be increased. In general, the data may be corrected for the angular resolution of the apparatus; however, the correlation which

is observed experimentally before correction tends to be washed out as the angular resolution becomes worse, and therefore the detectors cannot be placed too close to the source.[7] A compromise between counting rate and angular resolution must be reached.

4. Minimization of Systematic Errors and Effects Due to Electronic Drifts

In order to minimize systematic errors, data are taken as follows: a count is taken at a given angle for only a relatively short period of time (10-15 min.), and then the apparatus is changed to a new angle. The order in which angular data are taken is systematic, e.g. 90°, 135°, 180°, 270°, 225° and 180°. Data are taken twice at 180° for a single time at each of the other angles to maintain the same statistics at the three independent angles - 90°(270°), 135°(225°), and 180°. The variable delay is inserted periodically to determine the number of accidentals, and during the course of a day accidental counts are taken at all angles. The fact that data are only taken in relatively short counting intervals minimizes effects due to electronic drifts since the spectrometer gain may be reset fairly often.

5. Ratio of Time Spent Counting Real to Time Spent Counting Accidental Coincidences

This problem has been solved from the point of view of obtaining the best possible statistics in the shortest period of time in Appendix C.

---

[7] Consider an angular correlation curve taken with infintessimal angular resolution. It is easy to determine the experimental curve which would be measured with a given finite angular resolution; as the solid angle is increased the experimental curve becomes more nearly isotropic. Even though in principle it is possible to work from an experimental curve to the theoretical curve if the angular resolution is known, in practice it often becomes impossible to do. For example, if the solid angle is so large that an isotropic curve is obtained, then it is impossible to determine the anisotropic correlation function.

The result is in such a form that the time ratio can be calculated from a knowledge of the real and accidental counting rates.

6. Centering of the Source

The source is centered by ascertaining that the singles counting rate of the movable counter is the same at all angles. The source need not be centered exactly since the method of analysis of angular correlation data as described in Appendix D corrects for small errors in source centering.

7. Analysis of the Data

A complete discussion of the analysis of the data is given in Appendix D. In general, the following adjustments in the coincidence data must be taken into account.

(a) normalization to the singles counting rates to correct for slight shifts in electronics and inexact centering of the source.

(b) normalization to take into account decay of the source

(c) correction for the accidental coincidences

(d) correction for the finite angular resolution of the apparatus.

Consideration of the coincidence curves shown in Fig. 7 indicates that the following gamma-gamma angular correlation experiments can be performed: 300-300 kev, 468-300 kev, 468-416 kev, 600-300 kev, 600-600 kev and 205-485 kev. Experiments utilizing the 136 kev peak were omitted since the interpretation of such experiments would be very difficult due to the backscattering present in this peak. The 300-300 kev cascade contains three component cascades - 316-308 kev, 316-296 kev, and 396-308 kev cascade. No serious effort was devoted to this correlation because its interpretation is almost impossible since the contribution

from each cascade is unknown. Table 1 (page 37) is a summary of the data obtained in each of the above experiments. This table contains the correlation coefficients (both uncorrected and corrected for geometry), the anisotropy ratio, the number of real coincidences upon which the data are based, and the ratio of real to accidental coincidences. The following is a discussion of the particulars of each correlation experiment.

468-300 kev correlation experiment.--This experiment was very easy to perform because the coincidence and singles peaks rise very high above the background and because the counting rates were high. The detectors were placed 7.6 cm. and 8.1 cm. from the source. It was decided to set on the high energy ride of the 300 kev peak in order to obtain mostly 316 kev gamma counts. Data indicated that the coincidence rate per singles count on the 300 peak was not dependent strongly upon energy if the counting rate was maintained near 60 per cent peak rate on the high energy side. The angular correlation was run with one detector set directly on the 468 kev peak and the other set on the high energy side of the 300 kev peak at a position where the singles rate was close to 60 per cent of the peak singles rate. Fifteen minute counts were taken at each of five angles (90°, 135°, 180°, 270°, 225°0 and approximately 1400 real coincidence were obtained for each fifteen minute interval. The results as shown in Table 1 agree with those previously reported by Taylor and Pringle (29), Baggerly et al (28), and Kelley and Wiedenbeck (30).

468-416 kev correlation experiment.--This experiment was much more difficult than the above for three reasons. First, the 416 kev peak

Table 1. Experimental Gamma-Gamma Angular Correlation Data

Cascade (kev)	Uncorrected For Geometry A_2	A_4	A	Corrected For Geometry A_2	A_4	A	Total Real Coincidences at 180° R	Ratio of Real to Accidental Rates R/c
600-300	-0.195	-0.01	-0.271	-0.21	-0.01(2)	-0.29(2)	10 000	3.5
600-600	------	-----	-0.01	-----	-----	0.01(2)	5 000	2.8
417-468	0.019	-----	0.032	0.021(2)	-----	0.04(2)	9 000	2.0
468-300	0.082	0.000	0.129	0.088(6)	0.00(1)	0.14(1)	22 000	3.7
470-205	------	-----	-0.161	------	-----	-0.19(2)	8 500	6.9

Statistical errors in the last digit quoted are given in parentheses.

could not be seen on the singles spectrum; second, the 416-468 kev coincidence peak did not rise very high above background; and third, the coincidence counting rate was low. In order to improve the coincidence to background ratio the detectors were placed 4.7 and 5.2 cm. from the source. One counter was set directly on the 468 kev peak; the other one was kept near 416 kev by keeping the singles counting rate at a fixed percentage of the peak rate. This percentage was determined so that the spectrometer would be set directly on the 416 kev coincidence peak. Data were taken in fifteen minute counting intervals at each of five angles. Approximately 100 real coincidences were obtained for each fifteen minute run. In order to estimate the effect of interference from other cascades, an angular correlation experiment between the 468 kev peak and the valley between the 468 and 300 kev peaks was performed. An anistropy of 0.034 was obtained based on 7000 real coincidences at each of two angles (90° and 180°). It was estimated that the effect of this background interference was sufficiently large to make the data on the 417-468 kev angular correlations uninterpretable. Therefore, the data on the cascade as shown in Table 1 lack significance.

600-300 kev correlation experiment.--This experiment was performed in such a way that most of the contribution came from the 604-316 kev cascade. The detectors were placed 8.1 cm. and 7.6 cm. from the source. One spectrometer was set with a narrow window on the high side of the 300 kev peak so that the singles rate was 88 per cent - 94 per cent of the peak rate; the other spectrometer was set with a wide window on the high side of the 600 kev peak so that the singles counting rate was 47 per cent - 57 per cent of the peak. Data were taken in fifteen

minute counting intervals at five angles. Approximately 200 reals were obtained during each counting interval. The interpretation of these data required consideration of the various interfering cascades and will be discussed completely in the next chapter.

600-600 kev correlation experiment.--The principal difficulty in this experiment was the very small counting rate. The detectors were placed 8.1 and 7.6 cm. from the source. Both spectrometers were set directly on the 600 kev peak with wide windows. Data were taken at only three angles in fifteen minute counting intervals. Approximately 100 reals were obtained during each interval. Since a contribution from coincidences with the 296+316 kev sum peak is possible, data were taken of counting rate versus distance of detector from source. These data and numerical estimates indicated that no more than 9 per cent of the coincidences are due to sum peaks.

485-206 kev correlation experiment.--The detectors were placed 4.8 and 5.2 cm. from the source. One spectrometer was set slightly on the high energy side of the 468 kev peak, and the other directly on the unresolved peak at 205 kev. Care was taken to exclude as much as possible of the contribution from the 175 kev Compton edge due to the 316 kev gamma radiation; however, this experiment still suffers from interference effects due to coincidences between the 468 kev line and the Compton edge of the 316 kev line.

Beta-Gamma Work

As was the case in gamma-ray work, three types of experiments were performed using beta rays. These three types may be called

singles beta spectra determination, beta-gamma coincidence spectra determination and beta-gamma angular correlation experiments. The same type of source was used for each of these experiments, and the source preparation will be discussed first, followed by a discussion of each type of experiment.

Source Preparation

The sources used in the beta ray work were prepared in a manner similar to that used for gamma-ray sources. However, care must be taken to make the source and its backing as thin as possible since scattering of the electrons causes energy degradation and will tend to decrease any angular correlation (45). The same backing as was used for gamma-ray sources was used. In Ir^{192} the specific beta activity is high, and it was easy to obtain sources which were not thick[8] and still were sufficiently active.

Singles Beta Spectra

Since the scintillation type beta ray counter which was used in this research is sensitive to both beta and gamma radiation, care must be taken to correct all data for the gamma rays which are counted in the beta ray detector. This correction is made by determining the counting rate when a lucite absorber of approximately 0.5 cm. in thickness is inserted between the source and beta detector. Lucite is used because it contains elements of low atomic number and therefore few secondary electrons, which would reach the crystal, are produced in the

---

[8] One small drop of solution was evaporated forming a deposit of approximately 0.28 cm^2 in area.

absorber by the absorption of gamma-rays. Calculation shows that 0.5 cm. is the minimum thickness of lucite which will totally absorb beta-rays of the energies present in the decay.

The singles beta spectrum of Ir^{192} was obtained by running the beta spectrometer over the entire energy range with and without the lucite absorber. Figure 8 shows a plot of the results obtained with and without the absorber and a plot of the beta-ray spectrum obtained by subtracting out the gamma-ray background. The energy resolution of the beta spectrometer was found to be approximately 16 per cent using the conversion electron spectrum of Cs^{137}. Because beta-rays form a continuous energy spectrum, energy calibration in beta-ray work is somewhat difficult. For this research, the conversion electron lives of Cs^{137} (627 kev) and Bi^{207} (976 and 481 kev) were used as energy calibration points. In order to obtain calibration points at lower energies the amplifier gain was cut in half giving points at 313.5, 488 and 240.5 kev. It was found that a straight line energy calibration fits all six experimental points very well. This method of energy calibration was used in all the beta-ray work. More careful study of the singles beta spectra is unfruitful because of the superposition of several different beta spectra.

Beta-Gamma Coincidence Spectra

In order to single out one beta group for study, beta-gamma coincidence techniques were used. These coincidence studies are performed exactly as gamma-gamma coincidence studies. The only new difficulty is correcting for the gamma radiation detected by the beta

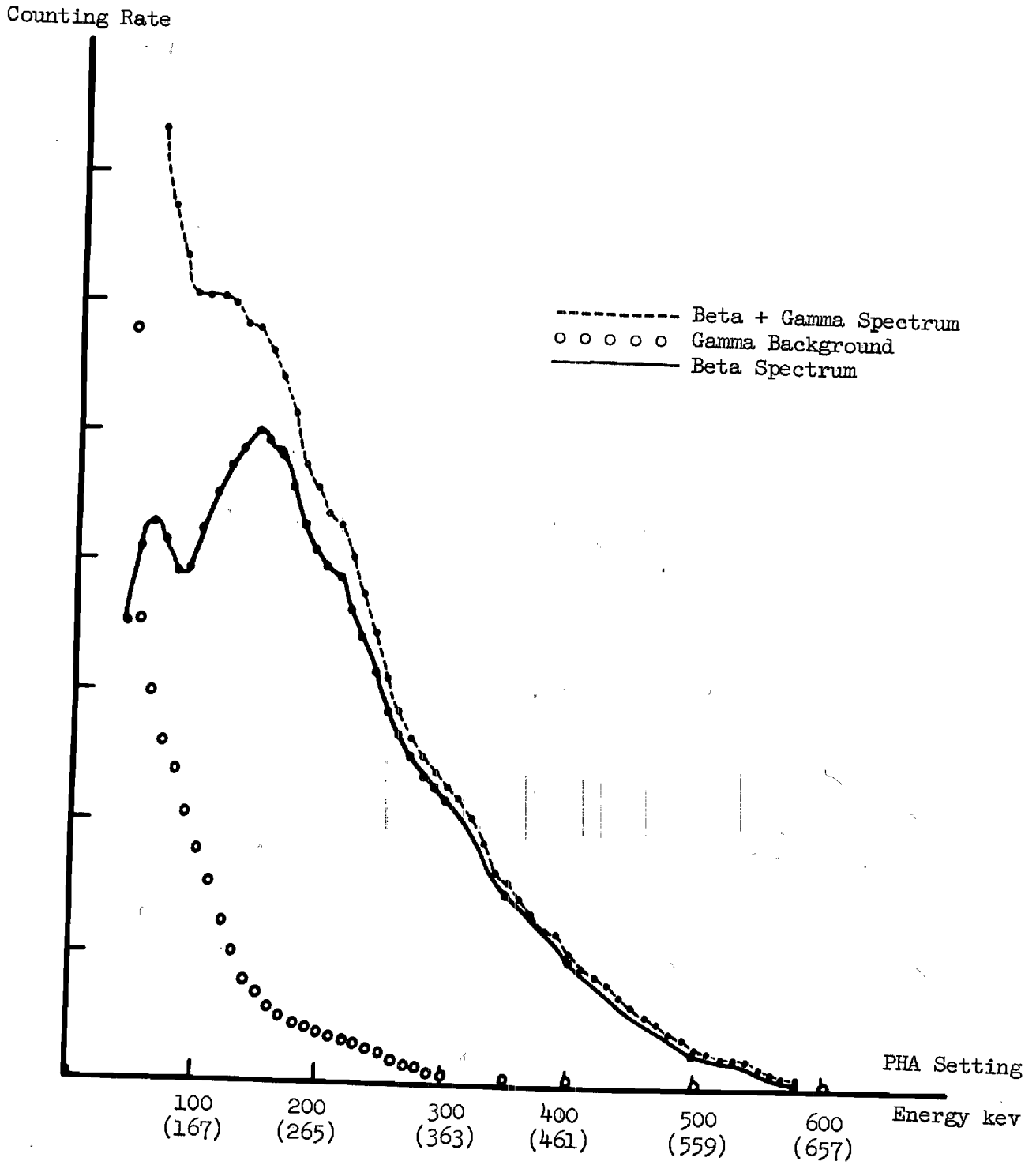

Figure 8. Beta-Ray Spectrum of Ir^{192}

counter. This leads to a certain gamma-gamma coincidence rate which must be subtracted along with the accidental rate from the observed coincidence rate. The correction is determined by periodic insertion of the lucite absorber and observation of the gamma-gamma coincidence rate. This rate is usually extremely low (below 5 real gamma-gamma coincidences per fifteen minute run) because the anthracene crystal used as a beta detector is thin and contains elements with very low atomic numbers.

Baggerly et al (28) have indicated the existence of three beta groups with endpoint energies of 670, 540 and 254 kev. The problem of electron scattering and its effect on angular correlation results grows progressively worse as the electron energy decreases; therefore, the low energy beta particles are not suitable for angular correlation studies unless extreme care is taken to secrue a thin source. Consideration of the decay scheme shows that the 670 kev beta group is in coincidence with the 468 kev gamma transition and that the 540 kev beta group is in coincidence with the 604 and 612 kev gamma lines; therefore, it appeared that angular correlation studies could be made of the 670-468 and 540-600 kev beta gamma cascades. In order to ascertain whether scattering in the source or the source backing was appreciable, coincidence studies of the 468 and 600 kev gamma-rays with the beta spectrum were made. The coincidence data are best presented in a Fermi plot. A discussion of this method of analysis is given in Appendix E. If the Fermi plot does not deviate from a straight line to any great extent, it is assumed that energy degradation of the electrons has not taken place and that the scattering of the source and backing is

negligible. One expects, therefore, to obtain Fermi plots which are very nearly straight in the higher energy region but begin to deviate from a straight line at lower energies due to scattering. The resulting Fermi plots obtained from coincidence studies of the 468 and 600 kev gamma-rays with the beta spectrum are shown in Figs. 9 and 10 respectively. From these figures one can see that the Fermi plots are reasonably straight over most of the energy range except near the beta group endpoint. The distortion near the beta group endpoint is due to the finite energy resolution of the beta spectrometer. This distortion can be corrected by an approximate method due to Owen and Primakoff (46); however, the method is not good if the beta spectrometer does not have excellent resolution. Since the energy resolution of a scintillation spectrometer is poor compared to a magnetic spectrometer, this correction has not been made. The uncorrected Fermi plots may be compared with numerous uncorrected Fermi plots for other decays in the literature (47) and in all cases the characteristic distortion near the beta group endpoint is present. The fact that the Fermi plots are reasonably straight in the region of interest indicates that energy degradation due to electron scattering is not appreciable.

Angular Correlation Measurements

From the beta-gamma coincidence data it appeared that angular correlation experiments between the 670 kev beta group and the 468 kev gamma-ray and between the 540 kev beta group and the composite 600 kev gamma line could be performed without scattering difficulties. The 670-468 kev correlation is particularly easy to study since there are

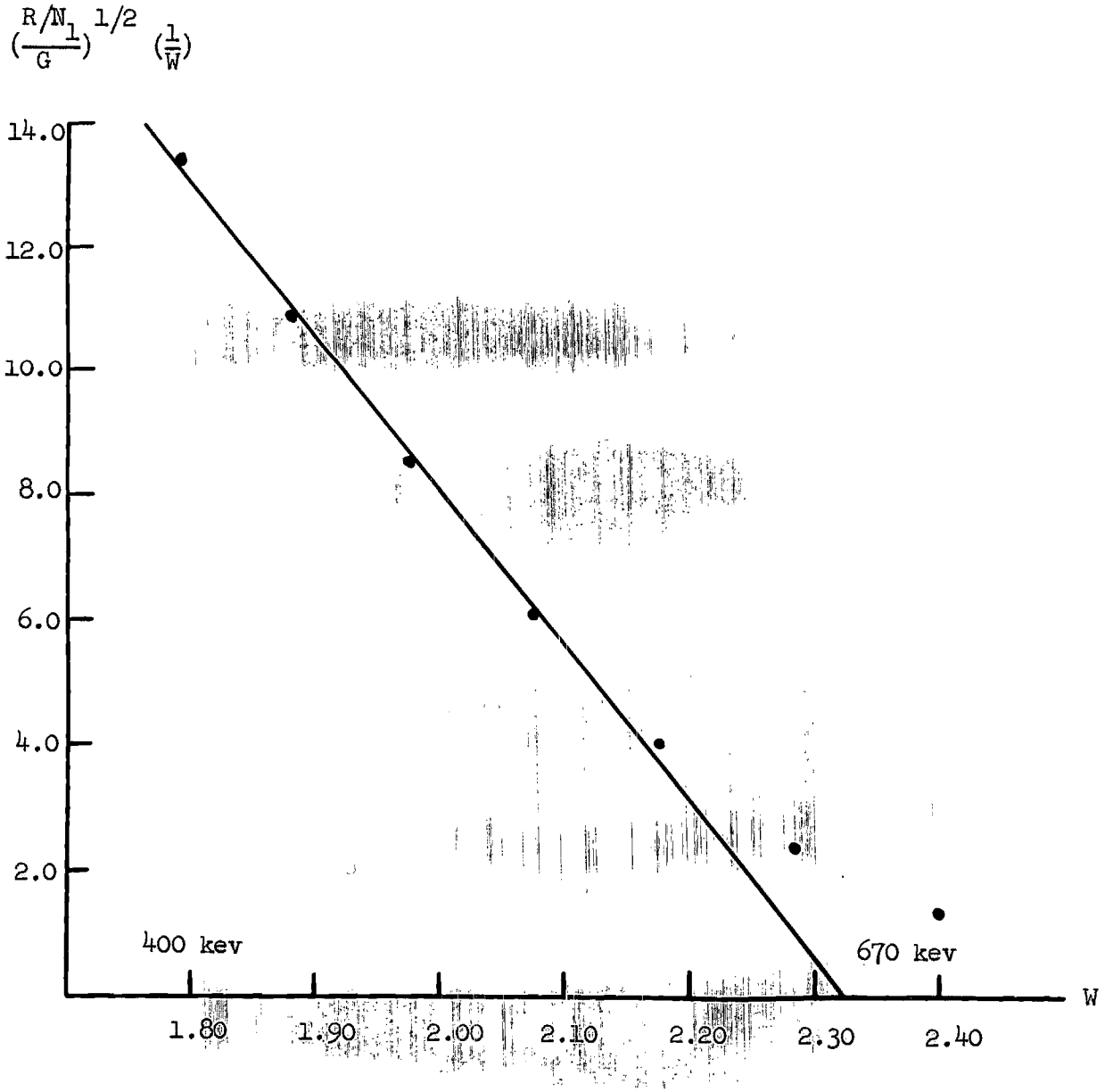

Figure 9. Fermi Plot of the Beta-Gamma Coincidences with the 468 kev Gamma-Ray

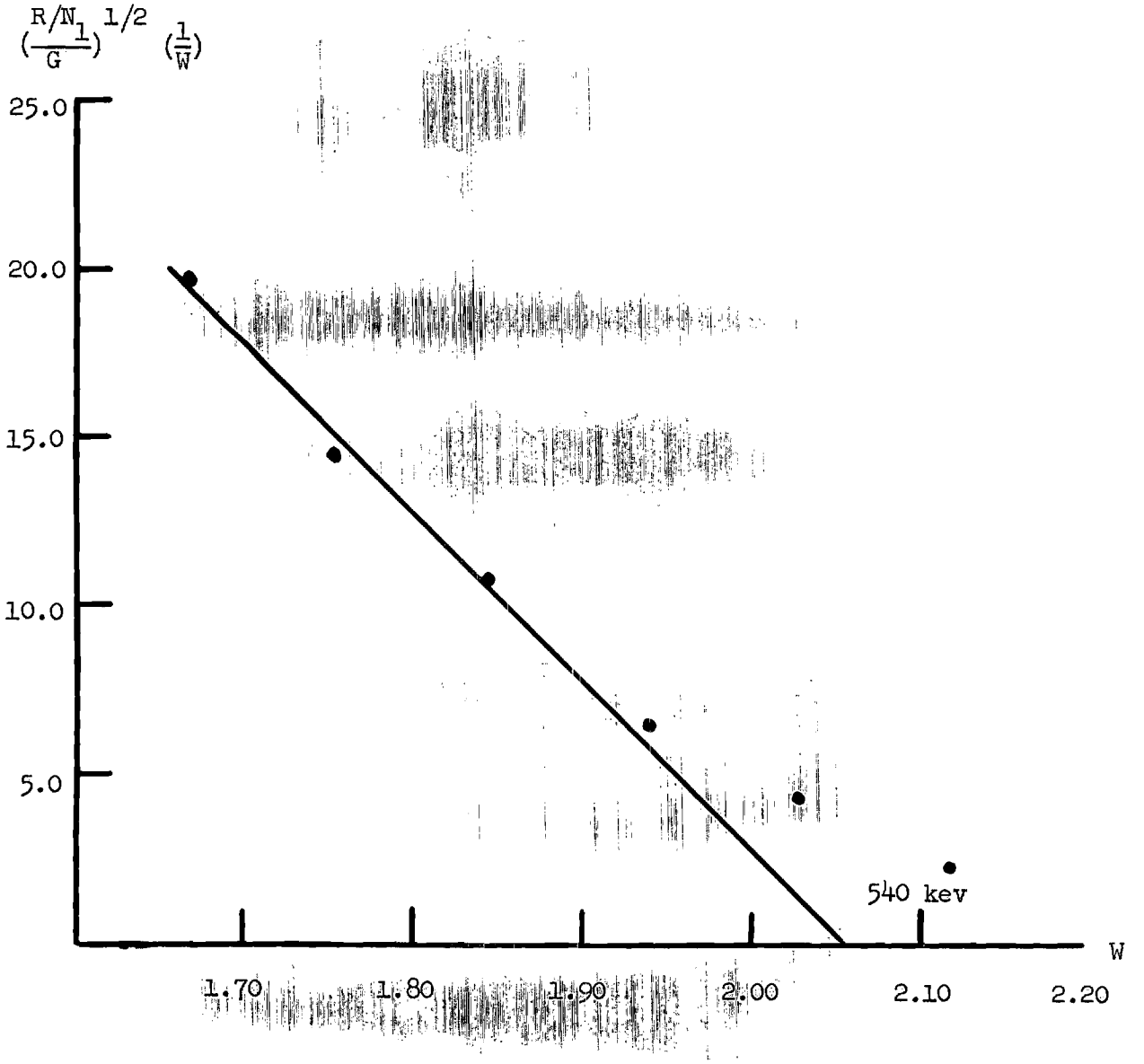

Figure 10. Fermi Plot of the Beta-Gamma Coincidences with the 600 kev Gamma-Rays

no complications from other beta-gamma cascades[10]. If the spin of Ir^{192} is five this correlation is isotropic, if the spin is six the correlation may be anisotropic (see Chapter IV); therefore, a study of this beta-gamma correlation is pertinent to a study of the spin of Ir^{192}. Furthermore if the correlation yields an anisotropic result, the results may be correlated with the matrix elements of the beta decay. The 540-600 kev correlation is much more difficult to interpret because of the complications arising from the coincidences between the 540 kev beta group and with both the 604 and 613 kev gamma lines. In this case if an anisotropic correlation results, one can say that the spin difference between the ground state of Ir^{192} and level E is greater than one (see Chapter IV).

The beta-gamma angular correlation experiments are performed in the same manner as are gamma-gamma angular correlation experiments. As in all beta decay work using scintillation detectors, one must make a correction for the gamma rays detected in the beta counter. The gamma-gamma coincidence rate was determined by insertion of the lucite absorber and was found to be very small (one gamma-gamma coincidence to several hundred beta-gamma coincidences). Since the gamma-gamma coincidence rate was so small, the angular correlation of the gamma-gamma coincidences need not be taken into account. The correlation function is a slowly varying function with respect to the beta particle energy having a maximum anisotropy at the beta group endpoint (4); therefore, it is

---

[10]The 468 kev gamma transition is not in coincidence with the 540 kev beta group except through the 136 kev gamma line which is very weak. Therefore, one may use beta energies below 540 kev and still have very little interference for other beta groups.

necessary to keep the beta-ray detector set accurately at the chosen energy. It is also desirable to set the beta spectrometer near the endpoint. The conversion lines of Cs^{137} and Bi^{207} were used as energy calibration points at the beginning and at the end of each run. The counting rate on the beta spectrum of Ir^{192} was kept constant during the course of the run by making small adjustments in the amplifier gain. If the calibration at the end of a run showed that the energy had not drifted more than 20 kev the data were regarded as valid; otherwise the data were discarded.

Angular correlation data were taken for the 670 kev beta group with the 468 kev gamma-ray by setting the beta spectrometer at approximately 550 kev with a window width corresponding to approximately 20 kev. The result was an almost isotropic distribution. Data were taken at a lower beta energy of approximately 420 kev and the same result was obtained. The angular correlation between the 540 kev beta group and the 600 kev gamma peak was measured by setting the beta spectrometer at approximately 450 kev with a window of approximately 30 kev. The result of this experiment was also an isotropic distribution. The results of these three beta-gamma angular correlation experiments are tabulated in Table 2.

Table 2. Experimental Beta-Gamma Angular Correlation Data

Cascade (kev)	Beta Energy (kev)	Uncorrected $N_{180°}$	Uncorrected $N_{135°}$	Total Real Coincidences at 180° R	Ratio of Real to Accidental Rates R/c	Ratio of Beta-Gamma to Gamma-Gamma Rates R/γ
670-468	550	1.016	1.012	10 260	6	(00)
670-468	420	1.008	1.026	10 054	8	200
540-600	450	0.971	-----	7 132	3	45

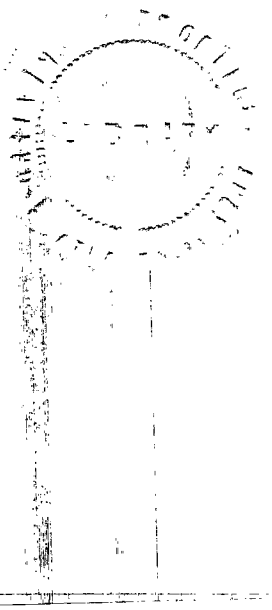

CHAPTER IV

CONCLUSIONS AND INTERPRETATION OF RESULTS

As was stated in the introduction, the main purpose of this research was to determine the spins of some of the energy levels involved in the decay of Ir^{192}. It should also be noted that this research lends support to the previously proposed decay scheme (28). All of the coincidence data, except for one discrepancy, can be interpreted using the existing decay scheme. In particular, the coincidences observed between the 468 kev and 416 kev, the 205 kev and 485 kev, and the K X-ray and 205 kev gamma radiations are original observations lending validity to the decay scheme. Also, the beta-gamma coincidence work showing coincidences between the 468 kev gamma and a beta group with endpoint near 670 kev and between the 600 kev gamma group and a beta group with endpoint energy of approximately 540 kev is strong support for the decay scheme. The strongest argument for the scheme is the fact that so much data, taken by many different investigators, is correlated by this decay scheme. The one discrepancy mentioned above is that in this research no evidence of a gamma line at 374 kev was observed either in singles or coincidence spectra. The fact that it is not visible in singles spectra is very likely due to its low intensity. The fact that no peak at approximately 374 kev was observed in coincidence with the 206 kev or a K x-ray line may also be due to low intensity; however, if the intensity of the 374 kev line as previously reported (27), (28), is correct a small coincidence peak should be observed.

Gamma-Gamma Correlation Experiments

The interpretation of the gamma-gamma angular correlation experiments is based on comparison of the experimental correlation coefficients, corrected for geometry, (tabulated in Table 1, Chapter 3) with the theoretical values as calculated by Biedenharn and Rose. Table 3 contains those theoretical coefficients and anisotropy ratios which will be useful for comparison purposes in the following discussion. The interpretation of each gamma-gamma angular correlation experiment will be discussed separately.

468-300 kev correlation.--Since the 468 kev gamma peak as observed in the singles spectrum is primarily composed of the 468 kev line[1] and since the 468 kev line is in coincidence only with one 300 kev line, the angular correlation measured is the correlation of the 468-316 kev cascade with very little interference from other cascades. This cascade connects levels D, B and A as shown in Fig. 1. As noted in the introduction, levels B and A have been assigned spins of 2 and 0 respectively; the 468 kev line is known to be very nearly pure E2; and the spin of level D is greater than one and less than five. Comparison of the corrected experimental coefficients with Table 3 (page 52) shows that the data are in agreement with a spin of four for level D and are in disagreement with spins of two or three. This interpretation has been given previously by Baggerly et al (28) and Kelley and Wiedenbeck (30).

600-300 kev correlation.--Consideration of the decay scheme shows that this correlation measurement contains contributions from four cascades - -

[1]Note that the other lines present in the 468 kev composite peak are weak. See Fig. 1, Chapter I.

Table 3. Theoretical Correlation Coefficients

Cascade	A_2	A_4	A
4(E2)2(E2)0	0.1020	0.0091	0.1095
3(E2)2(E2)0	-0.2041	-0.0815	-0.3335
2(E2)2(E2)0	-0.0766	0.3265	0.132

604-316 kev, 308-613 kev, 588-296 kev and 588-316 kev. In order to interpret these data it is necessary to estimate the contribution from each of these cascades. By using the intensities of the gamma transitions as given by Baggerly et al (28) and the measured resolution of the gamma spectrometers, curves were constructed which represented the composite 600 kev and 300 kev peaks. This was done assuming each gamma line yields a Gaussian distribution characterized by a peak height dependent upon intensity and width at half maximum dependent upon resolution of the spectrometer. From these curves it was estimated that the total coincidence rate was composed of the following: 604-316 kev (73 per cent), 308-613 kev (13 per cent), 588-316 kev (14 per cent), and 588-296 kev (<0.5 per cent).

The spin of level E is limited to values of two, three, or four by arguments which are similar to those applied to level D. If the spin is four then both the 604-316 kev and 308-613 kev cascades involve the same sequence of transitions - 4(E2)2(E2)0. Therefore, in this

case both cascades have the same correlation, and only 14 per cent of the total coincidence rate should be considered as interference. Comparison of the theoretical with experimental coefficients for this case indicates the spin of level E is not four. In fact the algebraic signs of the A_2 coefficients are different. The interference from the 588-296 kev cascade would not be expected to explain the large disagreement. If the spin of level E is either three or two, the possibility of mixing of magnetic dipole and electric quadrupole radiations must be considered for the transitions connecting levels E and B or levels E and C. In these cases if the mixing is different in the 604 kev and 308 kev line, then both the 588-296 kev and 612-308 kev cascades must be considered as interference. The data are in agreement with a spin assignment of three to level E if the 604 kev line is predominantly E2. Because of the interference it is not possible to be precise about the mixing ratio. Figure 11 shows graphs of A_2, A_4 and the anisotropy A versus δ^2, $(\delta^2 = \frac{\text{Intensity of E2 radiation}}{\text{Intensity of M1 radiation}})$, for the sequence 3(E2+M1)2(E2)0. From this graph it appears that the mixing of M1 in the 604 kev transitions is probably less than 5 per cent. If the spin of level E is taken to be two, the theoretical A_4 coefficient is much larger than the experimental A_4. Figure 12 shows plots of A_2, A_4 and the anisotropy A versus δ^2 for the sequence 2(E2+M1)2(E2)0. From this figure one sees that a very large mixing of M1, 50 per cent, in the 604 kev transition is required to obtain agreement between the A_4 coefficients. Baggerly et al (28) find these transitions to be predominantly E2; therefore, it seems very likely that the spin of level E is three.

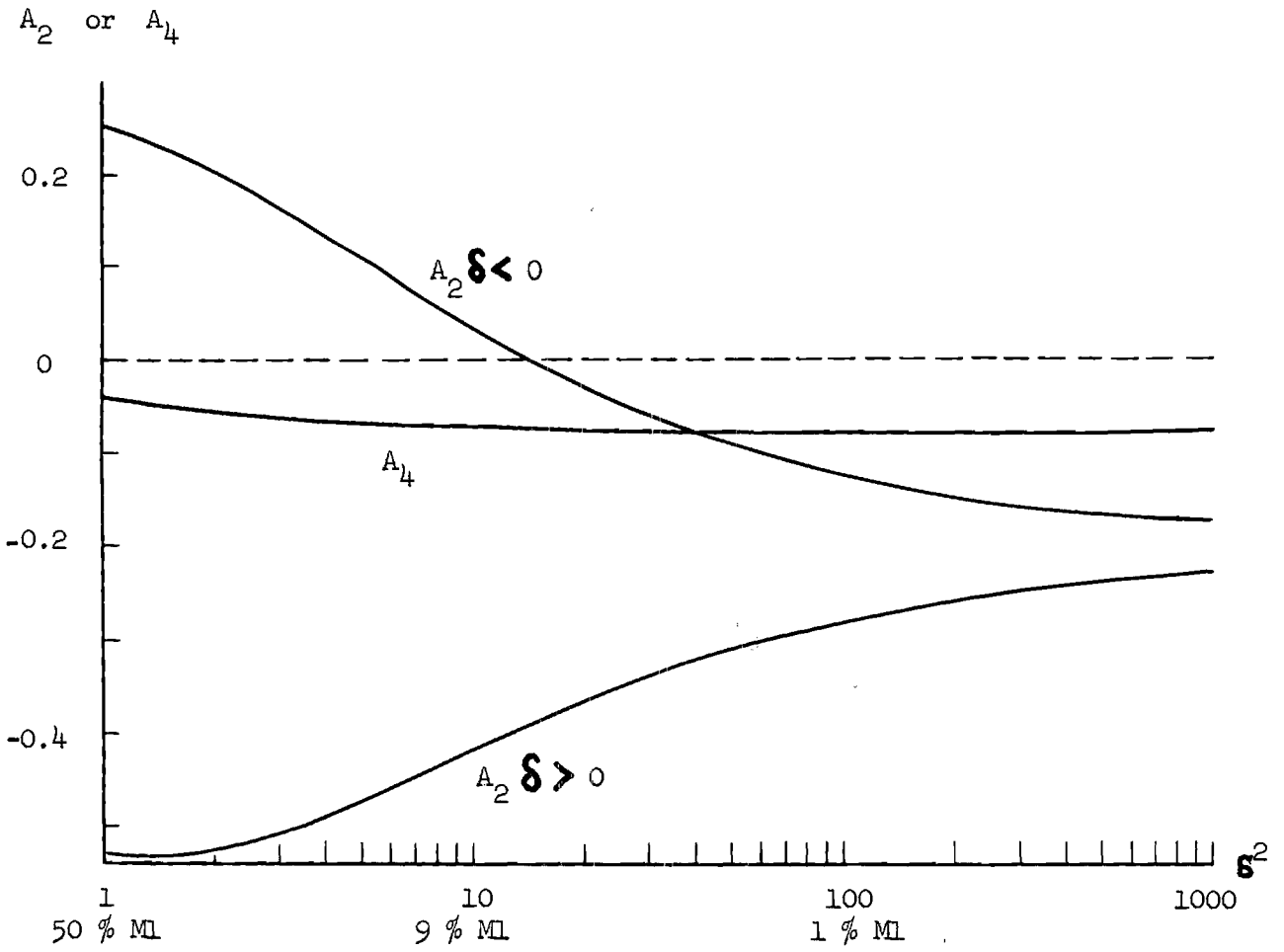

Figure 11a. Plot of the Theoretical Correlation Coefficients Versus the Mixing Ratio for the Sequence 3(E2+M1) 2(E2)0

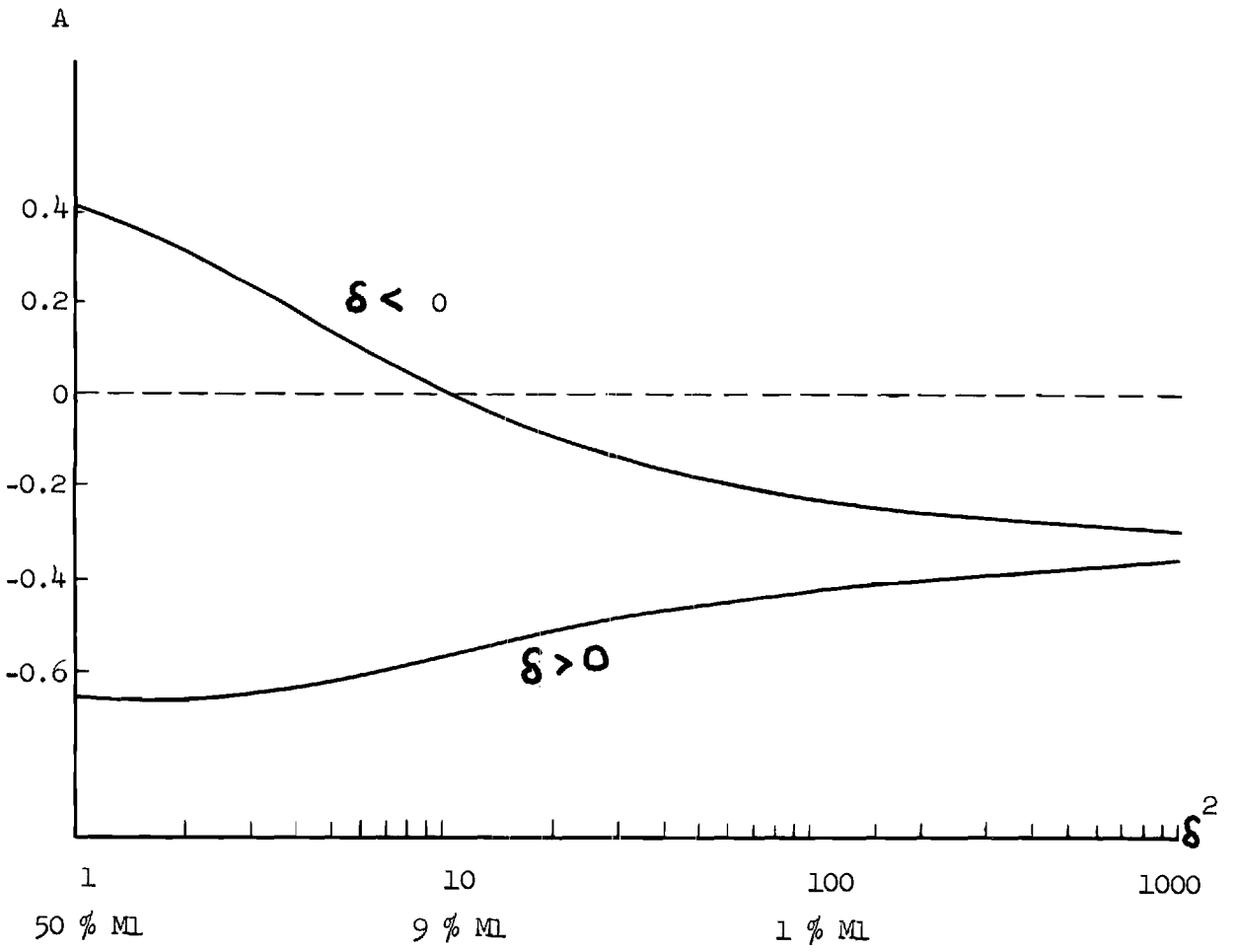

Figure 11b. Plot of the Theoretical Anisotropy Versus the Mixing Ratio for the Sequence 3(E2+M1)2(E2)0

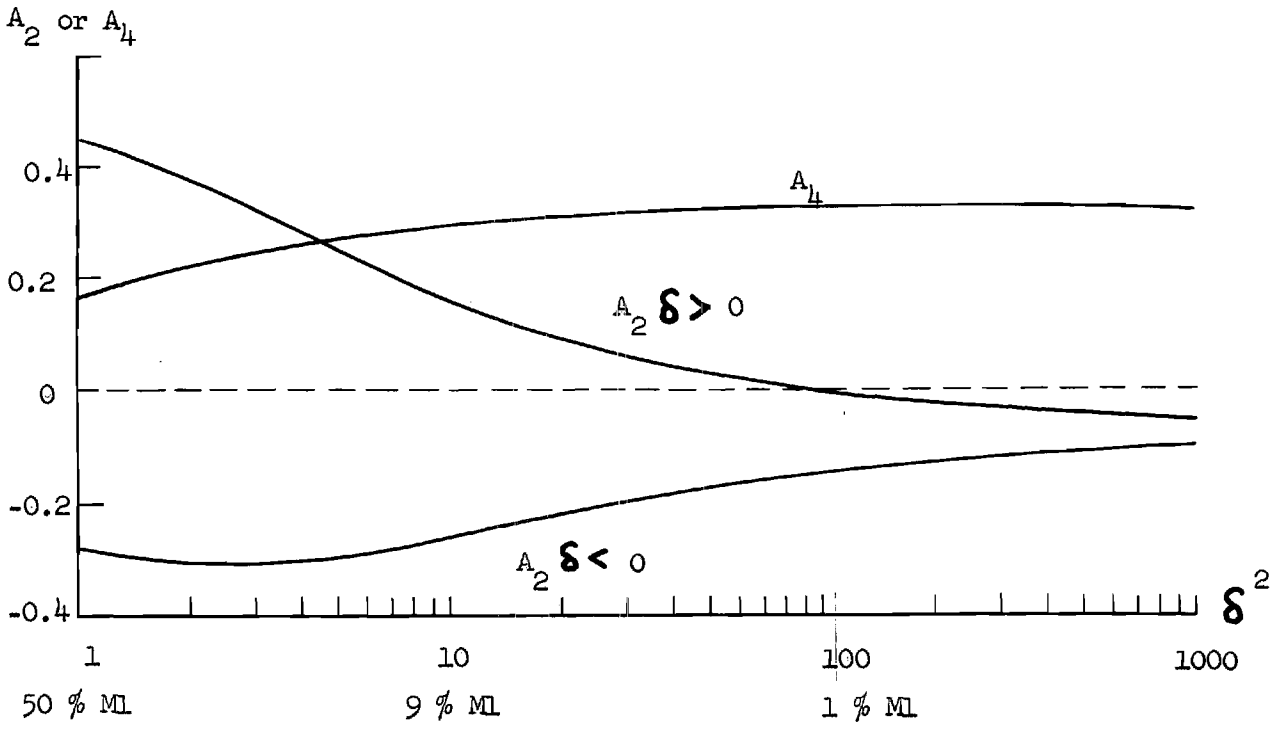

Figure 12a. Plot of the Theoretical Correlation Coefficients Versus the Mixing Ratio for the Sequence 2(E2+M1)2(E2)0

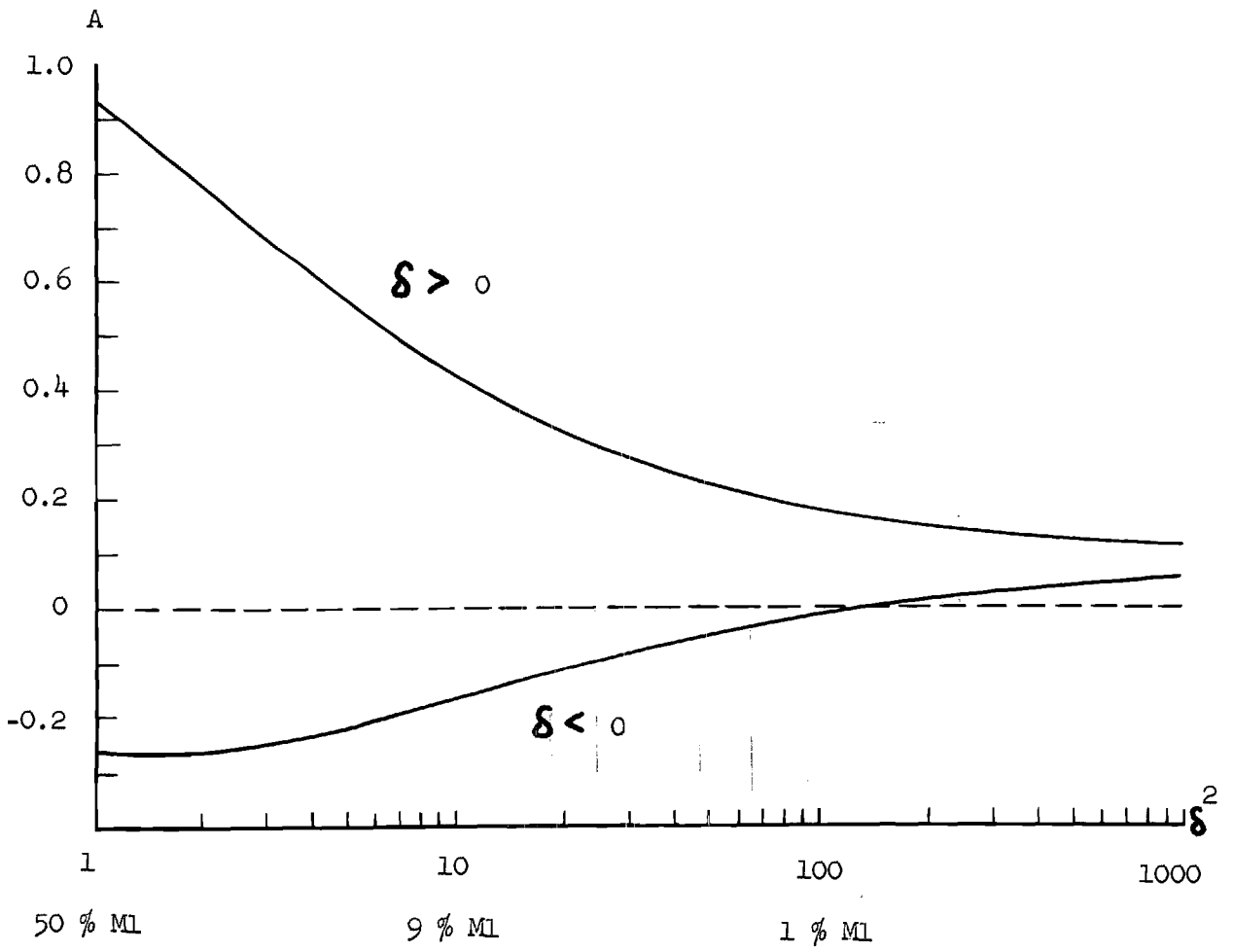

Figure 12b. Plot of the Theoretical Anisotropy Versus the Mixing Ratio for the Sequence 2(E2+M1)2(E2)0

600-600 kev correlation.--Consideration of the decay scheme shows the 600-600 kev experiment should be a measurement of the 588-613 kev correlation with a small amount of interference from sum peaks.[2] Since data were only obtained at three angles (90°, 180°, 270°) the coefficients A_2 and A_4 could not be determined explicitly; therefore, only the anisotropy ratio was determined experimentally and is to be compared with the theoretical values. The 588-613 kev cascade connects levels G, C and A. The spins of levels C and A are known to be two and zero respectively, and the 613 kev line is pure E2. The experimental data are not in agreement with a spin of four for level G. As in the case of level E, the other possibilities are spins of two or three.

If the spin is three, an admixture of M1 radiation in the 588 kev transition must be considered since the experimental data are not in agreement with a 3(E2)2(E2)0 correlation. Figure 11 shows the anisotropy ratio as a function of the admixture of M1 radiation in a 3(E2+M1)2(E2)0 correlation. From this figure one can see that the experimental anisotropy data agree with a spin assignment of three for level G and an admixture of 8.5(±1 per cent) M1 radiation with δ negative in the 588 kev transition. Interference from the 588-(296+316) kev cascade may introduce an additional error of a few per cent in δ, the mixing ratio. K, L_I, and L_{II} conversion coefficients for the 588 kev transition have been measured by Baggerly et al (28), and the L/K ratio has been measured by Bashilov et al (48). This admixture of 8.5 per cent M1 radiation in the 588 kev transition somewhat worsens the

---

[2]Sum peaks occur when two gamma-rays which are in coincidence with each other are counted by the detector simultaneously. In this case the interfering sum peaks are the 316+296 kev, 316+308 kev and 296+308 kev sum peaks. These three sum peaks give a count in the 600 kev region.

agreement of Rose's (49) theoretical conversion coefficients with the results of Baggerly et al (28) but tends to improve the agreement with the results of Bashilov et al (48).

If the spin of level G is taken to be two, consideration of Fig. 12 shows that the anisotropy data are in agreement if an admixture of a few per cent M1 radiation is assumed for the 588 kev transition. Figure 13 shows a plot of the ratio of the counting rate at 135° to the counting rate at 90° versus the mixing ratio for the cascade 2(E2+M1)2(E2)0. The more extensive experimental data of Kelley and Wiedenbeck (30), which were reported while this work was in progress and which are in agreement with the present data, are not consistent with the greatly reduced counting rate at 135° as shown in Fig. 13 for all admixtures of M1 radiation up to about 50 per cent. Therefore, a spin of two for level G seems unlikely and a spin of three is the best choice.

416-468 kev correlation.--An examination of this correlation is also pertinent to a discussion of the spin of level G. The correlation experiment was performed; however, since the intensity of the 416 kev line is small, interference from other cascades (468-316 kev) is large compared to the 416-469 kev coincidence rate. Therefore, no attempt is made to interpret the data, and no conclusions are based upon this experiment.

485-206 kev correlation.--This experiment also contains interference from other cascades; however, the fact that a large negative value for the anistropy was obtained makes the experiment interpretable. The

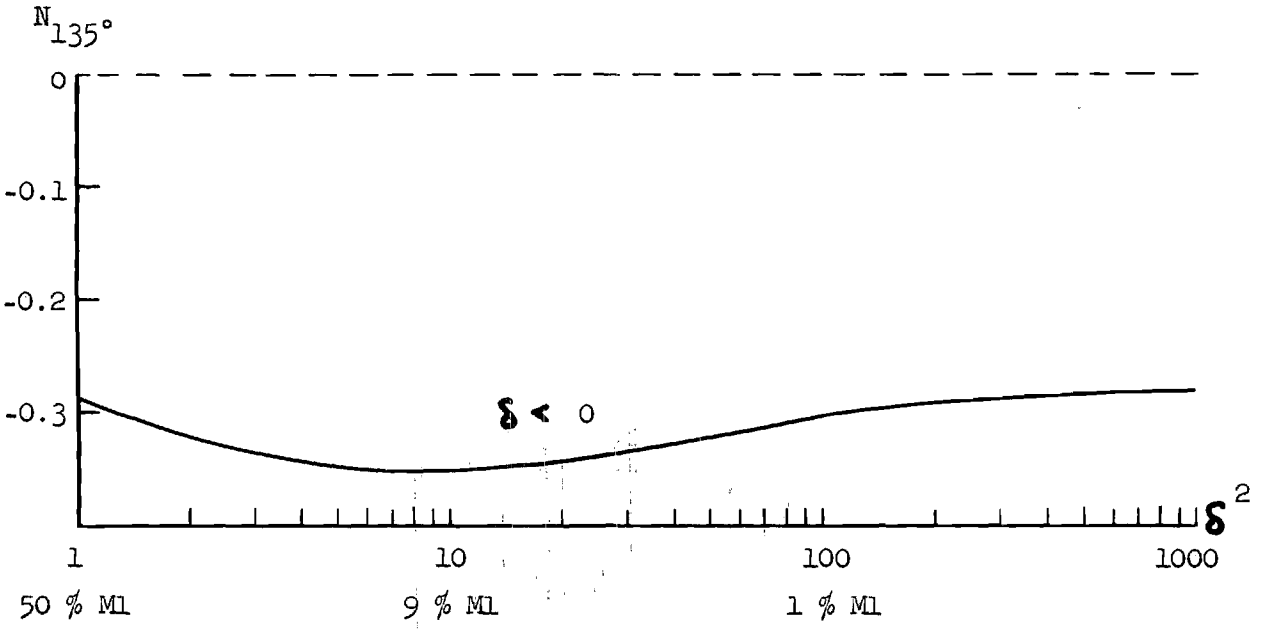

Figure 13. Plot of the Ratio of the Counting Rate at 135° to the Counting Rate at 90° Versus the Mixing Ratio for the Sequence 2(E2+M1)2(E2)0

major portion of the interference is probably due to the 468 kev radiation in one detector and the Compton distributions from the 316 kev line being counted in the other detector. This cascade would give a positive anisotropy. (See 468-316 kev correlation discussion.) Therefore, it is very likely that the value obtained for the anisotropy is somewhat smaller in absolute value than it would be if no interference was present. The 485-206 kev cascade connects levels d, b and a in Os^{192}. The spins of levels b and a are known to be two and zero respectively. Level d must have a spin of two, three or four. A spin of four is not in agreement with the correlation experiment. The data are consistent with a spin of three; however, the interference in the experiment prevents an accurate assignment of the admixture of M1 radiation in the 485 kev transition, but it is probably less than six per cent (see Fig. 11). This interference also makes it unfruitful to attempt to rule out a spin of two for level d on the basis of the angular correlation experiment. The absence of a crossover transition of appreciable intensity from level d to the ground state suggests that the spin of level d should be greater than two, otherwise this crossover ought to be M1 or E2 which would compete favorably with the other E2 transitions connecting levels d and b or b and a. Note that a similar argument applied to Pt^{192} suggests that the spins of levels E and G should not be two.

Beta-Gamma Correlation Experiments

All the beta-gamma angular correlation experiments gave results which were almost isotropic thereby limiting the number of conclusions

which may be obtained by examination of the data. In general, any beta-gamma angular correlation experiment will yield an isotropic result if the beta spectrum has the allowed shape (14). First forbidden beta transitions with a spin change $\Delta J=0$ or 1 have allowed shapes (14). First forbidden beta transitions with $\Delta J=2$ may deviate from the allowed shape and hence have a non-isotropic angular correlation (4). The Fermi plots obtained in this research with scintillation spectrometers are not sufficiently accurate to determine the shapes of the beta spectra.

468 kev gamma-670 kev beta group angular correlation.--The 670 kev beta group is first forbidden (28) with $\Delta J=1$ if we assume the ground state spin of iridium to be five.[3] Therefore, an isotropic angular correlation is expected. If the ground state spin were six, $\Delta J=2$, and an anisotropic result is expected. The fact that no anisotropy was observed is consistent with a spin of five for the ground state of Ir^{192}.

600 kev gamma-540 kev beta group angular correlation.--If the ground state spin of Ir^{192} is five, the 540 kev beta group is also first forbidden but has $\Delta J=2$. This is the so-called first unique beta transition and should give an anisotropic angular correlation with a single gamma ray. If the ground state spin of Ir^{192} is six, then $\Delta J=3$ and the 540 kev beta transition cannot be first forbidden. In this case the transition must be third forbidden, (second forbidden is ruled out by parity arguments), and again an anisotropic result is expected if no interference from other cascades occurs. However, the coincidence rate

---

[3]The 670 kev beta group proceeds to level D which has a spin of four.

as observed in this experiment is a composite of three cascades - 540 kev beta group and 604 kev gamma, 540 kev beta group and the 613 kev gamma, and 540 kev beta and the (308+296) kev sum peak. Therefore, even if each cascade had an anisotropic correlation, the composite might be very nearly isotropic. The experiment was performed with the above facts in mind. If an anisotropic result had been obtained, then one could have said that $\Delta J \geq 2$; however, the isotropic result does not limit the values of ΔJ.

Ground State Spin of Ir^{192}

The data on the 604-316 kev gamma-gamma angular correlation experiment and the data on beta-gamma angular correlations indicate that the spin of Ir^{192} is five and not six.[4] Since the 604-316 kev gamma-gamma correlation experiment fixes the spin of level E to three and since the log ft value of the 540 kev beta group connecting the ground state of Ir^{192} with level E indicates a first forbidden transition (28), then the spin difference between the Ir^{192} nucleus and level E can be no greater than two. Therefore, the ground state spin of Ir^{192} must be five. Furthermore, a spin of five is in agreement with the results of the 670-468 kev beta-gamma angular correlation.

The recent successes of the shell model in predicting the ground state spins of nuclei require an attempt to correlate a spin of five for Ir^{192} with the shell model. A great deal of the terminology used in this discussion is standard and will not be defined explicitly here;

---

[4] The spin of Ir^{192} is delimited to values of five or six by arguments based on the fact that first forbidden beta transitions proceed to levels of spin 3 or 4 (levels D, E, G) but not to levels of spin 2(levels B, C).

a complete description of the fundamentals of the shell model can be found in Mayer and Jensen's Elementary Theory of Nuclear Shell Structure (1). Ir^{192} is an odd-odd nucleus with proton number Z=77 and neutron number N=115. In order to predict its spin, one must decide into which orbitals the 77th and 115th nucleons must be placed.[5] One assumes, in the spirit of the shell model, that all other nucleons couple to zero. Figure 14 is a plot of the energy levels for protons and neutrons as predicted by the shell model with strong spin-orbit coupling (51). From this figure one can see that in the region of Z=77 and N=115 the energy levels are closely spaced. In such cases the shells may not fill up in the order shown, and the nearby levels may compete for the next nucleon. For the 77th proton the competing levels are $6h_{11/2}$, $4d_{3/2}$, and $3s_{1/2}$; for the 115th neutron the competing levels are $4p_{3/2}$, $7i_{13/2}$, and $4p_{1/2}$. In order to obtain information as to just which are the proper levels for these last odd nucleons, one might consider nearby odd-even and even-odd nuclei. Klinkenberg (51) and Blin-Stoyle (52) have extensive tables of the measured spins, j, of various nuclei and of the corresponding orbital assignments in the shell model. For Z=77 two examples are given -- Ir^{191} and Ir^{193}. Both have j=3/2, and assignment of the last proton is to the $4d_{3/2}$ state with the $6h_{11/2}$ state filled and the $3s_{1/2}$ state empty. For N=115 no

---

[5] If the angular momenta of the odd proton and neutron are known one must still find a coupling rule to predict the total spin of the nucleus (1). Nordheim (50) has formulated empirical rules which seem to fit the observed spins of odd-odd nuclei. However, for heavy nuclei very few spins of odd-odd nuclei have been measured; therefore, it is unknown whether Nordheim's coupling rules apply in this region. Furthermore, Nordheim's rules do not always predict a unique spin.

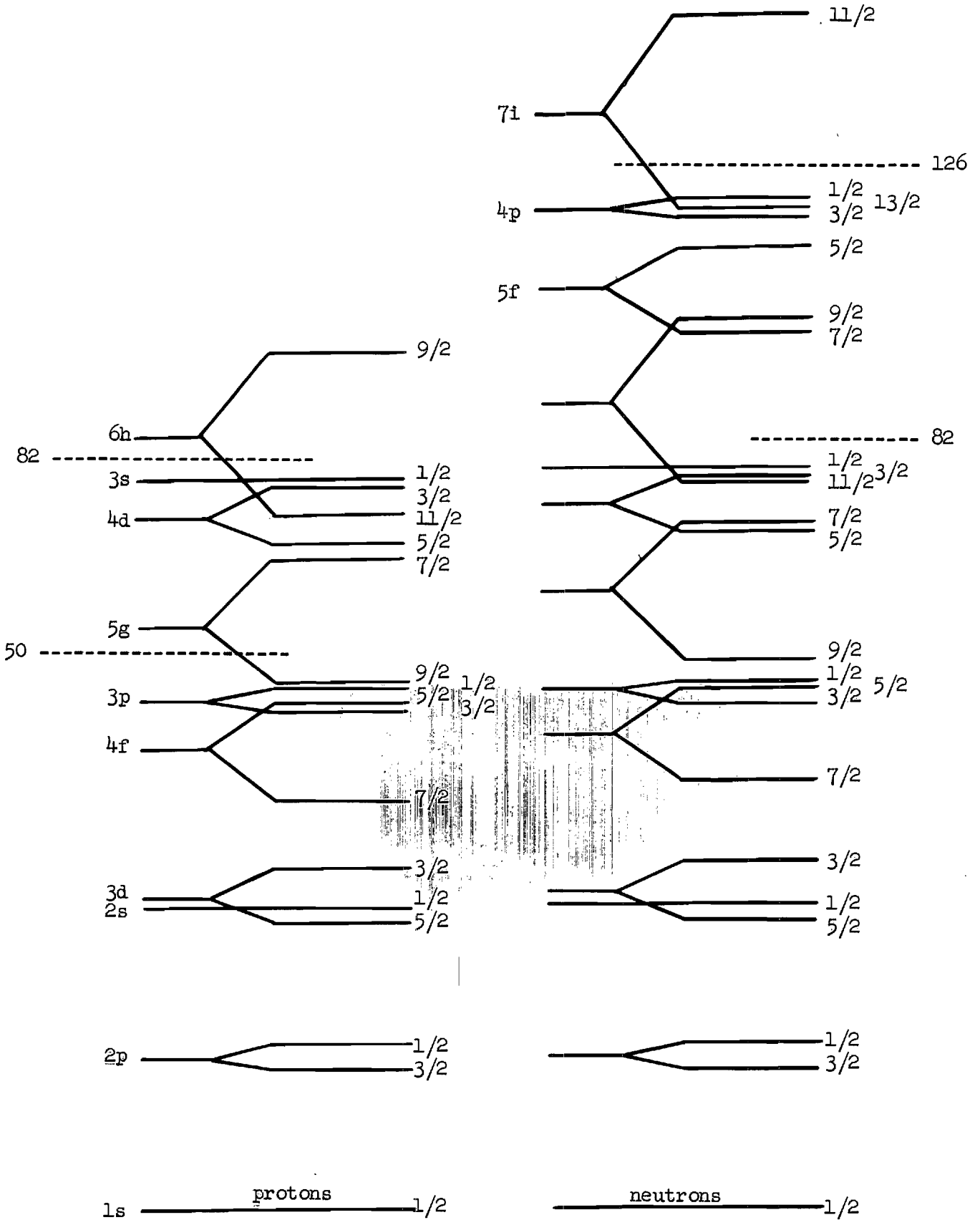

Figure 14. Energy Levels for Protons and Neutrons as Predicted by the Shell Model with Strong Spin-Orbit Coupling

examples are known; however, for N=113 (Os^{189}) the spin is 3/2 with the assignment of the last neutron to the $4p_{3/2}$ state. In this case the $7i_{13/2}$ state is only partially filled and the $4p_{1/2}$ level is empty. For N=117 (Pt^{195} and Hg^{199}) the measured spin is 1/2, and the assignment of the last neutron is to the $4p_{1/2}$ state with the $7i_{13/2}$ level partially filled and the $4p_{3/2}$ level empty. These arguments would indicate the odd proton should be in the $4d_{3/2}$ state and the odd neutron in $4p_{1/2}$ or $4p_{3/2}$ state. These assignments could give a nuclear spin of at most 3; therefore, some other assignment is necessary. In order to obtain a spin of five the following assignments are possible: proton in $6h_{11/2}$ and neutron in $4p_{3/2}$, $4p_{1/2}$, or $7i_{13/2}$ levels, or neutron in $7i_{13/2}$ and proton in $6h_{11/2}$ or $4d_{3/2}$ levels. As stated in the introduction the parity of Ir^{192} is known to be odd; the only one of the above combinations which gives an odd parity is the assignment of the odd proton to the $6h_{11/2}$ level and the neutron to the $7i_{13/2}$ level. This assignment is not expected from the nearby odd-even and even-odd nuclei mentioned above. This must mean the ordering of the levels in odd-odd nuclei is somewhat different from that in odd-even or even-odd nuclei. A similar case occurred in the odd-odd nucleus $_{71}Lu^{176}$, with N=105 and Z=71. The spin of Lu^{176} is known to be greater than six (53). This requires the odd nucleons to be assigned to states with high angular momenta, and as in the case of Ir^{192}, nearby odd-even and even-odd nuclei do not indicate these assignments.

CHAPTER V

THEORY OF ANGULAR CORRELATIONS

Introduction

An elementary discussion of some of the concepts used in this chapter is given in Appendix A which may be consulted by the reader as needed. The purpose of this chapter is to explain why an angular correlation should exist between successively emitted radiations. Major emphasis will be placed upon the correlation between successively emitted gamma-rays, and beta-gamma correlations will be discussed only briefly. The theory will not be developed in its most general form (for such treatment, see Biedenharn and Rose (12)); however, special emphasis will be placed upon a treatment which provides insight into the physics of the correlation mechanism. The development presented here closely follows that of Frauenfelder (4).

The probability of emission in a particular direction of radiation by a radioactive nucleus is a function of the relative orientation between the nuclear spin axis and the direction of emission. If the nuclear spin axes are randomly oriented in space, then the observed radiation pattern is necessarily isotropic. In order to observe an anisotropic pattern, it is necessary to select an ensemble of nuclei which are not randomly oriented. A direct method of selecting such an ensemble is to place the sample at a low temperature in a strong magnetic field. Under such conditions the angular distribution of the emitted radiation with respect to the magnetic field direction may be anisotropic (4).

A more indirect method is to selectively observe the radiation from only those radioactive nuclei whose spins lie in a preferred direction. This method of selective observation is possible if the radioactive decay is accompanied by the successive emission of two radiations R_1 and R_2. The observation of R_1 in a fixed direction serves to select an ensemble of nuclei of limited spin orientations. The succeeding radiation R_2 may show an angular correlation with respect to R_1.

Experimentally, one records the coincidences between R_1 and R_2 as a function of the angle between the lines joining the two counters and the radioactive source. After proper normalization and geometrical correction (see Appendix D), one derives the experimental correlation function $W(\theta)$, where $W(\theta)d\Omega$ is defined as the relative probability that R_2 is emitted into the solid angle $d\Omega$ at an angle θ with respect to R_1. Information regarding the nuclear levels may be obtained only if it is possible to derive expressions for $W(\theta)$ for various nuclear spin sequences and various types of emitted radiations.

Gamma-Gamma Angular Correlations

In this section we assume that both R_1 and R_2 are electromagnetic quanta (gamma-rays). Furthermore, we assume the nuclei are not reoriented after the emission of R_1 and before the emission R_2. Usually the excited states are very short-lived (i.e. $< 10^{-9}$ second) and this assumption is justified. If perturbations of the intermediate state are appreciable, then the observed correlations will be smaller than the unpeturbed correlation. Comprehensive discussions of this problem have been given by numerous authors (8), (4).

Consider a single gamma-transition R_2 connecting two nuclear levels B and C with spins $\vec{J}_B$ and $\vec{J}_C$ respectively. R_1 is characterized by the angular momentum quantum number L_2. The Z axis defines a polar coordinate system and may be arbitrarily chosen. The component of L_2 along Z is called the magnetic quantum number and is denoted by M_2. M_2 can have integral values subject to the restriction:

$$-L_2 \leq M_2 \leq L_2$$

The total angular momentum and magnetic quantum numbers characterizing the nuclear states B and C may be denoted by j_B, m_B and j_C, m_C respectively, where $J_B^2 = j_B(j_B+1)\hbar^2$, $J_C^2 = j_C(j_C+1)\hbar^2$, $-j_B \leq m_B \leq j_B$ and $-j_C \leq m_C \leq j_C$ (m_B and m_C are integral or half-integral as j_B and j_C are integral or half-integral). Conservation of angular momentum requires that $\vec{J}_B = \vec{J}_C + \vec{L}_2$ and $m_B = m_C + M_2$.

Figure 15 shows a single E2(L_2 = 2) gamma-transition connecting nuclear levels of spin $j_B = 3$ and $j_C = 1$. If the radiation resulting from a transition between a particular pair of m-states is called a component, then the gamma-transition shown in Fig. 15 has 15 components. Each component with a definite value of M_2 has a characteristic directional distribution which is independent of j_B and j_C. If Θ denotes the angle between the direction of propogation of the emitted gamma-ray and the Z axis, then the directional distribution for a particular component may be denoted by $F_L^m(\Theta)$. One calculates $F_L^m(\Theta)$ by evaluating the Poynting vector as a function of Θ for the multipole radiation characterized by M and L. The result is as follows (53), (54):

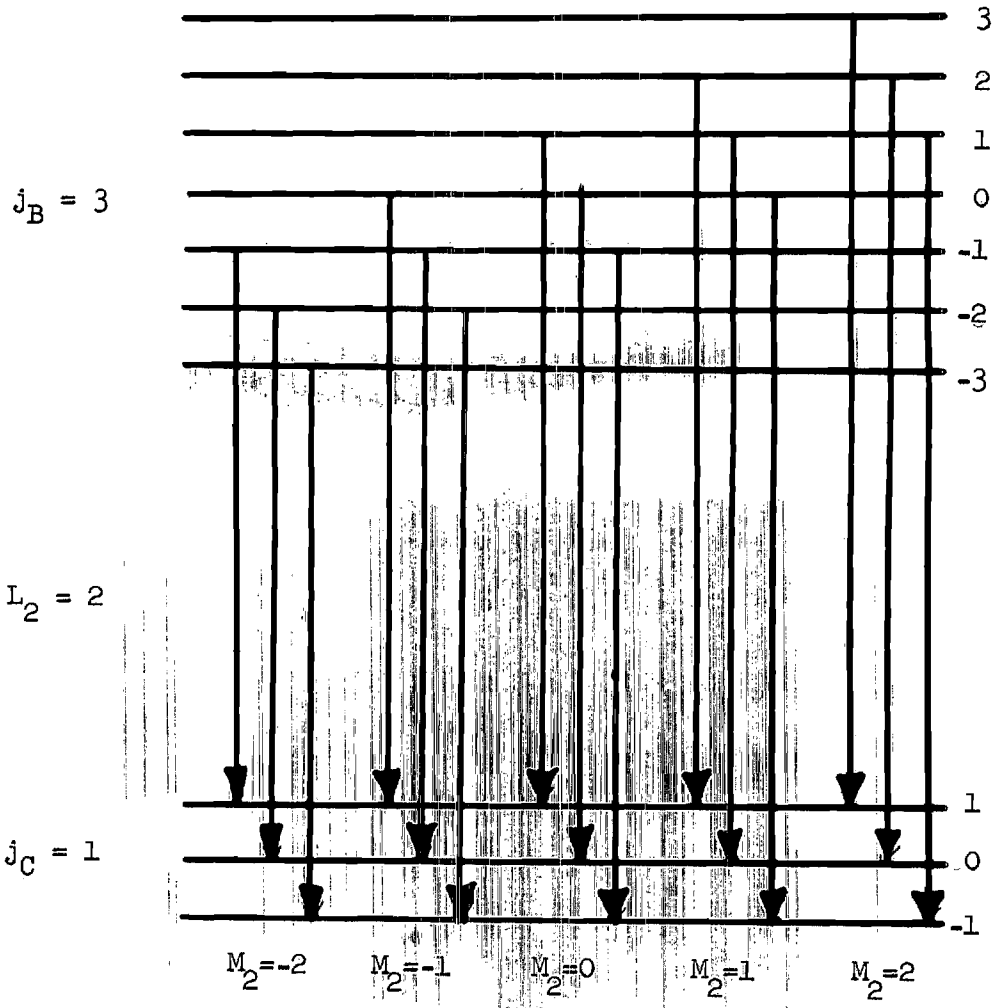

Figure 15. The Components of an E2 Gamma-Transition Connecting Nuclear Levels of Spin $j_B = 3$ and $j_C = 1$

$$F_L^m(\Theta) = 1/2 \left[1 - \frac{m(m+1)}{L(L+1)} \right] \left| Y_{L,m+1} \right|^2 + 1/2 \left[1 - \frac{m(m-1)}{L(L+1)} \right] \left| Y_{L,m-1} \right|^2 + \frac{M^2}{L(L+1)} \left| Y_{Lm} \right|^2 \quad (1)$$

where Y_{Lm} are the normalized spherical harmonics defined as normalized simultaneous eigenfunctions of the operators L^2 and L_z.[1]

In the Zeeman effect of atomic spectroscopy, one can observe the directional distributions of the individual components since the different states are split up in a magnetic field and the components have different energies. In nuclear spectroscopy the splitting of the levels even in a very strong magnetic field is only of the order of 10^{-8} ev (4). Therefore, it is impossible to separate the components, and one always observes the unresolved line R_2. Its directional distribution, $F_{L_2}(\Theta)$, depends upon $F_{L_2}^m(\Theta)$, the relative population of each magnetic substate in state B, $P(m_B)$, and the relative transition probability, $G(m_B m_C)$, for each component $M_2 = m_B - m_C$ as follows:

$$F_L(\Theta) = \sum_{m_B, m_C} P(m_B)\, G(m_B m_C)\, F_L^m(\Theta) \quad (2)$$

where the summation extends over all the magnetic substate of levels B and C.

The absolute transition probability $G'(m_B, m_C)$ for radiation of multipole order L is proportional to the square of matrix element of the multipole moment operator Q:

---

[1] See Blatt and Weisskopf, Theoretical Nuclear Physics, Appendix B (54).

$$G'(m_B m_C) \propto \left| \int \Psi_C^* \, Q \, \Psi_B \, d\tau \right|^2 .$$

This matrix element may be written as a product of a "nuclear" factor depending upon the radial wave functions and a "geometrical" factor depending explicitly on m_B and m_C. The geometrical factor yields the desired relative transition probability because the nuclear factor does not depend upon m_B and m_C explicitly. To clarify this discussion, consider, for example, the radiation from an electric dipole lying along the Z axis. Then the matrix element apart from numerical factors becomes $\int \Psi_C^* Z \Psi_B d\tau$. Assume the nuclear wave functions, Ψ_C and Ψ_B, may be separated into products of radial and angular functions:[2] $\Psi = R(r) Y_{jm}(\Theta, \Phi)$ and set $Z = r \cos\Theta$; then, the matrix element becomes a product of two integrals. One integral depends only upon the radial part of the wave function and the other upon the values of m_B and m_C.

In general, the multipole moment operator may be written as the product of a radial factor and the complex conjugate of a spherical harmonic $Y_{LM}^*(\Theta, \Phi)$ (54). The separation of the matrix element into a radial factor independent of m_B and m_C and an angular factor then follows (4). The angular factor may be written as $\int Y_{j_C m_C}^* \, Y_{j_B m_B} \, Y_{LM}^* \, d\tau$ where $Y_{j_C m_C}$ and $Y_{j_B m_B}$ are the angular parts of the wave functions representing the initial and final states and Y_{LM}^* is the angular part of the multipole moment operator. In order to take advantage of the orthogonal properties of the spherical harmonics, one expands $Y_{j_C m_C}^* \, Y_{LM}^*$ in terms of the complete set of functions on the unit sphere, $Y_{j_B' \, m_B'}^*$.

---

[2] This is equivalent to the assumption of a single particle wave function with a spherical potential.

This expansion is given by the expression (4)

$$Y^*_{j_C m_C} Y^*_{LM} = \sum_{j_B' m_B'} (j_C L m_C M \,|\, j_B' m_B') \, Y^*_{j_B' m_B'} .$$

The coefficient $(j_C L m_C M | j_B' m_B')$ is the so-called Clebsch-Gordan or vector addition coefficient (54). The Clebsch-Gordan coefficients are the coefficients of the expansion of a wave function characterized by angular momentum $\vec{J}_B$ in terms of wave functions characterized by angular momenta $\vec{J}_C$ and $\vec{L}$ where $\vec{J}_B = \vec{J}_C + \vec{L}$. Utilizing the orthogonality properties of the spherical harnomics, one obtains the result that the matrix element of the multipole moment operator is proportional to the Clebsch-Gordan coefficient $(j_C L m_C M | j_B m_B)$, and the relative transition probability $G(m_B m_C)$ is given by

$$G(m_B m_C) = (j_C L m_C M | j_B m_B)^2 \qquad (3)$$

A general derivation of the above result may be obtained by group theoretical methods (4), (12).

Consider now a nucleus which decays through a cascade A-B-C by successive emission of two gamma rays R_1 and R_2 of multipolarities L_1 and L_2 respectively. We seek the directional correlation function $W(\Theta)$ between R_1 and R_2.

Let the Z axis coincide with the direction of propogation of R_1. In this case, $W(\Theta)$ is identical with $F_{L_2}(\Theta)$ -- the directional distribution of R_2 with respect to the Z axis. Therefore, $W(\Theta) = F_{L_2}(\Theta)$ can be calculated from equations (2) and (3) if the relative population of state B, $P(m_B)$, is known. $P(m_B)$ is given by the sum of all transitions

leading into state m_B. Assuming all the magnetic substates of level A are equally populated, then

$$P(m_B) = \sum_{m_A} G(m_A m_B) F^{M_1}_{L_1} (\theta = 0°) \tag{4}$$

Where the summation extends over all the magnetic substates of A, and $M_1 = m_A - m_B$ for conservation of the Z component of angular momentum. The transverse nature of electromagnetic radiation restricts the values of M_1 to be ± 1 for a photon propogated along the Z axis. Therefore,

$$P(m_B) = \sum_{m_A} G(m_A m_B) F^{M_1}_{L_1} (\theta = 0°) \tag{5}$$

and $$W(\theta) = F_{L_2}(\theta) = \sum_{m_B m_C} \left[\sum_{m_A} G(m_A m_B) F^{M_1}_{L_1} (\theta = 0°) \right] G(m_B m_C) F^{M_2}_{L_2}(\theta)$$

where $M_2 = m_B - m_C$ and $M_1 = m_A - m_B$. Finally, putting in explicit expressions for the relative transitions probabilities in terms of the Clebsch-Gordan coefficients, one obtains

$$W(\theta) = \sum_{m_B m_C m_A} (j_B L_1 m_B M_1 | j_A m_A)^2 \; F^{\pm 1}_{L_1}(0) \; (j_C L_2 m_2 M_2 | j_B m_B)^2 F^{M_2}_{L_2}(\theta) \tag{6}$$

where $M_2 = m_B - m_C$, $M_1 = m_A - m_B$. In a simple case, the correlation function may be calculated from equation (6). The Clebsch-Gordan coefficients are tabulated by Condon and Shortley (55). The functions F^M_L may be found by using equation (1), and expressions for spherical harmonics may be found in Blatt and Weisskopf (54).

The general theory of angular correlations has been discussed by many authors (12), (4). The progress in the theory since Hamilton's (5) original work is largely due to the use of three tools: group theory,

Racah algebra, and density matrix formalism (4). A discussion of this more general theory will not be presented here; however, some of the results will be mentioned.

The correlation function $W(\Theta)$ for gamma-gamma correlations is not an infinite sum of even order Legendre polynomials but only contains a finite number:

$$W(\Theta) = 1 + A_2 P_2(\cos\Theta) + A_4 P_4(\cos\Theta) + \ldots . P A_{\nu_{max.}} P_{\nu_{max.}}(\cos\Theta)$$

The highest term in this expansion is given by $\nu_{max.} = \text{Min.}\ (2j_B, 2L_1, 2L_2)$ where Min. represents taking whichever one of the numbers $2j_B$, $2L_1$, $2L_2$ is the smallest (4). The explicit calculation of A_ν in the expression $W(\Theta)$ is facilitated by the fact that it can be broken up into two factors, each depending upon only one transition of the cascade. If we denote these factors by F_ν, then

$$A_\nu = F_\nu\ (L_1 j_A j_B)\ F_\nu\ (L_2 j_C j_B) \qquad (7)$$

These factors, F_ν, have been numerically tabulated by Biedenharm and Rose (12), and the calculation of A_ν for pure gamma-gamma cascades is easily performed.

The general theory of gamma-gamma angular correlations may be extended to include the case in which one of the two gamma-rays is mixed, i.e. must be described by more than one L value. In this case, the correlation function for the cascade $j_A(L_1 L_1')j_B(L_2)j_C$, $W(\Theta)$, is given by

$$W(\Theta) = W_I + \delta^2 W_{II} + 2\delta W_{III}$$

where W_I and W_{II} are the correlation functions for the pure cascades $j_A(L_1)j_B(L_2)j_C$ and $j_A(L_1')j_B(L_2)j_C$ and can be calculated from equations (7). δ is called the mixing ratio and is given by $\delta = \frac{(j_B \| L_1' \| j_A)}{(j_B \| L_1 \| j_A)}$. The ratio of the total (i.e. angle-integrated) intensity of the L_1' multipole to that of the L_1 multipole is equal to δ^2 (4). For a given intensity ratio δ^2, the mixing ratio δ can have either a positive or negative sign. W_{III} is a contribution due to the interference between L_1 and L_1' and is given by

$$W_{III} = \sum_{\substack{\nu \neq 0 \\ \text{even}}} A_\nu^{III} \; P_\nu(\cos\Theta)$$

with $$A_\nu^{III} = F_\nu(L_1 L_1' \; j_A j_B) F_\nu(L_2 j_C j_B)$$

and $$F_\nu(L_1 L_1' \; j_A j_B) = (-1)^{j_B - j_A - 1} \left[(2j_B+1)(2L_1+1)(2L_1'+1)\right]^{1/2}$$

$$G_\nu(L_1 L_1' \; j_A j_B)$$

The function $G(LL' \; j_A j_B)$ has been tabulated for the case[3] $L_1 = L + 1$ by Biedenharn and Rose (12).

Beta-Gamma Angular Correlation Theory

The correlation between a beta-particle and a subsequent gamma-ray is much more difficult to treat theoretically than the preceeding problem. In beta decay the nucleus emits a beta-particle and a neutrino simultáneously. In the correlation experiment only the direction of the beta-particle is observed; therefore, the theoretical calculations must average over all neutrino directions and over all the spins of the neutrino

[3] This is the only case of interest because the gamma-ray transition probability decreases rapidly with increasing multipolarity (56).

and the beta-particle. Furthermore, the beta-decay interaction Hamiltonian is not well understood. The interaction may be some combination of the five relativistically invariant "pure" forms (57). If more than one of these pure interactions is responsible for beta decay, then the beta-gamma correlation function must contain interference terms (4). As in gamma-decay, one can classify the beta-transitions according to the angular momentum, L, carried away by the electron-neutrino pair. However, in the beta-decay several operators exist for a given L even if one considers a pure interaction (4). Finally, interference can also occur between matrix elements belonging to different L values, usually L and L + 1. These three types of interference greatly complicate the theoretical calculations and only a discussion of a few of the pertinent results will be presented here (4).

The beta-gamma correlations depend in general upon the beta-interaction Hamiltonian and the particular matrix elements responsible for the transitions. It also depends upon the spins of the three nuclear states, the parity change in the beta-transition, and the multipolarity of the gamma-ray. It is a function of the energy of the beta-particle. The beta-gamma correlation function for beta particles in the energy region between E and E + dE is called the differential correlation $W(\Theta,E)$ and in general $W(\Theta,E)$ has its maximum anisotropy for the maximum beta energy and always becomes isotropic as E approaches zero. Finally, all allowed and some additional matrix elements cause isotropic distribution. In fact if shape of the energy spectrum is strictly identical with that of an allowed transition (gives a straight line Fermi plot), $W(\Theta,E)$ is isotropic. For anisotropic correlations there

is a close connection between the correction factor by which an allowed spectrum has to be multiplied to give the desired forbidden distribution and the behavior of the correlation function (4).

APPENDIX A

BASIC PROPERTIES OF NUCLEAR STATES AND NUCLEAR RADIATION

The purpose of this appendix is to describe the basic properties of nuclear states and radiations and to discuss briefly how a knowledge of the properties of the nuclear radiations aids in determining the properties of the nuclear states involved in the transitions. The discussion will be a summary of the theoretical results, and no attempt will be made to derive these results; however, some mention will be made of the experimental methods used to determine the properties of nuclear radiations. Further discussions of the theoretical arguments may be found in the following references: (57), (58), (59), (60), (61). Since this thesis is concerned with a study of beta and gamma radiations only, other types of radiation will not be discussed, and special emphasis will be placed upon methods and basic arguments which can be applied to the decay of Ir^{192}.

The state of a nucleus may be characterized by various quantities, of which we are particularly interested in three: energy, total angular momentum (spin), and parity.[1] The energies of the various excited states in a nucleus are determined by measurement of the energies of the gamma-rays by which these excited states decay to the ground state. The problem with which this thesis is primarily concerned is the determination of the spin, j, and the parity of these states, which may be determined by studies of additional properties of these gamma-rays.

Gamma radiations are conveniently classified by multipole orders L, according to the angular momentum (in units of $\hbar$) carried by each

---

[1] Parity refers to the symmetry property of the wave function under coordinate inversion. (See for example Schiff (62)).

quantum of radiation (57). The possible classifications are L=1, 2, 3, ... called respectively dipole, quadrupole, octopole, ...radiation. The tranverse nature of an electromagnetic wave excludes the case L=0 (57). Furthermore, for each multipole order it is convenient to divide the radiations into two classes depending upon parity. These two classes are referred to as electric 2^L pole (EL) and magnetic 2^L pole (ML). Classically EL and ML refer to radiation emitted by a vibrating electric or magnetic 2^L pole (57). Multipolarity refers to both the class (electric or magnetic) and the multipole order of the radiation. Application of the conservation of angular momentum to the system nucleus plus gamma-ray imposes certain selection rules on the possible multipolarities of a gamma transition. For transitions between two nuclear states specified by angular momenta ($\vec{J}_i$, $\vec{J}_f$) and parities (π_i, π_f) where i refers to the initial state and f to the final state, these selection rules are as follows:

$$|J_i - J_f| \leq L \leq J_c + J_i$$

$$\text{and } \Delta\pi \equiv \pi_i/\pi_f = (-1)^L \quad \text{for EL radiation}$$

$$= (-1)^{L-1} \quad \text{for ML radiation}$$

where $\Delta\pi = +1$ represents no parity change and $\Delta\pi = -1$ represents a parity change. Calculation of the transition probability for gamma-decay (56) shows the probability of emission decreases rapidly with increasing multipole order. Therefore, one expects to find only the lowest multipole order satisfying the selection rules or, at most, a mixture of the two lowest permissible multipole orders. Parity conservation excludes

the simultaneous occurrence of electric and magnetic radiation of the same multipole order.

A knowledge of the multipole classification of the gamma transitions accompanying decay will place restrictions on the possible nuclear spins and parities. A common method of determining the multipolarity is by measuring the internal conversion coefficients; i.e. the ratio of the number of conversion electron transitions to the number of gamma-ray transitions. The internal conversion coefficients depend upon the energy and multipolarity of the gamma-ray, the particular atomic orbit out of which the electron is ejected, the wave function of the electrons, but not on the nuclear wave function. It is this lack of dependence upon nuclear wave functions that makes the measurement of internal conversion coefficients highly adapted to determinations of gamma-ray multipolarities.[2] Theoretical values for the K and L shell conversion coefficients have been tabulated for various multipolarities as a function of energy and nuclear charge by Rose (49). Both the absolute magnitude of the conversion coefficients and the ratios of the coefficients (i.e. K shell to L shell or various L subshells) are sensitive to changes in multipolarity. Experimentally, the value of the ratio of two conversion coefficients is more apt to be accurate than an absolute determination of a conversion coefficient, and frequently the ratio of two conversion coefficients is much more sensitive to multipolarity than is the absolute conversion coefficient. In any event small

---

[2]However, recent work by Sliv (63), (64) on the effect of the finite size of the nucleus on internal conversion coefficients has shown that in some cases at least nuclear wave functions are important.

admixtures of other multipolarities in the case of a transition involving two (or more) multipolarities cannot be detected by internal conversion coefficient measurements.

If the spin and parity of the ground state are known, definite parities and a restricted number of possible spins may be assigned to the excited states from a knowledge of multipolarities. A number of ground-state spins have been measured[3] and a recent tabulation has been given by Blin-Stoyle (52). A study of the measured spins yields certain general empirical rules which aid in predicting ground state spin. One such rule, with no known exceptions (1) is: the spin of an even-even nucleus is zero. The class of even-even nuclei comprises approximately 75 per cent of the stable nuclei. If the spin has not been directly measured and if no empirical rule exists which is applicable, then a nuclear model may be used to predict the ground-state spin. The shell model has proved itself very valuable in this respect. The shell model is of further advantage because it accurately predicts the parity of the ground state.

Additional information which may aid in delimiting the spin of an excited state often may be obtained from even very crude measurements of the relative intensities of gamma radiations connecting the same nuclear states. Theoretical calculation shows an increase of gamma-ray transition probability (56) with an increase in energy but a decrease with an increase in multipolarity. If a choice of spin is available for a given nuclear excited state, it is profitable to see if transitions occur to all other

---

[3] A common method is the molecular beam technique perfected by Rabi (65).

states with spins very near the possible spins of the state considered. If some of the transitions do not occur, it may be possible to further eliminate some of the spin choices which were possible in the light of the multipolarity selection rules.

The application of gamma-gamma angular correlation techniques to the study of nuclear spin states is likely to prove profitable after the spin possibilities have been narrowed down to a few in number and after the dominant multipolarity of the gamma transition is known. This method offers the distinct advantage of being able to determine with good precision the exact mixing of the radiations in those cases of an admixture of two radiations. A discussion of the theory underlying this method of determination of spins is given in Chapter 5.

The determination of the spin and parity of the radioactive parent nucleus which decays by beta emission requires a knowledge of the properties of the beta decay connecting the parent with the daughter nucleus. The theory of beta decay is discussed in many books (57), (59), (14), (66) and only a summary of the pertinent results will be mentioned here.

Fermi's theory of beta decay predicts on the assumption of zero rest mass for the neutrino the following energy spectrum for the beta particles:

$$N(W)dW \sim W\sqrt{W^2 - 1}\,(W_o - W)^2 dW,$$

where W is the beta energy (in units of mc^2) and W_o is the maximum energy. The experimentalist wishes to determine W_o; he does so by making a Fermi plot. Consider

$$F(W) = \sqrt{\frac{N(W)}{W(W^2 - 1)^{1/2}}}$$

Then $F(w) \sim W_o - W$ and a plot of $F(W)$ as a function of W yields a straight line for allowed transitions cutting the axis at W_o. A first order calculation gives the transition probability or the reciprocal of the lifetime to be:

$$1/\tau = G^2 \frac{mc^2}{2\pi^3 \hbar} \left|M^2\right| F(W_o)$$

where τ is the life time, G describes the interaction strength between electron and neutrons, M is the matrix element of the transition and

$$F(W_o) = \int_1^{W_o} W\sqrt{W^2 - 1}\ (W_o - W)^2\, dW.$$

A more detailed calculation shows $F(W_o)$ is also a function of the nuclear charge $F(Z, W_o)$. Beta decay is subject to certain selection rules just as in atomic spectra. Beta transitions are classified by the terms: allowed, first forbidden, second forbidden, etc. according to the value of the matrix element M. M is approximately 1 for allowed transitions. From the expression for the reciprocal of the lifetime it may be seen that the value of $\tau F(Z, W_o)$ (usually abbreviated ft) should be approximately constant for a given class of interactions. Even though the theory of beta decay is far from complete, the class of a given beta interaction is characterized by selection rules governing the spin and parity change in the decay. Table 4 shows the selection rules.

Table 4. Beta-Decay Selection Rules

Classification	Nuclear Spin Change	Nuclear Parity Change
Allowed	$0, \pm 1$	No
First Forbidden	$0, \pm 1, \pm 2$	Yes
Second Forbidden	$\pm 2, \pm 3$	No

In summary, the experimentalists may determine the maximum energy of a beta group by making a Fermi plot. In addition from the log ft values the class of decay may be determined and limitation may be placed on the spin and parity changes in the beta decay from the selection rules. As in the case of gamma transitions further limitations may be placed by observing the relative intensities of the beta groups. The lack of a particular transition implies a higher order of forbiddenness and therefore a larger spin change than in the observed transition (see Chapter I).

APPENDIX B

ANALYSIS OF COINCIDENCE DATA

The major correction in coincidence work was for the accidental background due to the finite resolving time of the coincidence circuit. The resolving time is determined from the accidental rate with a delay inserted in one channel. The accidental rate is very low, and long counting times are necessary to accurately determine the resolving time. By checking the accidental rate periodically throughout the experiment, a large number of counts are accumulated for the resolving time determination, and furthermore, periodic checks are obtained on the proper operation of the coincidence circuit.

Table 5 is a sample of the recorded data and the necessary analysis for one day's data on the coincidence spectrum with the 468 kev gamma-ray. The calculations required to analyze the data as shown in the table are described below.

1. The value of 2τ (τ = resolving time of the apparatus) is calculated for each run in which a delay of 0.45 microsecond was inserted in one channel. This calculation is made utilizing the expression $N_{acc} = 2\tau N_1 N_2$ where N_{acc} = accidental coincidence counting rate observed, N_1 = counting rate observed on spectrometer number 1, N_2 = counting rate observed on spectrometer number 2.

2. The average value of 2τ , ($\overline{2\tau}$), is calculated for the day. If trends indicating something other than statistical fluctuations in the calculated resolving times were observed, data for that day would be discarded, but, fortunately, no such cases arose. When accidental

Table 5. Sample of the Recorded Data and Analysis for the Gamma Coincidence Spectrum with the 468 Kev Gamma Rays

Spectrometer No. 1 Pulse Height Anal. Setting	Spectrometer No. 1 Singles Counts ÷ 256 N_1	Spectrometer No. 2 Pulse Height Anal. Setting	Spectrometer No. 2 Singles Counts ÷ 256 N_2	Variable Delay Micro-Second	Counting Interval Second	Discriminator Setting on Spect. No. 1	Product of the Singles Counts on 1 and 2 N_1N_2	Total Number of Coinc. Ncc.	Total Number of Accidental Coinc. Nacc.	Total Number of Real Coinc. N_R	Total Number of Real Coinc. ÷ Singles Count on Spect. 2: $N_R/N_2 \times 10^5$	Micro-Second 2τ
50	1921	400	7668	0.000	900	2.1	1473	550	259	291	379	
70	2007	410	7841	0.000	900	3.9	1574	704	277	427	545	
90	2570	400	8440	0.000	900	4.0	2169	1034	382	652	773	
110	3061	400	8324	0.000	900	5.3	2548	1174	449	725	871	
110	3086	398	8407	0.45	900	5.3	2594	481	481	0	----	0.254
130	2534	398	8303	0.000	900	7.0	2104	976	370	606	730	
150	2043	405	8082	0.000	900	8.7	1651	709	291	418	518	
170	1901	402	8168	0.000	900	10.4	1553	650	274	376	460	
190	1514	402	8010	0.000	900	12.6	1213	580	214	366	457	
190	1516	400	8007	0.45	900	12.6	12.4	225	225	0	----	0.255
210	1274	400	7930	0.000	900	12.6	1010	534	178	356	449	
230	1676	405	7905	0.000	900	13.0	1325	764	234	530	670	
250	3019	403	8215	0.000	900	14.3	2480	1339	437	902	1098	
250	3008	400	8216	0.45	900	14.3	2471	509	509	0	----	0.283
270	5311	403	8079	0.000	900	15.2	4290	1949	756	1193	1477	
290	8524	405	8155	0.000	900	16.9	6951	2821	1225	1596	1957	
290	8723	403	8158	0.45	900	16.9	7116	1054	1255	0	----	0.204
310	8049	410	8066	0.000	900	18.9	6492	3062	1145	1917	2377	
330	3409	410	7976	0.000	900	20.5	2719	1368	476	889	1115	
330	3272	400	7916	0.45	900	20.5	2590	408	408	0	----	0.216
350	916	407	7945	0.000	900	22.1	728	334	128	206	259	

determinations are made at different energies on one spectrometer, then $\overline{2\tau}$ is determined by weighting each determination according to the singles counting rate obtained at that energy.

3. The product $N_1 N_2$ is calculated for each run.

4. The number of accidental coincidence counts, $N_{acc.}$, which are contained in each run of duration T is calculated utilizing the expression

$$N_{acc.} = \frac{\overline{2\tau} N_1 N_2}{T} .$$

5. The number of real coincidence counts N_R, in each run is determined by subtracting $N_{acc.}$ from the total number of coincidence counts observed in one run, $N_{cc.}$.

6. The ratio N_R/N_2 is calculated for each run. It is necessary to normalize to the counting rate on the fixed spectrometer, N_2, to correct for small shifts in N_2 due to electronic drifts in the spectrometer. The ratio N_R/N_2 represents the number of coincidences observed at a given energy (as determined by the energy setting of the channel that counts N_2) per gamma-ray detected in spectrometer number two. This also corrects for the decay of the source with time.

7. Finally, N_R/N_2 and N_1 are plotted versus the pulse height base line setting on spectrometer number one (essentially the energy of the gamma-ray detected by counter number one). A curve as shown in Fig. 7 results. The N_1 plot may now be used as a reference for energy calibration.

The above discussion has described the analysis of gamma-gamma coincidence data. The analysis of beta-gamma data is similar with the

added complication of undesirable gamma-gamma coincidences which must be subtracted from the total coincidence rate. The analysis proceeds as in the case of gamma-gamma work up through step 4 as described above. In general at this point one must determine the number of gamma-gamma coincidence counts $N_{\gamma\gamma}$, which are present and calculate

$$N_R = N_{cc.} - N_{acc.} - N_{\gamma\gamma} .$$

However, in the beta-gamma coincidence work described in this thesis it was observed that, when the lucite absorber was inserted to determine the gamma-gamma background, the coincidence rate was reduced to such an extent that no gamma-gamma correction was needed. Therefore, the data analysis was done as described above in steps 1 through 6. However, the best way to present the data is not as in 7 but in the form of a Fermi plot, and this method will be discussed in Appendix E.

APPENDIX C

COINCIDENCE COUNTING

The object of this discussion is the determination of the optimum way in which coincidence counting experiments should be performed in order to secure the maximum precision for a prescribed total counting time. The source strength and the way in which the counting time should be divided amongst the various types of counts, e.g. total coincidences, accidental determination, etc., will be discussed. In section 1 a list of symbols is given. In sections 2 and 3 a simple beta-gamma coincidence experiment is investigated, and sections 4 and 5 discuss a problem based on a beta-gamma angular correlation experiment. In either case the results can be applied to other experimental problems, i.e. gamma-gamma experiments.

1. Symbols.--Assume counter number 1 counts beta particles and counter number 2 counts gamma-rays. The experimental problem to be investigated is the determination of the real beta-gamma coincidence counting rate. Complications arise because both counters detect unwanted background coincidences due to cosmic rays and radioactivity in the surroundings. Further complications arise because the beta counter detects some gamma-rays, giving a number of gamma-gamma coincidences and because the coincidence circuit has a finite resolving time, giving a number of accidental coincidences. The following notation is used throughout this appendix:

N_1 - singles rate, due to source only, counted by counter number 1

N_2 - singles rate, due to source only, counted by counter number 2

N_1' - singles rate, total, counted by counter number 1

N_2' - singles rate, total, counted by counter number 2

n - total coincidence rate

g - coincidence rate when absorber is placed in front of beta counter to absorb out all the beta particles

b - background coincidence rate if no source is present

a_n' - coincidence rate when a delay is inserted in one channel

a_n - computed accidental rate when n is counted

a_g - computed accidental rate when g is counted

a_b - computed accidental rate when b is counted

t - time spent counting n (at a particular angle in section 4)

t_g - time spent counting g (at a particular angle in section 4)

t_a - time spent counting a_n'

T - total counting time

τ - resolving time of the coincidence circuit

a - defined by the equation $a = a_n - a_g$

r - real beta-gamma coincidence rate $(r = n - g - a)$[1]

c - beta-gamma coincidence rate normalized to the singles rate on counter number 2 $(c = r/N_2)$

The statistical error in any rate is indicated by prefixing the symbol Δ to the rate. For large numbers of counts the counting distribution is approximately Gaussian, and it is assumed that the statistical error is the square root of the total number of counts obtained (43). In general, the singles rates are always very much greater than the coincidence rates; therefore, the relative error in the singles rate may be neglected.

---

[1]Notice that the background coincidence rate, b, is contained in g. Further g includes a_g, but a_n also includes a_g.

2. Simple coincidence experiment -- counting times.--The quantity to be determined in a simple beta-gamma coincidence experiment is the beta-gamma coincidence rate normalized to one of the singles rates due to the source, i.e. c, where

$$c = r/N_2 = \frac{n-g-a}{N_2} . \qquad (1)$$

The statistical errors in n, g, and a are truly independent because of the way in which each of these quantities is determined. The observed total coincidence rate n is counted for a period of time, t, resulting in nt counts. The relative error in nt is

$$\frac{\sqrt{nt}}{nt} = (nt)^{-1/2}; \text{ thus}$$

$$\Delta n = (nt)^{-1/2} (n) = (n/t)^{1/2}. \qquad (2)$$

The rate g is determined by placing an absorber in front of the beta counter and counting for time t_g. The rate g includes gamma-gamma coincidences, background coincidences, and accidentals. The relative error in $n_g t_g$ is

$$(n_g t_g)^{-1/2}; \text{ thus}$$

$$\Delta g = (g/t_g)^{1/2} .$$

Each accidental correction is made using the relation $a_i = 2N_1' N_2' \tau$ ($a_i = a_n$ or a_g). Assuming the statistical errors in the singles rates are negligible the error in a_i is entirely due to the error in τ. τ is commonly determined by an independent measurement, e.g. by insertion of a suitable time delay in one channel. It may be noted that

this delay method also eliminates all true coincidences due to the background. If the delay method is used (as is the case in this research), then τ is determined by counting the accidental rate, a_n', for a time t_a. The relative error in τ, $\frac{\Delta\tau}{\tau}$, is given by

$$\frac{\Delta\tau}{\tau} = \frac{(a_n' t_a)}{a_n' t_a} = (a_n' t_a)^{-1/2}.$$

The error in a ($a = a_n - a_g$) is given by

$$\Delta a = \frac{a}{(a_n' t_a)^{1/2}} .$$

From the above discussion one can see that n, g, and a are determined by three independent measurements, and therefore, the errors are mutually independent.

The relative error in c can now be given as

$$(\frac{\Delta c}{c})^2 = \left[(\Delta n)^2 + (\Delta g)^2 + (\Delta a)^2\right] \frac{1}{N_2^2 c^2} = \frac{n/t + g/t_g + \frac{a^2}{a_n' t_a}}{r^2} \quad (3)$$

In order to determine the optimum counting time, one must minimize $(\frac{\Delta c}{c})^2$ subject to the constraint that $T = t + t_g + t_a$. Using the method of Lagrangian multipliers (67), one obtains the three equations

$$t^2 = \frac{n}{\lambda r^2} \quad (4)$$

$$t_g^2 = \frac{g}{\lambda r^2}$$

$$t_a^2 = \frac{a^2}{\lambda a_n' r^2}$$

where λ is a Lagrangian multiplier. The solution of the system of equations (4) combined with the constraint equation yields expressions for the optimum counting times in terms of readily determined counting rates:

$$T/t = 1 + \frac{\sqrt{g} + \frac{a}{\sqrt{a'_n}}}{\sqrt{n}} \tag{5a}$$

$$T/t_g = 1 + \frac{\sqrt{n} + \frac{a}{\sqrt{a'_n}}}{\sqrt{g}} \tag{5b}$$

$$T/t_a = 1 + \sqrt{\frac{a'_n}{a}}\ (\sqrt{n} + \sqrt{g}\ ) . \tag{5c}$$

The relations obtained in this section may be applied to gamma-gamma coincidence work if r is interpreted as the gamma-gamma coincidence rate. Of course, no absorber experiment to determine g is required; however, in its place an experiment to determine the background rate b may be necessary. The equations (5) then become

$$T/t = \frac{1 + \sqrt{b} + a/\sqrt{a'_n}}{\sqrt{n}} \tag{6a}$$

$$T/t_b = \frac{1 + \sqrt{n} + a/\sqrt{a'_n}}{\sqrt{b}} \tag{6b}$$

$$T/t_a = 1 + \sqrt{\frac{a'_n}{a}}\ (\sqrt{n} + \sqrt{b}\ ). \tag{6c}$$

If the background coincidence rate is negligible and if the background singles rates are so low that the accidental coincidences due to the background are negligible, then $b = 0$; $a_b = 0$ and $a = a_n - a_b = a_n$. In

this case

$$T/t = 1 + \frac{a_n/\sqrt{a_n'}}{\sqrt{n}}$$

$$T/t_a = 1 + \sqrt{a_n'}/a_n \quad (\sqrt{n}) \ .$$

noticing that $a_n = a_n'$,[2] the equations become

$$T/t = 1 + \sqrt{a_n/n} \tag{7a}$$

$$T/t_a = 1 + \sqrt{n/a_n} \ . \tag{7b}$$

3. Simple coincidence experiment -- source strength.--In order to investigate the effect of the source strength on the precision it is necessary to express $(\Delta c/c)^2$ in terms of the source strength S. One needs to consider the relationship between n, a, and g and S.

The total coincidence rate n is the sum of three terms. The first term represents the total real coincidence rate due to the source; the second term the total accidental rate due to the source; the third term the total coincidence rate due to the background. It is well known (43) that these terms are functions of the source strength as follows: the real rate due to the source is proportional to S; the accidental rate due to the source is proportional to S^2; the background rate is independent of S; therefore,

$$n = w_n S + w_1 S^2 + b, \tag{8}$$

---

[2]The symbols a_n and a_n' were both introduced because a_n' represents an observed quantity and a_n represents a calculated quantity. In all cases a_n and a_n' are assigned the same numerical value.

where w_n and w_1 are proportionality factors depending upon the efficiency of the counters (including any effect due to a finite window width if a pulse height analyzer is used), the solid angles subtended by the counters, the loss of radiations due to absorption and scattering, and branching ratios pertinent to the radiation detected. The quantity g is composed of terms similar to n and can be written as:

$$g = w_g S + w_2 S^2 + b. \tag{9}$$

a_n and a_g are composed of two terms and may be written as:

$$a_n = w_1 S^2 + a_b \tag{10}$$

$$a_g = w_2 S^2 + a_b \, . \tag{11}$$

Therefore,

$$a = a_n - a_g = (w_1 - w_2) S^2 \, . \tag{12}$$

Using equation (3) and the above relations one obtains

$$\left(\frac{\Delta c}{c}\right)^2 = \frac{1}{(w_b - w_g)^2} \left[\frac{w_1}{t} + \frac{w_2}{t_g} + \frac{(w_1 - w_2)^2}{(w_1 + a_b/S^2)t_a} + 1/S\left(\frac{w_n}{t} + \frac{w_g}{t_g}\right) + 1/S^2(b/t + b/t_g) \right] . \tag{13}$$

The precision is improved by using an arbitrarily strong source if the term in a_b/S^2 is neglected, in which case the terms $1/S$ and $1/S^2$ do not make appreciable contribution. However, little is gained after the source is sufficiently strong to make the error contributed by terms independent of S approximately equal to the error contributed by the

term dependent upon S (3). The behavior of $\Delta c/c$ as a function of S is best illustrated by consideration of a simple case in which there is no background and no interference in the beta-gamma experiment from gamma-gamma coincidences. In this approximation $w_g = w_2 = b = g = a_b = 0$ and $a = a_n' = a_n$. Consideration of w_1 and w_n as determined by equations (8) and (9) shows that in the above approximation $w_1/w_n = 2\tau$ subject to simplifying assumptions about the particular radiation detected by the counters.[3] For these conditions equation (13) becomes

$$(\frac{\Delta c}{c})^2 = \frac{2\tau + 2\tau t/t_a + 1/S}{w_n t} . \qquad (14)$$

If one further assumes that the optimum counting times are used in (14), one obtains

$$(\frac{\Delta c}{c})^2 = \frac{2\tau}{w_n} \frac{1}{t} \left[1 + (\frac{2\tau S}{2\tau S + 1})^{1/2} + \frac{1}{2\tau S} \right] = K^2 \qquad (15)$$

$$\left[1 + (\frac{p}{1+p})^{1/2} + 1/p \right] .$$

where

$$K^2 = \frac{2\tau}{w_n t} \text{ and } p = 2\tau S.$$

Inspection of (15) reveals certain well known relations (43): the precision is improved by making the resolving time, τ, short; or by

---

[3] $n = w_n s + a_n$. $a_n = w_1 s^2$. $n - a_n = r$. $w_1/w_n = a_n/Sr$, but $r = N_1 N_2/S$ if one assumes that N_1 and N_2 include only contributions that can lead to real coincidences. Also $a_n = 2\tau N_1 N_2$. Therefore, $w_1/w_n = \frac{2\tau N_1 N_2}{S(N_1 N_2/S)} = 2\tau$.

making w_n large, which requires that the counter efficiencies and/or solid angles be made large.

The dependence of the error $\Delta c/c$ (in terms of K) upon the parameter p is given in Fig. 16. For $p = 1, (S = 1/2\zeta)$, almost maximum precision is obtained. For this value of S, $n/a_n = 2$. That is, the accidental coincidence rate is equal to the real coincidence rate. In this case relations (5) for the optimum counting times are $T/t = 1.7$ and $T/t_a = 2.4$. One should, therefore, spend 60 per cent of the time counting total coincidences and 40 per cent of the time counting accidental coincidences.

4. Angular correlation experiment -- counting times.--In the determination of beta-gamma angular correlation coefficients knowledge of the absolute coincidence rates at various angles is not essential. The required quantity is the ratio of the coincidence rates at the angle Θ to that at some reference angle, say 90°. When pertinent, the angle between the counters is indicated in parenthesis, e.g. $n(\Theta)$ is the total coincidence rate observed for an angle Θ. It is usually best to normalize coincidence rates to the product of the singles rates in angular correlation work in order to better compensate for instrumental drifts and changes in solid angle subtended with variation in angle between the counters. (This overcorrects for the decay of the source.) The quantity to be measured is thus:

$$R \equiv \frac{r(\Theta)}{r(90)} f = \frac{n(\Theta) - g(\Theta) - a(\Theta)}{n(90) - g(90) - a(90)} f \qquad (16)$$

where

$$f = \frac{N_1(90)N_2(90)}{N_1(\Theta)N_2(\Theta)} \quad \text{(usually } f = 1\text{)}$$

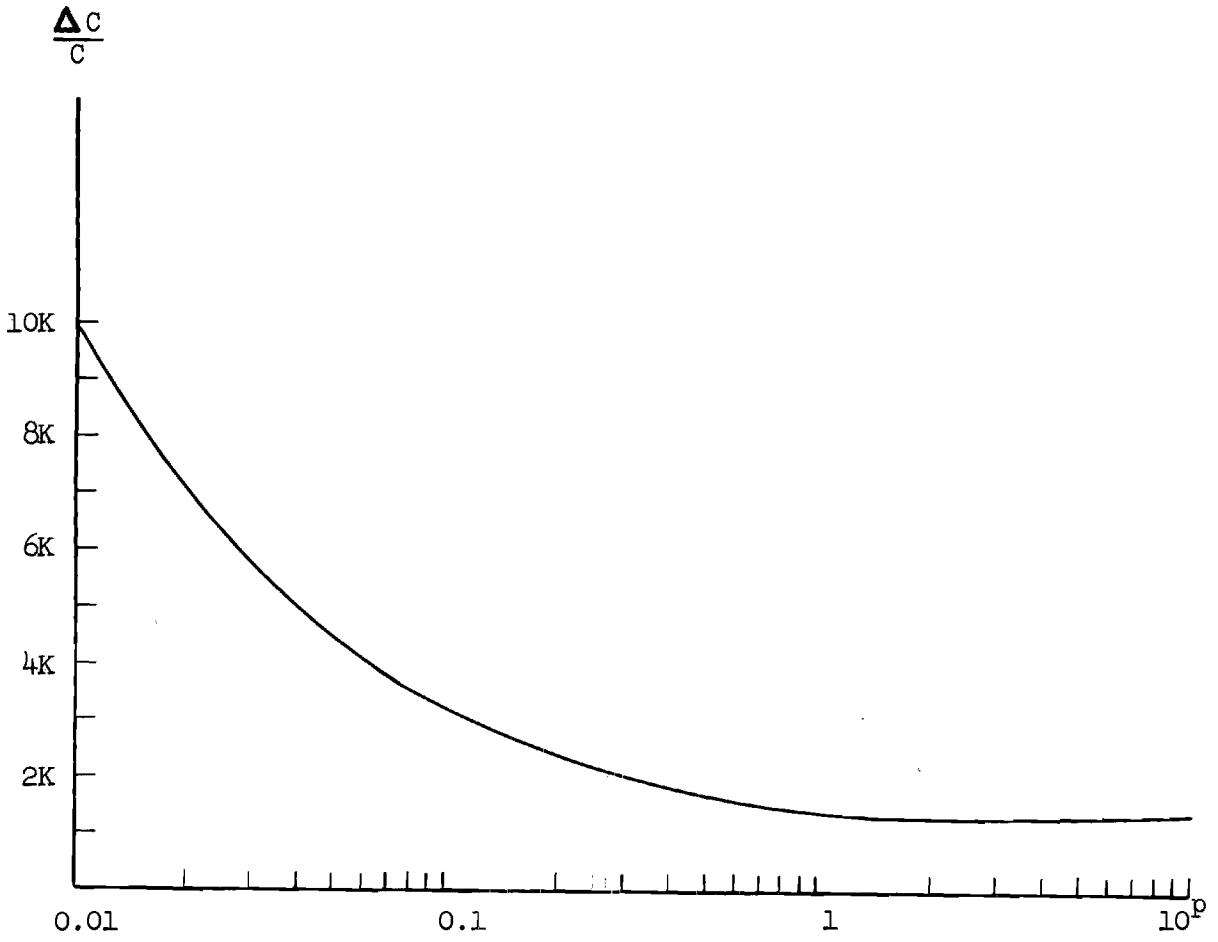

Figure 16. Relative Statistical Error in the Coincidence Rate Versus p

The error in $a(\Theta)$ is not independent of the error in $a(90)$ because both are computed from the same data -- namely, the resolving time of the coincidence circuit. In fact $a(\Theta) = a(90)/f$. We assume throughout that singles rates contain negligible statistical error; therefore, f is exactly known.

The errors in $g(\Theta)$ and $g(90)$ may be independent or, in some experiments, we may have apriori knowledge of how $g(\Theta)$ depends on angle. For example, the gamma-gamma angular correlation that is interfering with the beta-gamma experiment may be known. In the latter event we define G by the relation:

$$G = \frac{g(\Theta)}{g(90)} f \tag{17}$$

We carry through the subsequent analysis for the case in which errors in $g(\Theta)$ and $g(90)$ are treated as independent and the case in which they are not independent. Equations that refer to the latter condition will be indicated by a prime attached to the equation number. Such equations may also be recognized by the appearance of the quantity G. The independent errors in R due to statistical errors in $n(\Theta)$, $n(90)$, $g(\Theta)$, $g(90)$, and $a(90)$ are, respectively, $f\Delta n(\Theta)/r(90)$, $R\Delta n(90)/r(90)$, $f\Delta g(\Theta)/r(90)$, $R\Delta g(90)/r(90)$, and $(R-1)\Delta a(90)/r(90)$. If $g(\Theta) = g(90)/f$ the independent errors in R are $f\Delta n(\Theta)/r(90)$, $R\Delta n(90)/r(90)$, $(R-G)\Delta g(90)/r(90)$, and $(R-1)\Delta a(90)/r(90)$.

The statistical error in R, ΔR, is the quantity to be minimized and it may be written in the usual way as:

$$(\Delta R)^2 = \frac{f^2\Delta n(\Theta)^2+R^2\Delta n(90)^2+f^2\Delta g(\Theta)^2+R^2\Delta g(90)^2+(R-1)^2\Delta a(90)^2}{r(90)^2} \tag{18}$$

$$(\Delta R)^2 = \frac{f^2 \Delta n(\Theta)^2 + R^2 \Delta n(90)^2 + (R-G)^2 \Delta g(90)^2 + (R-1)^2 \Delta a(90)^2}{r(90)^2} . \quad (18')$$

The errors are given by expressions similar to those used in section 2. We express ΔR in terms of the counting times:

$$(\Delta R)^2 = \frac{1}{r(90)^2} \left[f^2 \frac{n(\Theta)}{t} + R^2 \frac{n(90)}{t} + f^2 \frac{g(\Theta)}{t_g} + \frac{R^2 g(90)}{t_g} + \frac{(R-1)^2 a(90)^2}{a_n(90) t_a} \right] \quad (19)$$

$$(\Delta R)^2 = \frac{1}{r(90)^2} \left[f^2 \frac{n(\Theta)}{t} + R^2 \frac{n(90)}{t} + \frac{(R-G)^2 g(90)}{t_g} + \frac{(R-1)^2 a(90)^2}{a_n(90) t_a} \right] . \quad (19')$$

We minimize these relations with respect to t, t_g, and t_a subject to the restriction that $T = 2t_g + t_a$ (t and t_g represent the time spent counting coincidences at one angle; $2t$ or $2t_g$ is the total time spent at both angles). We obtain three equations, where λ is a Lagrangian multiplier:

$$t^2 = \frac{1}{2\lambda r(90)^2} \left[f^2 n(\Theta) + R^2 n(90) \right] \quad (20)$$

$$t_g^2 = \frac{1}{2\lambda r(90)^2} \left[f^2 g(\Theta) + R^2 g(90) \right]$$

$$t_a^2 = \frac{1}{\lambda r(90)^2} \frac{(R-1)^2}{a(90)^2} \frac{a(90)^2}{a_n(90)}$$

$$t^2 = \frac{1}{2\lambda r(90)^2} \left[f^2 n(\Theta) + R^2 n(90) \right] \quad (20')$$

$$t_g^2 = \frac{1}{2\lambda r(90)^2} (R-G)^2 g(90)$$

$$t_a^2 = \frac{1}{\lambda r(90)^2} (R-1)^2 \frac{a(90)^2}{a_n(90)} .$$

The results are much simplified by noting that most angular distributions are almost isotropic; hence, in sums, we can put $n(\Theta) = n(90) = n$; $g(\Theta) = g(90) = g$; and $f = R = 1$; except the factor $(R - 1)$ and $(R - G)$ must be retained. We also drop the angle designations on a and a_n. Combination of relations (12) with the expression for T yields expressions for the optimum counting times in terms of readily determined quantities.

$$T/t = 2 + 2\sqrt{g/n} + (R - 1)\, a/\sqrt{n\, a_n} \tag{21a}$$

$$T/t_g = 2 + 2\sqrt{n/g} + (R - 1)\, a/\sqrt{g\, a_n} \tag{21b}$$

$$T/t_a = 1 + \frac{2\sqrt{n a_n}}{(R - 1)a} + \frac{2\sqrt{g a_n}}{(R - 1)a} \tag{21c}$$

$$T/t = 2 + \sqrt{2}\,(R - G)\sqrt{g/n} + (R - 1)\, a/\sqrt{n\, a_n} \tag{21'a}$$

$$T/t_g = 2 + \frac{2\sqrt{2}}{(R - G)}\sqrt{\frac{n}{g}} + \frac{2\,(R - 1)}{(R - G)}\,\frac{a}{\sqrt{g\, a_n}} \tag{21'b}$$

$$T/t_a = 1 + \frac{2\sqrt{n a_n}}{(R - 1)a} + \frac{\sqrt{2}\,(R - G)}{(R - 1)}\,\frac{\sqrt{g\, a_n}}{a} \tag{21'c}$$

These results are similar (except for trivial factors of 2 due to the new definition of T) to those of section 2, except for the factors $(R - 1)$ and $(R - G)$. The factor $(R - 1)$ is a consequence of the fact that an error in the resolving time determination tends to cancel out because it affects both numerator and denominator in the expression for R. In the limit of an isotropic angular distribution there is no need to spend time counting accidentals. The factor $(R - G)$ is also a consequence of the non-independence of errors in g that appear in both numerator and denominator of the expression for R.

The relations obtained in this section may be applied to gamma-gamma work by putting $g = 0$, then $a = a_n$, where it is assumed that no appreciable interference in the angular correlation work results from background due to cosmic rays and the surroundings.

5. Angular correlation experiment -- source strength.--We examine only the case in which $g(\Theta)$ and $g(90)$ are treated as independent. Equation (11) is now expressed in terms of the source strength, with the approximations introduced that $n(\Theta) = n(90) = n$; $g(\Theta) = g(90) = g$; $f = R = 1$ except that $(R - 1)$ is retained.

$$(\Delta R)^2 = \frac{1}{(w_n - w_g)^2}\left[\frac{2w_1}{t} + \frac{2w_2}{t_g} + \frac{(R-1)^2(w_1 - w_2)^2}{t_a(w_1 + a_b/S^2)} + \frac{1}{S}\left(\frac{2w_n}{t} + \frac{2w_g}{t_g}\right) + \frac{1}{S^2}\left(\frac{2b}{t} + \frac{2b}{t_g}\right)\right] \quad (22)$$

This expression is essentially like (13) considered in section 3; hence the conclusions drawn there about the source strength still apply.

APPENDIX D

ANALYSIS OF ANGULAR CORRELATION DATA

The purpose of this analysis is to determine the coefficients A_2 and A_4 in the correlation functions.

$W(\Theta) = 1 + A_2P_2(\cos\Theta) + A_4P_4(\cos\Theta)$ as defined in Chapter I. It is assumed that higher order terms may be neglected.[1]

As in the case of coincidence spectra determinations data are analyzed on a day to day basis.[2] During the course of a day approximately equal amounts of time are spent taking data at each angle. Table 6 is a sample of one day's data and the necessary analysis of this data for the 600-300 kev angular correlation experiment. The calculations required to analyze the data as shown in the table are described below.

1. The value of 2τ (τ = resolving time of the apparatus) is calculated for each run in which a delay is inserted. The calculation utilizes the expression

$$N_{acc.} = \frac{2\tau N_1 N_2}{T}$$

$N_{acc.}$ = accidental coincidence counts observed during a run of duration T.

---

[1] The determination of higher order terms if they exist requires greatly improved angular resolution. Chapter V discusses restrictions on the highest order term which may appear.

[2] For the angular correlation experiments described in this thesis the data are normalized to the product of both the singles counting rates since small drifts in amplifier gain affect these rates. This overcorrects for the decay of the source. Therefore, it is necessary to analyze the data in periods of time which are short as compared to the half-life of the source or make an explicit correction for the decay of the source.

Table 6. Sample of Recorded Data and Analysis for the Gamma-Gamma Angular Correlation in the 600-300 kev Cascade

Spectrometer No.1 Pulse Height Anal. Setting	Singles Counts ÷ 256 N_1	Spectrometer No.2 Pulse Height Anal. Setting	Singles Counts ÷ 256 N_2	Variable Delay Micro-Second	Counting Interval Seconds	Angle Degrees	Product of Singles Counts on 1 and 2 ÷ 10^4 N_1N_2	Total Number Coinc. N_{cc}	Total Number Accidental Coinc. N_{acc}	Total Number Real Coinc. N_R	2τ Micro-Second	Total Number of Reals ÷ $N_1N_2 \times 10^4$ N_R/N_1N_2
402	1594	295	9093	0.00	900	90°	1449	363	148	215	-----	1484
404	1557	295	9571	0.00	900	180°	1490	334	152	182	-----	1221
404	1570	295	9322	0.45	900	180°	----	113	---	---	0.106	----
405	1488	295	9426	0.00	900	135°	1403	339	143	196	-----	1397
405	1659	295	9409	0.00	900	180°	1561	308	159	149	-----	955
406	1645	295	9391	0.00	900	270°	1545	379	158	221	-----	1430
406	1630	295	9733	0.45	900	270°	----	173	---	---	0.150	----
407	1547	297	9306	0.00	900	225°	1440	337	147	190	-----	1319
406	1436	296	9845	0.00	900	180°	1414	284	144	140	-----	990
404	1550	300	9037	0.00	900	90°	1401	315	143	172	-----	1228
402	1542	298	9456	0.00	900	135°	1458	329	149	180	-----	1235
402	1765	298	9690	0.45	900	135°	----	169	----	----	0.136	----
406	1691	302	9552	0.00	900	180°	1615	359	165	194	-----	1201
407	1645	305	9447	0.00	900	270°	1554	434	159	275	-----	1770
407	1367	305	9240	0.00	900	225°	1263	310	129	181	-----	1433
403	1544	303	9483	0.45	900	225°	----	158	---	---	0.148	----
401	1498	299	9146	0.00	900	180°	1370	265	140	125	-----	912
400	1614	298	9101	0.00	900	90°	1469	375	150	225	-----	1532
399	1554	293	9685	0.00	900	135°	1505	364	154	210	-----	1395
397	1664	295	9656	0.00	900	180°	1607	335	164	171	-----	1064
397	1664	295	9474	0.45	900	180°	----	143	---	---	0.124	----
397	1719	297	9605	0.00	900	270°	1651	403	168	235	-----	1423
399	1516	297	9277	0.00	900	225°	1406	334	141	193	-----	1373
399	1432	297	9015	0.45	900	225°	----	167	---	---	0.177	----

$2\tau = 0.140$ $(R/N_1N_2)_{90°,270°} = 1478$ $(R/N_1N_2)_{180°} = 1057$ $(R/N_1N_2)_{135°,225°} = 1359$

$N_{180°} = 0.7250$ $N_{135°} = 0.9195$

N_1 = counting rate observed on spectrometer number 1; N_2 = counting rate observed in spectrometer number 2.

2. The average value of 2τ, $(\overline{2\tau})$, is calculated as in step 2 of Appendix B.

3. The product N_1N_2 is calculated for each run.

4. The number of accidental coincidence counts, $N_{acc.}$, which are contained in each run is calculated.

5. The number of real coincidence counts, N_R, in each run is determined by subtracting $N_{acc.}$ from the total number of coincidence counts observed in one run, $N_{cc.}$, i.e.

$$N_R = N_{cc.} - N_{acc.}.$$

6. The ratio N_R/N_1N_2 is calculated for each run.

7. The average of the quantity N_R/N_1N_2 is calculated for each angular position and is denoted by

$$(\overline{N_R/N_1N_2})_{180°},\ (\overline{N_R/N_1N_2})_{90°,\ 270°},\ \text{or}\ (\overline{N_R/N_1N_2})_{135°,\ 225°}.$$

8. The data are normalized to 90° as follows:

$$N_{180°} = \frac{(N_R/N_1N_2)_{180°}}{(N_R/N_1N_2)_{90°,\ 270°}} \quad ; \quad N_{135°} = \frac{(N_R/N_1N_2)_{135°,\ 225°}}{(N_R/N_1N_2)_{90°,\ 270°}}$$

9. After the quantities $N_{180°}$ and $N_{135°}$ are calculated for each day the average of these quantities for the entire experiment is calculated. In determining this average the result from each day is weighed statistically according to the time spent counting coincidences during that day. From the number $N_{180°}$ and $N_{135°}$ the coefficients A_2 and A_4 are determined as follows:

$$W(90°) = 1 + A_2P_2(0) + A_4P_4(0) = 1 - 1/2A_2 + 3/8A_4$$

$$W(180°) = 1 + A_2P_2(-1) + A_4P_4(-1) = 1 + A_2 + A_4$$

$$W(135°) = 1 + A_2P_2(-.707) + A_4P_4(-.707) = 1 + 1/4A_2 - 13/32\ A_4;$$

therefore, $N_{180°} = \dfrac{1 + A_2 + A_4}{1 - 1/2A_2 - 3/8A_4}$, and $N_{135°} = \dfrac{1 + 1/4A_2 - 13/32A_4}{1 - 1/2A_2 + 3/8A_4}$.

Solving these two equations for A_2 and A_4 yields

$$A_2 = \frac{0.78125\ N_{180°} + 0.625\ N_{135°} - 1.40625}{0.109375\ N_{180°} + 0.875\ N_{135°} + 0.65625}, \text{ and}$$

$$A_4 = \frac{0.75\ N_{180°} - 1.5\ N_{135°} + 0.75}{0.109375\ N_{180°} + 0.875\ N_{135°} + 0.65625}.$$

The experimentally measured coefficients A_2 and A_4 represent a correlation which is the average of the true correlation over the finite angles subtended by the two detectors; therefore, it is necessary to correct the experimental coefficients before a comparison with theory is made. A method of estimating these geometrical corrections has been discussed by Rose (68). The necessary corrections are made by multiplying A_2 and A_4 by certain correction factors $1/J_2$ and $1/J_4$. These correction factors are actually products of factors corresponding to each detector as follows:

$J_2 = J_2(1)\ J_2(2)$ and $J_4 = J_4(1)\ J_4(2)$ where $J_2(1)$ or $J_2(2)$ refers to the correction of A_2 due to the finite angular resolution of detector number 1 or 2 and J_4 to the correction to A_4. These correction factors are functions of the following quantities:

r - radius of the crystal in the detector,

h - distance from the source to the front face of the crystal,

τ - absorption coefficient of the crystal for the particular gamma-ray energy being observed, and

t - thickness of the crystal.

Rose has tabulated J_2 and J_4 for crystals of size r = 1.9 cm. and t = 2.54 cm. with h = 7 cm. and h = 10 cm. and values of τ ranging from 0.123 $cm.^{-1}$ to 40.0 $cm.^{-1}$. Since h = 7 or 10 cm. does not apply to all the experiments performed in this research, it is necessary to make an interpolation or extrapolation of Rose's tables. In order to make this method more accurate, plots of J_2 and J_4 versus h for the case of total absorption of the gamma-ray have been drawn[3] and are shown in Fig. 17.

In order to make this discussion more concrete, the geometrical correction for the A_2 coefficient in a definite experiment, the 416-468 kev angular correlation experiment, will be calculated. If the two detectors are denoted by 1 and 2, then in this experiment h_1 = 5.2 cm., and h_2 = 4.7 cm. The approximation is made that $h_1 = h_2 = 5$ cm. Referring to Fig. 16, one observes that in the case of complete absorption $J_2(h = 5 \text{ cm.}) = 0.952\, J_2(h = 7 \text{ cm.})$. Next, it is necessary to compute the absorption coefficient in $cm.^{-1}$ of the NaI crystal for gamma-rays in the region of 400-500 kev energy. Using data published by National Radiac,

---

[3]The explicit form of J_2 and J_4 for the case of total absorption is as follows:

$$J_2 = \frac{P_1(X_o) - X_o P_2(X_o)}{(3)(1 - X_o)} \quad ; \quad J_4 = \frac{P_3(X_o) - X_o P_4(X_o)}{(5)(1 - X_o)} \quad ,$$

where $X_o = \cos\gamma$, $\gamma = \tan^{-1}\frac{r}{h}$ and $P_i(X_o)$ are the Legendre polynomials.

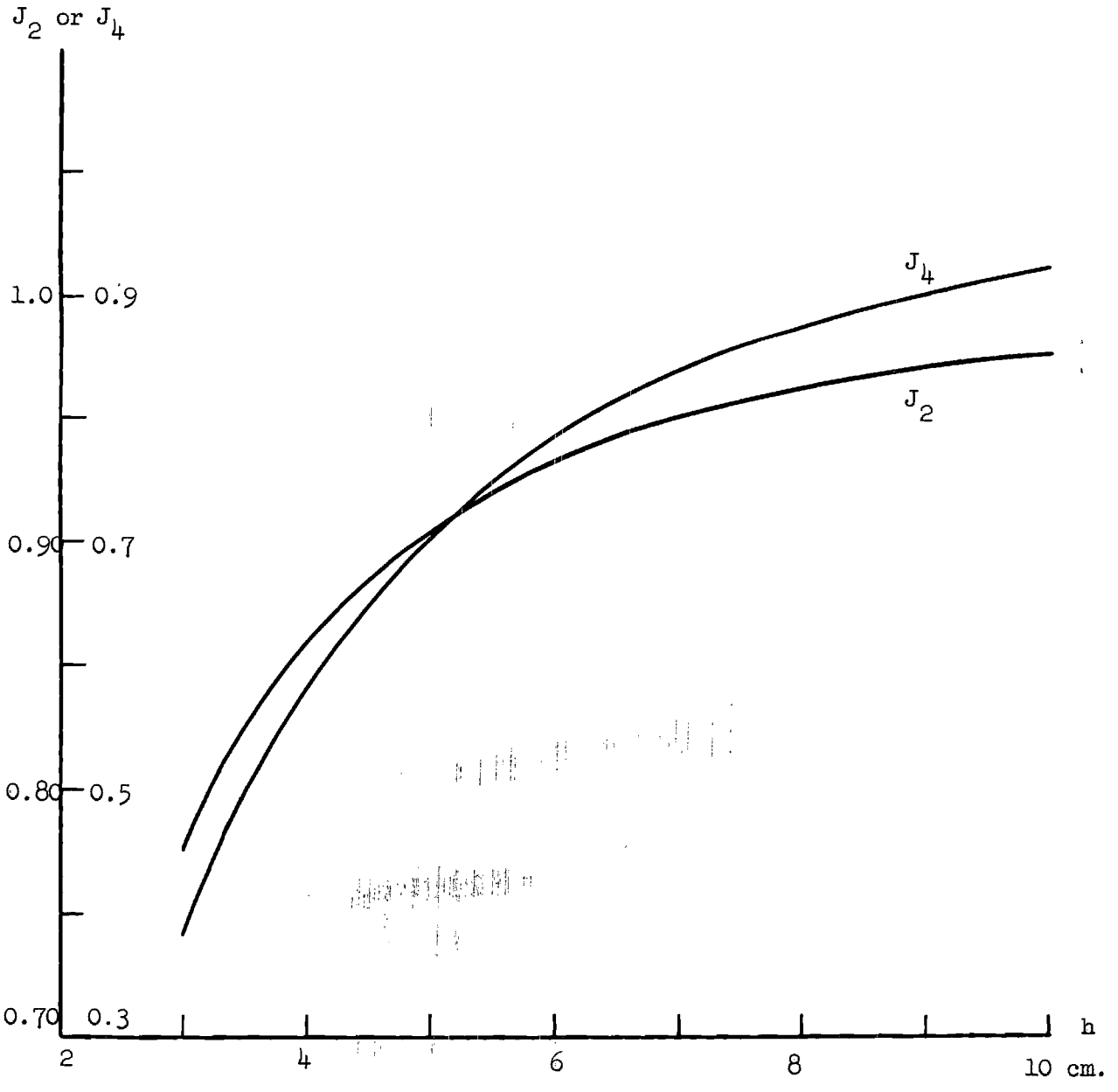

Figure 17. J_2 and J_4 Versus h for the Case of Infinite Absorption

Inc. (69) one finds that $\tau = 0.422$ cm.$^{-1}$ for a gamma-ray of energy 450 kev. It is not necessary to calculate τ to any great degree of accuracy since the correction factors do not vary rapidly with τ. Rose's tables give $J_2(h=7cm.) = 0.95851$ for $\tau = 0.300$ cm.$^{-1}$ and $J_2(h=7cm.) = 0.95565$ for $\tau = 1.000$ cm.$^{-1}$. Therefore, for $\tau = 0.400$ cm.$^{-1}$, $J2(h=7cm.) = 0.9581$. Using the relationship between $J_2(h=7cm.)$ and $J_2(h=5cm.)$ one calculates that $J_2(h=5cm.) = 0.912$ for $\tau = 0.400$ cm.$^{-1}$. Under the above approximations $J_2(1) = J_2(2)$ and $J_2(1)^2 = (0.912)^2 = 0.832$. Therefore, the experimental value of A_2 is to be multiplied by $1/0.832 = 1.202$ before comparing with the theoretical value.

If data are only taken at two angles, 90° (270°) and 180°, then the coefficients A_2 and A_4 cannot be determined. Instead the anisotropy ratio A defined by

$$A = \frac{N_{180°} - N_{90°,\,270°}}{N_{90°,\,270°}}$$

is calculated. It can be shown from the expression given earlier that

$$A = \frac{1.5A_2 + 0.625A_4}{1 - 0.5A_2 + 0.375A_4} \quad .$$

Using theoretical values for A_2 and A_4 one can then calculate the theoretical value of the anisotropy ratio and compare it with the experimentally determined quantity.

In beta-gamma angular correlation work the data are analyzed in a similar way to gamma-gamma angular correlation data. However, an additional correction due to the gamma-gamma coincidence background must be made. In general this correction should take into account the angular

correlation of this background; however, in all of the beta-gamma experiments performed in this research the gamma-gamma background was very low, approximately 1 per cent of beta-gamma rate, and it was not necessary to examine the angular correlation of this background. The gamma-gamma coincidence background correction is made as described in Appendix C. The remainder of the analysis is as described in the section on gamma-gamma angular correlation analysis. Furthermore, the geometrical correction may be handled in the same way as in gamma-gamma work noting that the beta detector is essentially one hundred per cent efficient and the analytic expressions for J_2 and J_4 given in footnote number 3 may be used.

APPENDIX E

FERMI PLOT ANALYSIS OF BETA DECAY DATA

In the theory of beta decay, it becomes evident that it is possible to devise coordinates such that an allowed beta-ray spectrum may be plotted as a straight-line graph (14) (see Appendix A). It has become common practice to use such coordinates also for transitions which are not allowed even though the graph may not be a straight line (66). Such a graph is called a Kurie plot or Fermi plot. The appropriate coordinates for a Fermi plot are as follows: The ordinate is taken to be $(N(W)W^{-2}/F(Z,W))^{1/2}$ where W represents the total energy of a beta particle in M_oC^2 units, N(W) is the number of beta particles emitted in the energy range extending from W to W + dW, and F(Z, W) is the Fermi function described in Appendix A. The abscissca is taken to be W in M_oC^2 units.

Table 7 shows the calculations necessary to obtain the Fermi plot pertaining to the 670 kev beta group arising in the decay of Ir^{192}. In the table, W is calculated from E (the kinetic energy of the beta particle in kev) using the relations $W = 1 + E/M_oC^2$ and $M_oC^2 = 511$ kev. The momentum (in MoC units) P is calculated from W using the relation $W = 1 + P^2$. The Fermi function F(Z, W) has been tabulated by Rose et al (70) in the form of (P/W)F(Z, P). N(W) is taken to be the real coincidence rate at the energy W, normalized to the singles rate on the gamma counter.

Table 7. Sample Calculations for the Fermi Plot Analysis of the 670 Kev Beta Group

E	W	P	F	R/N_1	$(\frac{R/N_1}{F})$	$(\frac{R/N_1}{F})^{1/2}$	$1/W$	$(\frac{R/N_1}{F})^{1/2}(\frac{1}{W})$
398	1.780	1.470	17.62	10 015	568.4	23.84	0.562	13.40
448	1.878	1.585	17.28	7 261	420.2	20.50	0.532	10.91
498	1.977	1.700	16.96	4 853	286.1	16.91	0.506	8.56
549	2.075	1.815	16.66	2 668	160.1	12.65	0.482	6.10
600	2.174	9.930	16.36	1 244	76.0	8.72	0.460	4.01
656	2.283	2.050	16.07	479	29.8	5.46	0.438	2.39
714	2.400	2.175	15.79	161	10.2	3.19	0.417	1.33

BIBLIOGRAPHY

BIBLIOGRAPHY

1. Mayer, M. G. and J. H. D. Jensen, Elementary Theory of Nuclear Shell Structure, New York: John Wiley and Sons, Inc., 1955.

2. Bohr, A. and B. R. Mottelson, "Collective Nuclear Motion and the Unified Model," in Beta- and Gamma-Ray Spectroscopy, ed. by K. Siegbahn, New York: Interscience Publishers Inc., 1955, pp 468-493.

3. Shiel, V., L. D. Wyly, and C. H. Braden, Physical Review, 105, (1957), 1521.

4. Frauenfelder, H., "Angular Correlation," in Beta- and Gamma-Ray Spectroscopy, ed. by K. Siegbahn, New York: Interscience Publishers Inc., 1955, pp 531-599.

5. Hamilton, D. R., Physical Review, 58, (1940), 122.

6. Dunworth, J. V., Reviews of Scientific Instruments, 11, (1940), 167.

7. Kibuchi, S., Y. Watese, and J. Stoh, Zeitschrift für Physik, 119, (1942), 185.

8. Goertzel, G., Physical Review, 70, (1946), 897.

9. Brady, E. L. and M. Deutsch, Physical Review, 72, (1947), 870.

10. Brady, E. L. and M. Deutsch, Physical Review, 74, (1948), 1541.

11. Brady, E. L. and M. Deutsch, Physical Review, 78, (1950), 558.

12. Biedenharn, L. C. and M. E. Rose, Reviews of Modern Physics, 25, (1953), 729.

13. Falkoff, D. L. and G. E. Uhlenbeck, Physical Review, 79, (1950), 334.

14. Rose, M. E., "The Theory of Allowed Beta-Decay," Beta- and Gamma-Ray Spectroscopy, ed. by K. Siegbahn, New York: Interscience Publishers Inc., 1955, pp 273-291.

15. Fuchs, M. and E. S. Lennox, Physical Review, 79, (1950), 221.

16. Yamada, M. and M. Morita, Progress in Theoretical Physics, 8, (1952), 431.

17. Morita, M. and M. Yamada, Progress in Theoretical Physics, 10, (1953), 111.

18. Morita, M., Progress in Theoretical Physics, 10, (1953), 363.

19. Morita, M. and M. Yamada, Progress in Theoretical Physics, 10, (1953), 161.

20. Fugita, J., M. Morita, and M. Yamada, Progress in Theoretical Physics, 11, (1954), 219.

21. Novey, T. B., M. S. Freedman, F. T. Porter, and F. Wagner, Jr., Physical Review, 103, (1956), 942.

22. Muller, D. E., H. C. Hoyt, D. J. Klein, and J. W. M. Dumond, Physical Review, 88, (1952), 775.

23. Dumond, J. W. M., Reviews of Scientific Instruments, 18, (1947), 626.

24. Cork, J. M., J. M. LeBlanc, A. E. Stoddard, W. J. Childs, C. E. Branyan, and D. W. Martin, Physical Review, 82, (1951), 258.

25. Pringle, R. W., W. Turchinetz, and H. W. Taylor, Physical Review, 95, (1954), 115.

26. Roulston, K. I. and R. W. Pringle, Physical Review, 87, (1952), 930.

27. Johns, M. W., and S. V. Nablo, Physical Review, 96, (1954), 1599.

28. Baggerly, L. J., P. Marmier, F. Boehm, and J. W. M. Dumond, Physical Review, 100, (1955), 1364.

29. Taylor, H. W. and R. W. Pringle, Physical Review, 99, (1955), 1345.

30. Kelly, W. H. and M. L. Wiedenbeck, Physical Review, 102, (1956), 1130.

31. Lu, D. C. and M. L. Wiedenbeck, Physical Review, 94, (1954), 501.

32. Heydenburg, N. P. and G. M. Temmer, Physical Review, 93, (1954), 906.

33. Jnanananda, S., Physical Review, 69, (1947), 570.

34. Levy, P. W., Physical Review, 72, (1947), 352.

35. Shpinel, V. S. and N. V. Forafontov, Zhurnal Eksperimental noi i Teoreticheskoi Fiziki, 21, (1951), 1376.

36. Siegbahn, K., ed., Beta- and Gamma-Ray Spectroscopy, New York: Interscience Publishers Inc., 1955.

37. McGowan, F. K., Physical Review, 79, (1950), 404.

38. McGowan, F. K., Physical Review, 93, (1954), 163.

39. Elmore, W. C. and M. Sands, Electronics, New York: McGraw-Hill Book Company, Inc., 1949.

40. Elmore, W. C., Review of Scientific Instruments, 21, (1950), 649.

41. Novey, T. B., Review of Scientific Instruments, 27, (1951), 841.

42. Bell, P. R., "The Scintillation Method," in Beta- and Gamma-Ray Spectroscopy, ed. by K. Siegbahn, New York: Interscience Publishers Inc., 1955, pp. 132-164.

43. Mitchell, A. C. G., "The Coincidence Method," in Beta- and Gamma-Ray Spectroscopy, ed. by K. Siegbahn, New York: Interscience Publishers Inc., 1955, pp. 201-223.

44. Stanford, A. L. and E. T. Patronis, private communication.

45. Frankel, S., Physical Review, 83, (1951), 673.

46. Owen, G. E. and H. Primakoff, Physical Review, 74, (1948), 1406.

47. Wu, D. C., "Experiments on the Shapes of Beta Spectra. The Interaction in Beta Decay," in Beta- and Gamma-Ray Spectroscopy, ed. by K. Siegbahn, New York: Interscience Publishers Inc., 1955, pp. 314-356.

48. Bashilov, A. A., N. M. Anton'eva, and B. S. Dzhelepov, Izvest. Akad. Nauk. Ser. Fiz. SSSR, 16, (1952), 264. Cited in Nuclear Science Abstracts, 7, No. 24B, (1953), 53.

49. Rose, M. E., "Internal Conversion Coefficients," in Beta- and Gamma-Ray Spectroscopy, ed. by K. Siegbahn, New York: Interscience Publishers Inc., 1955, pp. 905-909.

50. Nordheim, L. A., Reviews of Modern Physics, 23, (1951), 322.

51. Klinkenberg, P. F. A., Reviews of Modern Physics, 24, (1952), 63.

52. Blin-Stoyle, R. J., Reviews of Modern Physics, 28, (1956), 75.

53. Schüler, H. and H. Gollnow, Zeitschrift für Physik, 113, (1939), 1.

54. Blatt, J. M. and V. F. Weisskopf, Theoretical Nuclear Physics, New York: John Wiley and Sons, Inc., 1952, p. 769.

55. Condon, E. U. and G. H. Shortley, The Theory of Atomic Spectra, Cambridge, England: The University Press, 1935.

56. Blatt, J. M. and V. F. Weisskopf, Theoretical Nuclear Physics, New York: John Wiley and Sons, Inc., 1952, p. 590.

57. Blatt, J. M. and V. F. Weisskopf, Theoretical Nuclear Physics, New York: John Wiley and Sons, Inc., 1952.

58. Rose, M. E., Multipole Fields, New York: John Wiley and Sons, Inc., 1955.

59. Green, A. E. S., Nuclear Physics, New York: McGraw-Hill Book Company, Inc., 1955.

60. Evans, R. D., The Atomic Nucleus, New York: McGraw-Hill Book Company, Inc., 1955.

61. Sachs, R. G., Nuclear Theory, New York: Addison-Wesley Publishing Company, Inc., 1953.

62. Schiff, L. I., Quantum Mechanics, First Edition, New York: McGraw-Hill Book Company, Inc., 1949, p. 39.

63. Sliv, L. A. and I. M. Band, Zhurnal Eksperimental noi i Teoreticheskoi Fiziki, 31, (1956), 134.

64. Sliv, L. A. and I. M. Band, Soviet Physics (JETP), 4, (1957), 133.

65. Rabi, I. I., J. R. Zacharias, S. Millman, and P. Kusch, Physical Review, 53, (1938), 318.

66. Konopinski, E., "The Theory of Forbidden Beta Decay" in Beta- and Gamma-Ray Spectroscopy, ed. by K. Siegbahn, New York: Interscience Publishers Inc., 1955, pp. 292-313.

67. Hildebrand, F. B., Methods of Applied Mathematics, New York: Prentice-Hall, Inc., 1952, p. 139.

68. Rose, M. E., Physical Review, 91, (1953), 610.

69. National Radiac, Inc., 10 Crawford St., Newark 2, New Jersey, Bulletin No. 8.

70. Rose, M. E., N. M. Dismuke, C. L. Perry, and P. R. Bell, "Tables of Fermi Functions," in Beta- and Gamma-Ray Spectroscopy, ed. by K. Siegbahn, New York: Interscience Publishers Inc., 1955, pp. 875-883.

VITA

Vincent Wymore Shiel was born in Atlanta, Georgia on April 23, 1933. He received his secondary education in the City of Atlanta and Fulton County Public School Systems and was graduated from North Fulton High School in 1949. He attended Emory University and received the degree Bachelor of Arts in Physics in 1953. He was elected to the Phi Beta Kappa honorary society in 1952. He entered graduate school in the School of Physics at the Georgia Institute of Technology in September 1953. While enrolled in graduate school he held the position of Chemist with the Atlantic Steel Company during 1953 and 1954, and has held the position of Instructor in the School of Physics at Georgia Institute of Technology since 1954. He was the recipient of a Graduate Division Fellowship during 1955-1957. In 1956 he was elected to associate membership in Sigma Xi national research society, and in 1957 he was elected to full membership.